5-2015

The Effects of Methylmercury on Cell Proliferation and Apoptosis during Zebra Finch Neural Development

Monika E. Stančiauskaitė
College of William and Mary

The Effects of Methylmercury on Cell Proliferation and Apoptosis during Zebra Finch Neural Development

A thesis submitted in partial fulfillment of the requirement for the degree of Bachelor of Science in Neuroscience from the College of William and Mary

By

Monika Aleksandra Eiva Stančiauskaitė

Accepted for _____

_____
Margaret Saha, Ph.D., Director

_____
Randolph Coleman, Ph.D.

_____
Dan Cristol, Ph.D.

_____
John Griffin, Ph.D.

List of Tables

List of Figures

Acknowledgements

I would like to profusely thank my committee members, Drs. Saha, Coleman, Cristol, and Griffin for being kind enough to serve on my Honors committee and agreeing to read my Honors thesis. I look forward to hearing all of your comments and suggestions. I would also like to thank all of you for your patience and advice during all of the years I have known your respective selves.

To Dr. Saha, I give my greatest thanks for all of the fantastic opportunities you have given me and to have had you as a research mentor for all these years. I honestly have no clue what I would be doing right now if it was not for you. What I do know though is that I would lack a great deal of knowledge that I currently have, would not have been as successful as a student researcher, and would be a completely different person than I am now. Your great fervor for research has always been a source of inspiration for me. I would also like to thank Dr. Griffin. I am always grateful for having the opportunity to start out working in your lab. The experiences I had in your lab are what drew me into the research world. If I had not started out doing research in your lab as a freshman, there is a good chance I would gone down a different career path. To Dr. Cristol I am very thankful for all of your help and for getting the chance to know more about birds. I would never have thought that I learn or appreciate birds so much, especially in the span of the last couple years. Dr. Coleman, I would like to thank you for poking fun of some of my student sleeping habits and for all the campus walks. Lastly but not least, I would like to thank my family, friends, and the rest of Saha lab as well. Ačiū už kantrybęs, for understanding my odd quirks, and for listening to all of my nonsensical moments in life. I don't know if I could have handled

both research and volleyball during undergrad without all of you in my life. Finally, I would like to recognize the grants from the Howard Hughes Medical Institution (HHMI) through the Undergraduate Biological Sciences Education Program to the College of William & Mary, the DeFontes Fellowship award, and the NIH Grant 1 RI5N5067566-01 to Dr. Saha.

Abstract

Methylmercury is a widespread, highly neurotoxic, pollutant that is well known to cause neurological deficits and is particularly harmful during neural development. Many studies have investigated the neurotoxic effects of MeHg to better comprehend the threat that MeHg exposure poses to organisms. However, few studies have focused on the molecular and cellular effects that MeHg has on developing avian species, let alone altricial songbirds. Even less is understood how maternal MeHg deposits affect and disrupt the developing nervous system of songbird species. To address this issue, the objective of this study was to investigate the effects of maternally deposited MeHg on neural proliferation and apoptosis of the developing zebra finch (*Taeniopygia guttata*) embryo. The study also investigated the toxicokinetics of MeHg during embryonic zebra finch development, to provide insight into which stages of development may be more susceptible to the harmful effects of MeHg due to increased exposure. We used *in situ* hybridization (ISH) for proliferating cell nuclear antigen (PCNA), Terminal deoxynucleotidyl transferase dUTP nick end labeling (TUNEL) along with cell counting techniques to respectively determine any changes in proliferation and apoptosis in the developing neural regions of stage 25 embryos in control and 2.4ppm developmentally exposed embryos. We found a statistically significant decrease in neural proliferation in the midbrain of 2.4ppm embryos, but no significant difference was found in the amounts of apoptosis between control and MeHg exposed embryos. The mercury content was measured in a developing egg's pooled yolk and albumin, and embryo order to elucidate MeHg toxicokinetics at stage 25, stage 32, and stage 38 embryos. We found a trend of increased mercury accumulation in the embryo as development progressed.

1. Introduction

1.1: MeHg as an environmental contaminant

Methylmercury (MeHg) is a major environmental neurotoxin that is known to adversely affect organisms. MeHg, a heavy metal, is derived when natural and anthropogenic sources release inorganic mercury (Hg) into the environment[1]. Examples of natural sources that release Hg include volcanic eruptions and forest fires; however, the primary sources of Hg are due to anthropogenic production through mining and fossil fuel burning[1]. When Hg is released into the environment anaerobic bacteria and other soil and aquatic microorganisms methylate Hg and produce MeHg. MeHg accumulates in organisms and biomagnifies up the food chain, causing higher trophic levels to accrue the highest concentration of MeHg within their tissues.

Mercury (Hg) cycling between air and water phases contributes to the prevalence of MeHg in ecosystems[2]. When Hg is in its gaseous form, it is able to use the atmosphere as a vector to travel long distances and disperse in multiple soil and water sources where conversion to MeHg can take place. This is a cause for concern as the distribution properties of Hg vastly increase mobility. Studies have shown that due to Hg cycling in the environment, organisms in non-industrial Hg areas have high levels of MeHg[3]. As global warming is predicted to increase MeHg formation in the environment,[4] the ability of Hg to travel long distances away from its original source point and contribute to the contamination of MeHg is of a growing concern. Although it is not fully understood how higher climate temperatures will affect MeHg in aquatic ecosystems, elevated temperatures

have the potential to enhance Hg methylation and in turn increase MeHg bioaccumulation in organisms. Field and laboratory studies have demonstrated that MeHg concentrations can significantly increase at higher temperatures[26].

Hg is converted to MeHg mainly in aquatic ecosystems. However, studies have shown that terrestrial organisms can be exposed to MeHg[5] and organisms distant from Hg sources and aquatic habitats can reach MeHg concentrations similar to those found in aquatic ecosystems[6]. MeHg biomagnification in aquatic and terrestrial habitats poses as threat to organisms within numerous ecosystems and increases the risk of MeHg's neurotoxic effects.

1.2: MeHg Toxicity Overview

MeHg is widely considered to be the most toxic form of mercury based on its bioavailability, biomagnification in food chains, and bioaccumulation in tissues[7]. Unlike inorganic Hg and elemental Hg, which are poorly absorbed in the gastrointestinal tract of organisms, MeHg is highly absorbed at around 90-95%[8] compared to around 7-10% elemental/metallic Hg[9]. MeHg is able to easily accumulate into all tissue types, cross the placental barrier, and the blood brain barrier, enabling toxic events to occur[10]. Due to these characteristics, MeHg is known to preferentially target the central nervous system and exerts harmful effects during embryonic development[8][11].

Due to the occurrence MeHg poisoning in countries such as Japan and Sweden[11][12], it is well documented that acute, high-level exposure to MeHg during development causes

severe neurological impairments such as blindness, deafness, and mental retardation[11 13]. Other common neurological effects seen in adults include ataxia, dysarthria, auditory impairments, and tremors[14]. The Minamata MeHg poisoning incident in Japan which began in 1953, highlighted the sensitivity of high level MeHg embryonic exposure, as infants had symptoms similar to cerebral palsy as well as other deficits including mental retardation, cerebellar ataxia, and impaired motor reflexes[1415].

Chronic, low-level exposure to MeHg, however, is a far more prevalent problem worldwide. Recurrent exposure to MeHg is far more common as humans and other organisms consistently ingest low levels of MeHg in their diet through consumption of contaminated food[14]. Chronic, low-level exposure to MeHg is associated with various neurologic deficits. Chronic low-dose exposure to MeHg may play a role in the onset of epileptogenesis[16] and ADHD[17]. Low prenatal exposure may also be linked to irreversible behavior deficits that later emerge in adulthood. Rats prenatally exposed to low levels of MeHg displayed behavioral rigidity and affected reinforcement processing[18]. Studies also demonstrate that exposure to low, biologically relevant, levels of MeHg cause neurocognitive deficits by affecting learning and memory in children and animals [19,2021] which can be exemplified by contaminated songbirds that have less complex songs[22].

Understanding the sub-lethal effects of MeHg on birds is of importance for a number of reasons. First of all birds are excellent model organisms for understanding fundamental areas of human development, such as neurogenesis[23]. Chickens (*Gallus gallus*) have been used extensively to study limb development[24], neurogenesis[25], and somitogenesis[26], while zebra finches (*Taeniopygia guttata*) are an excellent model for understanding language development[2728]. Another major reason is that birds can, and have been, used as indicators

of ecosystem health[29]. As such, MeHg levels in birds are able to represent the bioaccumulation levels at multiple trophic, due to bird occupancy throughout the food chain levels[30]. MeHg accumulates in growing feathers, providing information on MeHg levels in the environment at selectable timepoints[3031]. The effects of sub-lethal levels of MeHg are also important to study in order to understand how it threatens a bird species' fitness. Sub-lethal levels of MeHg have been demonstrated to adversely affect reproductive success in birds by decreasing survival rates and the number of independent offspring a bird pair produces [32]. Reduced survival and reproductive success from MeHg combined with habitat loss and other environmental stressors are potentially serious threats to endangered bird species[33], particularly declining songbird species such as the saltmarsh sparrow (*Ammodramus caudacutus)* [34] and the ivory gull (*Pagophila eburnea*)[35]. As avian diversity is vital for ecosystem health it is paramount to better understand how sub-lethal MeHg exposure impact bird species.

1.3: Molecular Mechanisms of MeHg Toxicity

MeHg is well known to preferentially disrupt the nervous system however the molecular mechanisms by which MeHg exerts its toxic effects are unclear. There is evidence that MeHg disrupts Ca^{2+} homeostasis, increases oxidative stress, and impacts sulfhydryl group interactions, [1536] which can inhibit glutamate uptake[37]. More recently data has supported that MeHg induces neuronal apoptosis by inhibiting the tropomyosin receptor kinase A (TrkA) pathway[38].

One of the major mechanisms underlying MeHg toxicity is MeHg's ability to induce changes in calcium ion (Ca^{2+}) intracellular concentration. Cell culture studies demonstrate that increased micromolar concentrations of MeHg can perturb Ca^{2+} homeostasis by increasing intracellular Ca^{2+} levels. Disrupting normal Ca^{2+} concentrations can adversely impact cell survival, as Ca^{2+} is an intracellular signaling molecule that is important in the proper regulation of many cellular pathways and processes. To regulate metabolic and intracellular signaling, Ca^{2+} levels are tightly controlled in all cells and when the cell is at rest, extracellular Ca^{2+} concentrations are vastly higher than intracellular Ca^{2+} concentrations. MeHg disruption of Ca^{2+} homeostasis in cells is particularly pertinent for neurons, and may explain neuronal sensitivity to MeHg exposure. During normal neuronal cell signaling, Ca^{2+} rapidly enters neurons and subsequently slowly restores low Ca^{2+} intracellular concentrations in an energy dependent manner. Neurons expend great energy levels to restore low Ca^{2+} intracellular concentration[36] which is increased in the presence of MeHg Ca^{2+} dysregulation. Studies indicate that raised energy expenditure due to increase in intracellular Ca^{2+} levels lead to neuronal cell death and apoptosis[3911]. Elevated intracellular Ca^{2+} concentration is also associated with oxidative stress[11].

Another crucial mechanism behind MeHg toxicity which is associated with disruption of Ca^{2+} homeostasis, is glutamate dysregulation. Studies show that glutamate homeostasis is disrupted from MeHg exposure[3736]. Glutamate is a major excitatory neurotransmitter that is critical to properly regulate to prevent glutamate excitotoxicity. Glutamate excitotoxicity occurs when excessive neuronal activation by glutamate cause neuron cell death and injury in part due to increased Ca^{2+} influx. Glutamate excitotoxicity is also implicated in a number of conditions such as neurodegenerative diseases[40]. MeHg is

known to affect glutamate transporters. This occurs due to the soft electrophile property of MeHg. MeHg preferentially reacts with soft nucleophiles, such as sulfhydryl/thiol groups by covalently binding to cellular proteins containing such groups[378]. This ability allows MeHg to disrupt the proper functions of a wide array of thiol containing proteins, such as glutamate transporters, causing toxicological effects. MeHg's thiol binding ability inhibits the glutamate transporters GLAST and GLT-1 in astrocytes, thereby sustaining extracellular glutamate levels and excitation, potentiating excitotoxicity in neurons and neuronal cell death[36,37]. MeHg also disrupts proper glutamate homeostasis by inhibiting GABA receptors. GABA is the nervous system's predominant inhibitory neurotransmitter, and is also critical in maintaining the proper balance between neuronal excitation and inhibition. MeHg inhibits $GABA_A$ receptors, thereby impairing GABAergic inhibition and disrupting the proper inhibitory and excitatory balance[16]. Reduction of GABAergic inhibition leads to hyperexcitability as glutamate activation increases due to less inhibition. Low MeHg exposure may contribute to epileptogenesis by affecting glutamate and GABA activity[16].

It is widely known that MeHg causes oxidative stress in cells. MeHg increases the generation of reactive oxygen species (ROS) and the induction of lipid peroxidation in cells. The nervous system, especially the embryonic nervous system, is particularly vulnerable to oxidative stress induced by MeHg due to a developing antioxidant system and having a high content of oxidizable substrates such as lipids[41]. MeHg further increases oxidative stress by disrupting antioxidant defense systems such as glutathione (GSH) dependent enzymes. GSH is crucial in protecting against ROS damage and is a thiol-based antioxidant. Glutathione reductases are important for maintaining cellular redox homeostasis as they function to maintain reduced GSH. Glutathione peroxidases are essential in protecting the

lipid rich nervous system from oxidative damage, as they reduce reactive peroxides to prevent them from modifying lipids and proteins[42]. MeHg, due to its ability to covalently bind to thiol groups[37], inhibits proper glutathione activity. This interaction causes the formation of GSH protein adducts which are excreted from the cell. This formation has been suggested as a potential mechanism for depleted GSH levels in MeHg exposed cells, which disrupts normal redox balance of neurons leading to cell death[11].

Recently, evidence has shown that MeHg causes neuronal apoptosis by inhibiting the tropomyosin receptor kinase A (TrkA) pathway. The TrkA pathway plays an important function in neurons by regulating proper differentiation and cell death. TrkA signaling endosomes are involved in neuronal growth, gene expression, and survival[43]. A study by Fujimura and Usuki demonstrated that in PC12 cells (cells with a neural crest embryonic origin that are derived from the rat adrenal medulla) MeHg inhibits the TrkA pathway by inhibiting TrkA phosphorylation[38]. The study also showed that MeHg inhibition of the TrkA path caused exposed PC12 cells to have inhibited neurite extension prior to induced apoptosis, which was ameliorated by increasing TrkA pathway activation[38].

1.4: MeHg Neurotoxicity during Development

MeHg exerts its most neurotoxic effects during early development. Carefully coordinated processes such as cell proliferation, neuronal migration, and neuronal differentiation, all occur throughout development and the molecular disruptions caused by MeHg affect the tightly regulated developmental processes that are critical for normal brain

development. These critical developmental events either do not occur in the adult brain or occur on a much smaller scale, which suggests why the developing brain is more sensitive to MeHg[8]. Because the nervous system in developing organisms shows such sensitivity to MeHg, many studies have focused on understanding MeHg effect at the cellular level. Studies have demonstrated that during development MeHg, even at low biologically relevant levels, is able to disrupt proper neuronal migration in rodents [44], inhibit neuronal differentiation [45], decrease neural cell proliferation [46,47], and increase apoptosis[15,47]. The aforementioned neurotoxic effects during development are thought to mediate the neurologic and behavioral deficits caused by MeHg exposure[48].

A number of studies have examined the effect of MeHg on neural apoptosis and proliferation during development due to their critical roles in embryonic neural development. Alterations in the amount, location, and timing of apoptosis and cell proliferation can cause developmental disorders due to improper patterning of the nervous system. During normal embryonic development, the developing nervous system undergoes rapid proliferation as well as extensive apoptosis in order to establish proper neuronal populations. The timing and amount of proliferation and apoptosis are also essential in establishing patterns of normal neuronal connections and brain cytoarchitecture[46]. Changes within neural patterning can have long lasting effects. Alterations in neuronal proliferation and apoptosis are implicated in schizophrenia[49], autism [50], and other developmental disorders[51,52]. Numerous studies have demonstrated MeHg's impact on cell proliferation and apoptosis. *In vitro* cell culture studies have demonstrated that MeHg decreases cell proliferation in neural stem cells[53], cortical progenitor cells[46], and neurospheres in both human and rodent cells[45]. *In vitro* cell culture studies have similarly

shown that MeHg increases apoptosis in neural stem and progenitor cells[54,] in both human and rodent cells[45]. *In vivo* studies, using a variety of model organisms from rodent models to *Xenopus laevis*, have similar results where exposure to low levels of MeHg increases apoptosis and decreases proliferation during development in a dose[48,55,47]. Interestingly, an *in vitro* study demonstrated that decreased neural cell numbers, due to MeHg exposure, don't always occur alongside with increased apoptosis. MeHg reduced total cell numbers by decreasing neural stem cell proliferation, but did not increase apoptosis or necrosis, and this effect was even seen in daughter cells that had no direct MeHg exposure[5345].

1.5: MeHg and Avian Models

MeHg is considered to be a substantial threat to avian species and numerous studies have been conducted on how MeHg affects bird behavior, population, and adult reproductive success. However, although MeHg is a developmental neurotoxin, few cellular and molecular studies have been performed on bird development[56] (compared to rodent models) and even fewer studies have examined the effect of MeHg on neurodevelopment in birds[5758], let alone *in vivo* experiments[5960]. The few studies examining MeHg's neural developmental effects in birds have mainly been conducted using chickens (*Gallus gallus*) as the model organism. This is of note, as the majority of bird species are altricial songbirds and many endangered bird species are altricial, not precocial like chickens. Altricial species can differ significantly from precocial species in developmental processes, to the point where it is necessary to have different embryonic staging guides for precocial and altricial

species[61]. An example of developmental differences in precocial species is that organs such as the brain, muscle, and skeleton develop more rapidly during early development than altricial species[62]. Due to these differences in development, especially regarding brain development, MeHg has the potential to affect development differently in altricial species than what is observed in precocial species such as chickens.

Another problem regarding MeHg cellular and molecular avian studies is that the majority of studies are done either in cell culture or by directly injecting MeHg into the egg. Birds chronically exposed to MeHg from their diet accumulate MeHg into their tissues. During their laying period, females naturally deposit mercury from their tissue and diet into their eggs, which results in avian embryos being continuously exposed to MeHg throughout their entire embryonic development. Some studies show that the majority of MeHg is incorporated into the albumen during natural maternal MeHg transfer[63]. However, as mentioned before, all *in vivo* cellular and molecular studies regarding MeHg's impact on bird development inject MeHg directly into the egg. Also, many of such studies do not inject MeHg on day zero of development[63] (the day the egg is laid) but wait until incubation day three[59] or even incubation day five[64] . It is true that there are many practical benefits to expose bird embryos to MeHg via injections. Some benefits include eliminating individual variation regarding maternal MeHg transfer amounts and decreased cost due to not having to hand raise birds in a laboratory setting. Nonetheless, injections potentially decrease the biological relevance of such studies as direct MeHg injections may change the toxicokinetics and distribution of MeHg in the avian embryo and subsequently skew neurotoxic effects. The time course of MeHg accumulation into developing embryonic

tissues and subsequent neurological effects may especially be altered when injected later than day zero, as many sensitive developmental stages have already passed.

1.6: Experimental overview

As discussed in current literature, exposure to low doses of MeHg is a prevalent problem worldwide. Developmental exposure to low, chronic levels of MeHg causes an array of neurocognitive deficits such as affecting learning and memory in both children and animals[65,66]. Numerous studies, as mentioned in the literature, show that low MeHg developmental exposure causes neurotoxic molecular and cellular to occur and disrupts neural cell proliferation and apoptosis[38,48,44,47]. Although there are many studies examining the deleterious effects of developmental MeHg exposure, few to no studies have been conducted at the molecular cellular level investigating the effect that maternal MeHg transfer has on altricial embryonic neurodevelopment. Therefore, this study will address the effects that MeHg exposure via maternal transfer has on neural development using zebra finch (*Taeniopygia guttata*) as a model organism.

Zebra finch have been used in MeHg studies as they are easy to breed in captivity, have a large body of literature describing their physiology and behavior, and are the only songbird with a fully sequenced genome. Previous work conducted on zebra finches also demonstrates the impact MeHg has on reproductive success. Zebra finches exposed to low, biologically relevant MeHg doses for their entire lifetimes had significantly lower

reproductive capabilities and less successful offspring[32]. These results may be due to MeHg exposure affecting normal embryonic development.

Preliminary observations furthermore suggest that zebra finch embryos prenatally exposed to MeHg have altered cell proliferation and/or apoptosis. In the Saha lab it has been observed that dissected MeHg exposed embryos tend to be at an earlier stage of development compared to control embryos when dissected at identical time points. This difference may be explained by alterations in proliferation and/or apoptosis in MeHg embryos. However, as mentioned before, few molecular studies regarding MeHg neuro-developmental toxicity have been conducted in altricial species, let alone zebra finch, and few have researched how avian parental exposure to MeHg affects embryonic neural development at the molecular cellular level.

This project will examine the effect of low, prenatal MeHg exposure on cell proliferation and apoptosis in the developing nervous system of zebra finches. As previously discussed, changes in the amount, location, and timing of apoptosis and cell proliferation can cause developmental disorders by disrupting proper nervous system patterning. This project tested the hypothesis that changes in cell proliferation and apoptosis during embryonic development mediate the adverse effects that developmental MeHg exposure has on neural development in zebra finch. It was predicted that proliferating cell nuclear antigen (PCNA) expression levels will decrease and apoptotic levels will increase in embryos developmentally exposed to MeHg.

To prenatally expose zebra finch embryos to MeHg the parental generation was fed *ad libitum* a diet of 0.0ppm, or 2.4ppm MeHg. In order to analyze any changes in cell proliferation during embryonic development, gene expression for PCNA was examined at

stage 25 (day 4 ¾). PCNA is only expressed during DNA replication and acts as a marker of cell proliferation. During DNA replication, PCNA acts as a sliding clamp processivity factor of DNA polymerase δ, allowing the DNA polymerase to relax and regain its hold on DNA without losing its place at the replication fork [67,68]. Stage 25 was selected as it is easily distinguishable stage, is a relatively early stage of embryonic development, and the forebrain, midbrain, hindbrain, and spinal cord regions are well distinguished compared to earlier developmental stages. Whole mount *in situ* hybridization (ISH) was used to determine differences in spatiotemporal patterns of PCNA expression in control and mercury exposed embryos. The effect of MeHg on programmed cell death was also analyzed to determine changes in apoptosis. TUNEL (terminal deoxynucleotidyl transferase dUTP nick end labeling) was used in whole mount stage 25 zebra finch embryos to label apoptotic cells. The TUNEL assay functions by detecting DNA degradation that occurs in later apoptotic stages[69].

In order to quantitatively test if PCNA was downregulated and if there was an increase in apoptotic cells, ISH and TUNEL processed embryos were sectioned after ISH and stained with DAPI (4',6-diamidino-2-phenylindole, a fluorescent nuclear stain) in order to quantify the number of cells in given regions of the nervous system. Cell counting was done using plugins in Image J to determine if there was a difference in total number of cells. Cell counts were organized into forebrain, midbrain, hindbrain, and spinal cord neural regions in order to determine area-specific differences in cell proliferation and/or apoptosis.

Hg distribution in the developing embryo, eggshell, yolk and albumin, was also analyzed for a couple of reasons. One was to better understand MeHg toxicokinetics during early development of an altricial embryo. Second was to provide insight into early

developmental periods that are more susceptible to MeHg's adverse effects by determining when the embryo accumulates higher levels of Hg relative to the rest of the egg components. Very few studies have measured how MeHg spreads into different areas of the egg during embryonic embryo, and few to none have studied early embryonic stages of development[60,63]. To measure Hg distribution, eggs were dissected at stage 25 (day 4 ¾), stage 32 (day 6 ¾), and stage 38 (day 8 ½). For each developmental stage the eggshell and embryo were separated for Hg analysis on the Direct Mercury Analyzer (DMA-80, Milestone, Shelton CT). For each stage, the yolk and albumin were pooled together for Hg analysis. We predict that there will be a trend of increasing Hg content in the embryo compared to the rest of the egg as development progresses.

This methodology aims to determine if MeHg at biologically low, relevant doses affect proliferation and apoptosis during neural development of zebra finch embryos and to gain a better understanding of MeHg toxicokinetics during development. Analyzing these processes will provide information on how MeHg affects important cellular processes during neural development and exerts its effects as as a neurotoxin.

2. Materials and Methods

2.1. Animal Care

Unrelated zebra finches were paired together and housed on campus at the College of William and Mary in the Integrated Science Center. Pairs were kept in an environment to replicate breeding conditions on a 14hour light: 10 hour dark cycle. Each pair was kept in a wire cage (45 height x 45 width x 75 length cm) with two perches of a different width, a bowl for bathing, a nest box for breeding, hay for nesting material, cuttlebone as a calcium supplement, and feed cups containing digestive grit, food, or water. Food (ZuPreem Shawnee, Kansas, USA) was nutritionally complete and water enriched with vitamins (Vita-Sol Ultravite Multi-vitamin Supplement, 8 in 1, Pet Products, Islandia, NY). Both food and water were provided daily *ad libitum*. Pairs were designated into treatment groups and each treatment group was on a separate rack. There were three treatment groups kept in the same room but separated on different racks. The control was fed 0.0μg/g dietary methylmercury, and the two treatment groups respectively fed 1.2μg/g or 2.4μg/g dietary methylmercury. All animal care procedures were approved by the College of William and Mary's OLAW (Office of Laboratory Animal Welfare) and was IACUC approved (Institutional Animal Care and Use Committee).

2.2. Egg Collection and Care

Under breeding conditions zebra finch pairs can typically provide one egg per day. Eggs were collected daily within four to six hours after the light cycle began and labeled by pair number and collection date. Immediately after collection, eggs were put into a feed cup

lined flat with paper towels with six eggs maximum per cup and placed in a mechanical incubator (Picture Window Hova-Bator Incubator, Curciulated Air Model No. 158328.3 Watts 115 Volt AC, G. Q.F MFG CO INC, Savannah GA 31402-1552 USA). The lining and egg limit per cup allowed for a safe rolling environment during tilting within the incubator. Tilting simulated parental care and prevented embryos from adhering to the interior shell during development. The incubator was kept at 37.5°C +/- 1°C and 80-95% humidity to mimic parental incubation. 400mL of water was added daily to maintain humidity levels and egg care and collection was recorded daily in a binder next to the incubator.

2.3. Egg/Embryo Dissection

Eggs were dissected at developmental time points optimal to obtain embryo stages of interest. Eggs were candled by shining light from behind using fiber optic illuminator lamps (Dolan-Jenner Industries Fiber-Lite MI-150 High Intensity Illuminator) to visualize the interior. Day one embryos are unable to be seen by candling, however embryo vasculature can be seen Day two and later. It is important to know where the embryo is before cutting open the egg to avoid any damage. After determining embryo location, the eggs was cut from tip to base with a scalpel and the contents allowed to fall onto weigh paper. To better visualize the embryo and associated membranes, a dissecting scope was used (Olympus SZ61) as necessary. Fine tipped forceps were used to separate the embryo from its associated membranes. Early day one embryos were separated from the vitelline membrane while older stages, day three and older, were removed from the amniotic membrane and had the allantois removed. The embryo was washed with 1X PBS (phosphate buffered saline solution) to remove yolk granules. Embryos were staged

according to the Murray zebra finch staging guide[61]. Embryos to be used for later in situ hybridization were fixed with 4% PFA (paraformaldehyde) solution and later dehydrated in graded methanol solutions for storage at -20°C. Embryos for later RNA extraction were flash frozen in liquid nitrogen.

2.4. PCNA Primer Design

Primers were designed with Primer3 plus in order to amplify proliferating nuclear antigen (PCNA) mRNA (Taeniopygia guttata clone 0058P0040D09 putative proliferating cell nuclear antigen variant 1 mRNA, complete cds). Both forward and reverse primers contained around 50% GC content. The forward primer had an annealing temperature of 60.37°C and the reverse primer had an annealing temperature of 59.96°C. Both primers were 20 base pairs long. The primers covered 1006 base pairs for the target product size. Primers were checked on NCBI to ensure specificity for *Taeniopygia guttata* PCNA mRNA sequence.

2.5. Endpoint RT-PCR for PCNA

PCNA cDNA was amplified using the primers above designed to amplify the PCNA sequence. Reaction mix was prepared by combining 4µL dNTP 10mM mix, 5µL 10X buffer, 2µL 50mM $MgSO_4$, 2.5µL of forward and reverse primers, 1.5µL zebra finch embryo cDNA, 0.3µL Platinum Taq polymerase, and 32.2µL nuclease free water (NFW). After combining, the reaction mix was put into a thermocycler (GeneAmp PCR System 9700 thermocycler (Applied Biosystmes)) on the following cycle: 5 minutes at 94°C, 30 seconds for 35 cycles at

94°C, 30 seconds at 60°C, and 1.5 minutes at 68°C, 7 minutes at 68°C, and a subsequently cooled to a holding temperature of 4°C. PCR products were taken and run on a gel. Gel was made to be 1% agarose by combining 50mL 1X TAE, 0.5grams agarose, and 2.5 μL of ethidium bromide.

2.6. Cloning for PCNA

Cloning was done using the StrataClone PCR Cloning Kit and manual. Ligation reaction mixture was prepared by adding in order 3 μL StrataClone Cloning Bufer, 2μL of PCR product (obtained from the RT-PCR procedure above), and 1μL of StrataClone Vector Mix amp/kan (vector was StrataClone PCR Cloning Vector pSC-A-amp/kan). Reaction mixture was gently mixed and incubated for five minutes at room temperature. After incubation the reaction was put on ice. Transformation was done immediately after by adding 1μL of the cloning reaction to a thawed tube of StrataClone SoloPack competent cells and was gently mixed. The transformation mixture was incubated for 20 minutes on ice. As the mixture incubated, LB broth was warmed to 42°C. After incubation the transformation mixture was heat-shocked for 45 seconds at 42°C and 250μL of the pre-warmed LB broth was subsequently added. StrataCLone competent cells were allowed to recover for an hour and a half at 37°C while agitating horizontally in a shaker.

During competent cell recovery, LB-ampicillin plates were prepared by spreading 40μL of 2% X-gal on 2 LB plates. Ampicillin acts as a selection factor, as bacteria that took up the vector gain ampicillin resistance. X-gal acts as a screening factor, as colonies that had unsuccessfully taken up the vector are blue and colonies that were successful are white as the incorporation of the plasmid prevents them from being able to express β-

galactosidase and therefore are unable to hydrolyze X-gal. Spread 50μL and 100μL of the transformation mixture on the LB ampicillin and X-gal plates. Plates were incubated overnight at 37°C.

2.7. Miniprep (Wizard Plus SV Minipreps DNA Purification System kit)

Two different white colonies per plate were selected and placed into four respective culture tubes containing 4mL of LB broth and allowed to incubate in a 37°C shaker for 8 hours. Turbid cultures were taken out and placed into respective eppendorf tubes (2mL culture per tube). Tubes were spun for 5 minutes in the microcentrifuge to form a pellet (Microcentrifuge 5415 D) and resulting supernatant was poured off to remove culture media. To each tube 250μL of cell resuspension solution was added and vortexed for one minute to resuspend the pellet. Afterwards, 250μL of cell lysis solution was added and mixed by inverting the tubes for four times. 10μL of alkaline protease solution and also inverted four times and subsequently incubated at room temperature for 5 minutes. 350μL of neutralization solution was added to each tube and inverted four times. All eppendorf tubes were spun at max speed (13200 RPM) in the microcentrifuge for 10 minutes in order to pellet the cellular debris. Four spin columns were inserted into the vacuum manifold miniprep adaptor onto the vacuum manifold. Transferred cleared bacterial lysate to the prepared spin columns without allowing any white precipitate to fall in. Vacuum was applied and solution pulled through. 750μL of column wash solution was added to each column and vacuum applied. 250μL of column wash solution was subsequently added to columns and vacuum applied. Columns were allowed to dry with the vacuum on for 10 minutes. Afterwards the columns were transferred to 2mL collection tubes and spun for 2

minutes at max speed to dry completely. Spin columns were transferred to sterile eppendorf tubes and 30µL of NFW was added and allowed to stand for 1 minute then centrifuged at max speed for 1 minute. Afterward spin columns were discarded and purified plasmid DNA was stored at 4°C.

2.8. Restriction Digest for miniprep prepared plasmid DNA

Per each eppendorf tube 12.5µL sdd (sterile double distilled) H_2O, 2µL of 10X Buffer H, 5µL of miniprep purified plasmid DNA, and 0.5µL of EcoRI restriction enzyme was combined. Contents were gently mixed by flicking the tube and briefly spun down in a picofuge. Digest reaction was incubated at 37°C for 1-2 hours. After incubation, 4µL of the digest was run on a 1% agarose gel (as described above) to verify insert size.

2.9. Glycerol Stock preparation

-20°C and -80°C glycerol stocks were prepared from leftover mini culture taken from mini preps with desired restriction digest results. -20°C glycerol stocks were prepared by adding 500µL of sterile glycerol with 500µL of mini culture and completely mixing then storing at -20°C. -80°C glycerol stocks were prepared by adding 150µL of sterile glycerol with 850µL of mini culture and completely mixing then storing at -80°C.

2.10. Midiprep (Promega PureYield Plasmid Midiprep kit)

150mL of LB broth was inoculated with 10µL of glycerol stock and incubated in a 37°C shaker for approximately 12 hours. Once turbid, glycerol stocks were made (as described in methods section #12) from midi culture. Remaining midi culture was poured into a 200mL centrifuge tube and pelleted at 5,500RPM for 10 minutes using the

Thermoscientific Fiberlite F14 rotor and supernatant discarded. Pellet was resuspended with 6mL of cell resuspension solution, vortexed, and sterilely transferred to a smaller oakridge tube. 6mL of cell lysis solution was added and the oakridge tube was inverted 3-5 times then incubated for 3 minutes at room temperature. 10mL of neutralization solution was immediately added afterwards and inverted 5-10 times. Lysate in the oakridge tube was centrifuged (using HB-6 rotor) at 9,500RPM for 15 minutes. After centrifuging, cleared lysate was decanted into a blue PureYield Clearing Column placed on top of a white PureYield Binding Column on a vacuum manifold. Vacuum was applied until all liquid passed through both columns. Added 5mL of endotoxin removal wash to the white binding column and vacuum applied to pull liquid through. 20mL of column wash solution was added to the white binding column and liquid pulled through with the vacuum and the membrane was allowed to dry for 30-60 seconds. A 1.5mL eppendorf tube was added to the base of the vacuum eluator elution device and the binding column was placed on top. After sitting for one minute, 750µL of NFW was eluted through the DNA binding membrane of the white column and subsequently re-eluted. Purified plasmid DNA was nanodropped, digested as described in section #11 to verify insert size) and run out on a gel then stored at 4°C until usage.

2.11. Sequence verification

In order to verify plasmid insert sequence was PCNA for *Taeniopygia guttata*, two 0.2mL PCR tubes were prepared to be sequenced. Each PCR tube contained: 1.2µL of purified plasmid DNA, 0.32µL of diluted 10^{-2} M13 Forward primer or M13 Reverse primer, and 6.48µL NFW. Sequencing was done by the core lab of William and Mary. Once

sequenced, sequence was verified by blasting against Taeniopygia guttata clone 0058P0040D09 putative proliferating cell nuclear antigen variant 1 mRNA, complete cds.

2.12. Linearization for Transcription

To linearize plasmid DNA for subsequent use in transcription as a template, digests were set up containing 100µL per reaction. Each 1.5mL eppendorf tube contained: 10µL of appropriate 10X restriction enzyme buffer (Buffer E for antisense probe and Buffer H for sense probe), 20µg of plasmid DNA, 2-4µL of appropriate restriction enzyme (2µL of HindIII for antisense probe and 4µL of NotI for sense probe), and enough µL of NFW added to have 100µL total per reaction. Digests were incubated at 37°C for 2-3 hours. DNA was extracted by adding an equal volume of phenol/chloroform: isoamyl alcohol (25:24:1) then vortexed and spun down in a microcentrifuge for 5 minutes at max speed. The top aqueous layer was withdrawn and transferred to a new eppendorf, then the same process repeated after adding an equal volume of chloroform: isoamyl alcohol (24:1). 1/10 volume of 2M sodium acetate was subsequently added to precipitate linearized DNA and two volumes of cold 100% ethanol added. Linearized solution was frozen at -80°C for at least 30 minutes. Often linearized solution was left overnight due to time constraints. Linearized reaction was spun down in a refrigerated centrifuge (at 4°C) for 25 minutes at maximum speed (14000RPM). Supernatant was removed and DNA pellet was washed with 200µL of fresh 70% ethanol, inverted 2-3 times, and spun in the refrigerated centrifuge for 5 minutes at max speed. Supernatant was discarded and pellet dried in a speed vacuum for about 3minutes then resuspended in 20µL 1 X TE. Linearized DNA was run out on a gel to confirm success and nanodropped to determine concentration.

2.13. ISH RNA probe synthesis

Sense and antisense RNA probes were synthesized for later ISH usage to determine PCNA expression to label proliferating regions. A master mix of rNTPs was made containing: 7.5µL of 10mM rCTP, 7.5µL of 10mM rGTP, 7.5µL of 10mM rATP, 4.88µL of 10mM rUTP, and 2.63µL of 10mM dig-11 rUTP (Roch 11 209 256 910). Added to each respective sense or antisense eppendorf was: 10µL of 5X transcription buffer, 5µL of 0.1M DTT, 15µL of the 2.5mM rNTPmaster mix, 4µg of linearized plasmid, 0.5µL of RNAsin (Promega N2111), 1.5µL of appropriate RNA polymerase (T7 for antisense probe and T3 for sense probe), and enough NFW was added to make the total reaction volume per eppendorf be 50µL. Reactions were incubated at 37°C for 2 hours then had 1.5µL of appropriate RNA polymerase added and subsequently incubated for another 1.5 hours at the same temperature. To degrade the DNA template, 1µL of RQ1 DNAse (Promega M6101) was added to each eppendorf and incubated for 10 minutes at 37°C. 30µL of 7.5M lithium chloride precipitation solution was added to purify the RNA probes, and the solution placed at -20°C for at least one hour. Oftentimes solution stayed at -20°C overnight due to time constraints. Probe was pelleted in a 4°C refrigerated centrifuge by centrifuging for 25 minutes at max speed of 14000RPM. Pellet was washed with 1mL of 70% ethanol and spun for 5 more minutes at the same settings. Supernatant was subsequently removed, pellet dried in a speed vacuum for around 1-2 minutes, and resuspended in 20µL of NFW. Purity and yield were determined by nanodropping and the integrity was checked on a gel. Stock probe solution of 10X concentration was made by adding the appropriate amount of ISH buffer to dilute the concentrated probe solution. Occasionally, when probe yield was

particularly high, probe solution was diluted to 20-40X stock. All RNA probes were stored at -20°C.

2.14. Whole mount ISH for zebra finch embryos

Whole mount ISH was performed on stage 25 zebra finch embryos using the antisense PCNA probe to determine PCNA expression to label proliferating regions. Sense PCNA probe was used as a control to determine the level of background. Standard whole mount ISH procedures used for chick embryos were followed [70] with the following modifications: all washes were done using 5mL screw cap glass vials and vials were nutated vertically while placed in a Styrofoam rack to reduce any embryonic tissue damage. For day one, the concentration of Proteinase K for stage 25 embryos was 20µg/mL and embryos were treated for 18 minutes at room temperature. For day one embryos were incubated in 1µg/mL PCNA probe concentration and incubated overnight at 60°C. On day two, zebra finch embryo powder was used to prepare preabsorbed antibody. On day three, once sufficient signal developed after 20-30 minutes and color reaction was paused in order to image whole mount embryos on a dissecting scope (Olympus SZX7) using Olympus software. After imaging, embryos were returned to the color reaction solution in order to develop signal strong enough for cryosectioning.

2.15. Whole mount TUNEL assay for zebra finch embryos

The whole mount TUNEL assay in order to label apoptotic cells was performed on stage 25 zebra finch embryos. On day one, embryos were permeabilized in phosphate buffer saline (PBS) with 0.1% Triton X-100 three times for 20 minutes each, then bleached

and further permeabilized in 6% hydrogen peroxide for 1.5 hours. Afterwards, embryos were washed three times with PBT (PBS with 0.1% Triton X-100) three times for 5 minutes each and then kept in PBT for 1 hour and 30 minutes. In a 2mL eppendorf, embryos were equilibrated for two hours in terminal deoxynucleotidyl transferase (Tdt; Sigma-Aldrich) buffer at RT then incubated overnight at RT in TdT buffer with digoxigenin-dUTP (Roche) in a 1:100 dilution of TdT enzyme (Sigma-Aldrich) per 2mL eppe. For each TUNEL run, a negative control embryo was run to control for any potential background. Negative control embryos were accomplished by omitting the Tdt recombinant enzyme on the first day of the TUNEL assay. On day two, the enzyme reaction was stopped by washing embryos in PBT with 100mM EDTA solution at 65^{o}C two times for one hour each. To prepare for the antibody step, embryos were washed for one hour in maleic acid buffer with 0.1% Tween-20 (MABT) added. Embryos were subsequently washed for two hours in MABT with 2%BMB (Boehringer Mannheim Buffer), then washed for two hours in MABT with 2% BMB and 20% heat inactivated goat serum (GS). During the two hour wash, the alkaline phosphatase conjugated anti-digoxigenin antibody (Roche) was adsorbed in zebra finch embryo powder and diluted in MABT with 2% BMB and 20% heat inactivated goat serum (GS) for a final dilution of 1:2000 and incubated overnight at 4^{o}C in order to allow the antibody to label TUNEL positive cells. On Day three, after washing in MABT five times for 1 hour at RT, TUNEL positive cells were visualized by BCIP/NBT staining. All TUNEL assayed embryos were subsequently cross sectioned for further analysis.

2.16. Cryosectioning

Zebra finch embryos were prepared for cryosectioning by equilibrating in a 1.6M sucrose solution for at least 12 hours at 4°C and subsequently embedded in tissue freezing medium (TFM) for at least 4 hours at room temperature. Embryos were cross-sectioned on the cryostat (Cryostar NX70 microtome (Thermo Scientific) into 20μm sections and mounted onto triple coated gelatin slides.

2.17. Slide Imaging

Sectioned zebra finch embryos were imaged using the Olympus BX60 scope and QCapture Pro 7, and Amscope software. Both DAPI and RGB images were taken of the embryonic neural region for later cell counting purposes. All RGB images taken with QCapture were taken at 7.178msec exposure, with 2560 X 1920 (FF, Bin 1) resolution, at a bit depth of 24-bit color. DAPI exposure depended on strength of DAPI fluorescence. Due to QCapture camera breakage, Amscope software and camera was also used.

2.18. ROI Circling and Total Cell Counts

Regions of interest (ROIs) were used to outline developing neural regions of imaged zebra finch embryo sections. All forebrain, midbrain, hindbrain, and spinal cord regions were selected for on imaged DAPI sections. ROIs were created using Image J software and Saha lab plugins. DAPI ROIs were used to count total cells in neural regions. Cell counting was also done using Image J software and Saha lab plugins and relied on DAPI ROIs to define which areas to count. All cell counts were done using the same parameters to detect cells: 5 pixels for width, 2.5 pixels for minimum distance, and threshold was 0.3. As the cell counting process was automated, manual counts were done of select images representing

each respective neural region in order to test for the accuracy of automated counts. Manual counts were done using the ITCN plugin on Image J.

2.19. PCNA-DAPI overlay creation and PCNA cell counts

In order to count labeled PCNA cells, DAPI and PCNA images had to be combined into one single image. PCNA-DAPI overlay images were created using Image J software by using the threshold tool to highlight only PCNA labeled regions of interest. RGB images were converted to 8-bit and regions of PCNA expression were defined with a threshold value. The threshold used to label PCNA expression was determined by using sense embryo images to find a value too low to highlight background but was high enough to pick up PCNA signal in antisense embryo images. DAPI images were combined with converted RGB images, resulting in a PCNA-DAPI overlay image that only showed cells in areas of PCNA expression. Cell counting PCNA-DAPI overlay images was done using Image J software and Saha lab plugins and relied on DAPI ROIs to define which areas to count. All cell counts were done using the same parameters to detect cells: 5 pixels for width, 2.5 pixels for minimum distance, and threshold was 0.3. As the cell counting process was automated, manual counts were done of select images in order to test for the accuracy of automated counts. Manual counts were done using the ITCN plugin on Image J.

2.20. TUNEL cell counts

In order to count TUNEL positive apoptotic cells, cell counting was done using Image J software and Saha lab plugins and relied on DAPI ROIs to define which areas to count. All cell counts were done using the same parameters to detect TUNEL positive cells:

6 pixels for width, 3 pixels for minimum distance, and threshold was 5. The program was told to detect dark peaks on RGB image files. As the cell counting process was automated, manual counts were done of select images representing each respective neural region in order to test for the accuracy of automated counts. Manual counts were done using the ITCN plugin on Image J.

2.21. Data organization

PCNA and TUNEL cell counts were used to determine the respective number of proliferating or apoptotic cells in developing neural regions and DAPI cell counts were used to determine the total number of cells in developing neural regions for each zebra finch embryo. All cell counts were organized by neural region (forebrain, midbrain, hindbrain, spinal cord) in order to determine the total number of cells as well as proliferating cells and to compare cell count data for MeHg exposed embryos to control embryos. Hindbrain was defined as the region anterior to the midbrain in imaged sections, and both hindbrain and midbrain regions ended at the beginning of the eye. The forebrain was defined as the neural region from the beginning to end of the eye. The spinal cord region was defined as the beginning of the eye when the hindbrain ended.

2.22. Statistical analysis

Statistics and all graphs were performed in Microsoft Excel 2010 using the Analysis ToolPak and Solver Add-in. For both PCNA and TUNEL data, average counts and percentages were obtained per embryo for each respective neural region. For comparisons

between two populations of data (control embryos and 2.4ppm exposed embryos) a two tailed, unpaired Student's t-test was used.

2.23. Blood and feather collection for Hg concentration analysis

The blood, tail and neck feathers, of all control and 2.4ppm paternal adult pairs were collected to determine blood and feather mercury concentration. Adult birds were bled by pricking the brachial vein with a 30-gauge needle (Becton-Dickenson, Franklin Lakes, NJ) and collecting 15-40µL of blood was collected from each adult bird in a 75µL heparinized capillary tube(Fisher Scientific, Pittsburgh, PA). Capillary tubes were capped with critocaps (Oxford Labware, St. Louis, MO) and put in 10mL vacutainers (Becton-Dickinson, Franklin Lakes, NJ) to protect them from breaking. Blood samples were frozen at -20^{o}C until later analysis using a Direct Mercury Analyzer-80 (DMA, Milestone, Shelton CT). Feathers were collected by plucking approximately 9 feathers (taken from the breast and nape regions) and stored at RT until later analysis using the DMA-80.

2.24. Embryo and egg component collection for Hg distribution analysis

To measure Hg distribution, eggs were dissected at stage 25 (day 4 ¾), stage 32 (day 6 ¾), and stage 38 (day 8 ½). For each developmental stage the eggshell and embryo were separated by placing each component in its own respective 1.5mL eppendorf. For each stage, the yolk and albumin were pooled together and placed in a separate 1.5mL eppendorf. For each developmental stage, to analyze whole egg Hg concentration, a whole egg was dissected (to check for the proper developmental stage) and put entirely in a 1.5mL eppendorf. Wet weight was recorded for every sample. All samples were kept at

-20^{o}C until taken to the Keck lab for lyophilization. After lyophilization, samples were homogenized before being run on the DMA-80.

2.25. Blood, feather, and embryo Hg concentration analysis

All blood samples were analyzed on a wet weight basis, feather and embryo samples on a dry weight basis, by atomic absorption spectroscopy on the DMA-80. Before running samples, the DMA-80 was calibrated by running beginning standards of three blanks, two empty boat (sample) containers, then by using standard reference materials (two DORM-4 samples then two DOLT-4 samples), and two blanks. Standard reference materials were kept within 7.5-10% of the manufactured provided values. After 20 samples were run, end standards were run. End standards were two blanks, one empty boat, the standard reference materials, then two blanks. With every 20 samples, duplicates of the same sample were run to check for quality control.

3. Results

3.1. Results overview

The project determined how developmental exposure to low levels of MeHg affected proliferation and apoptosis in stage 25 zebra finch embryos and observed a trend for MeHg toxicokinetics during zebra finch embryonic development. A number of detailed experiments were used to determine the effects of MeHg on zebra finch embryonic development. We performed ISH to mark PCNA expression and after processing embryos and determining neural cell counts, we found a significant decrease in midbrain proliferation for treatment embryos. To label apoptotic cells we used the TUNEL assay and analyzed zebra finch embryos to determine cell counts. We found no significant difference in apoptosis between control and treatment embryos. Using the DMA-80 to measure mercury content in eggshell, combined yolk and albumin, and embryo across different developmental stages we observed a trend for mercury accumulation to increase in embryonic tissue as development progressed.

3.2. PCNA expression in stage 25 embryos during development

3.2.1. Whole mount ISH PCNA expression

Whole mount *in situ* hybridization (ISH) for PCNA was performed on a stage 25 (day 4 ¾) embryos for both control and 2.4ppm groups to measure proliferation. A total of two ISH runs were performed, with two embryos in each treatment group per run for an n of four embryos in each treatment group. **Figure 1** displays whole mount ISH examples for antisense (**a** and **b**) and sense probe (**c**) of PCNA for stage 25 embryo. The lower right-

hand column (**d**) is a stage 25 embryo from the Murray et al., 2013 zebra finch staging guide[61] which shows the common accepted form of the embryo. The upper right-hand panel (**c**) in **Figure 1** displays an embryo after incubating with the sense PCNA probe. The sense PCNA probe is the complementary RNA sequence to the antisense PCNA probe, meaning that it has the same sequence as the mRNA for PCNA. The sense embryo image shows a clear expression lack of background. Background from non-specific binding of probe, or when the reagents used for color production are not completely washed away during the ISH run. The left-hand column in **Figure 1** shows what stage 25 embryos appeared after incubating with the antisense PCNA probe from a whole mount ISH for a stage 25 embryo for both a control and 2.4ppm exposed embryo. The visible purple color indicates a positive result for PCNA mRNA. Due to massive amounts of proliferation (PCNA expression) no qualitative difference could be observed between the control and 2.4ppm whole mount embryos.

Figure 1. Example whole mount ISH expression of PCNA

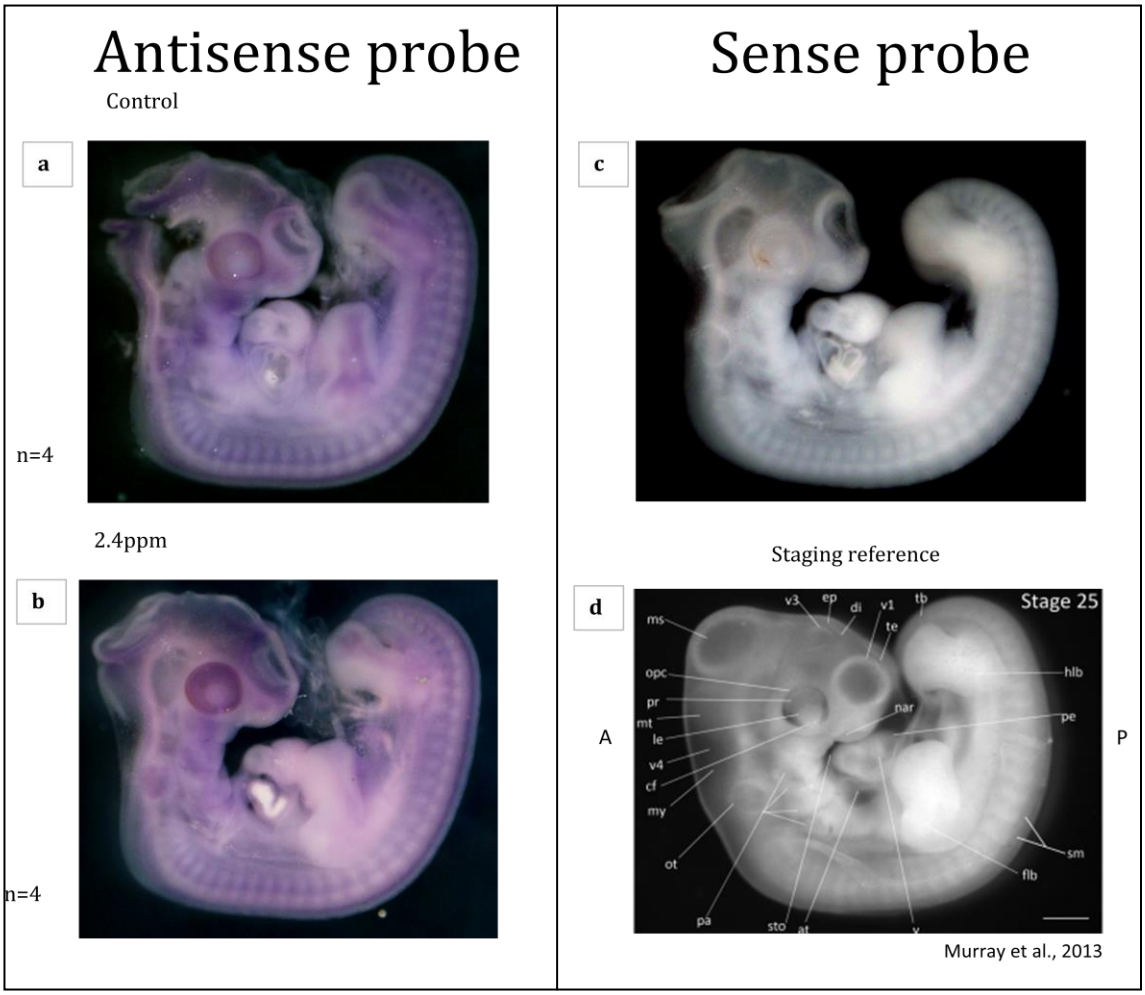

Figure 1: Left hand panel (**a**) displays a control stage 25 embryo incubated with antisense PCNA probe. Left hand panel (b) displays a treatment 2.4ppm stage 25 embryo incubated with antisense PCNA probe.

3.2.2. PCNA expression in embryo sections

Cross sectioned whole mount ISH zebra finch embryo images show PCNA signal with a DAPI nuclear stain. Spinal cord, forebrain, midbrain, and hindbrain regions were imaged and cell counts were obtained for each respective neural region. **Figures 2a-h** show how each respective neural region appeared in control and treatment embryo sections after imaging. For each image in **Figures 2a-h**, the left image is the DAPI image and the right image is the red green blue (RGB, color saved file) image to show PCNA expression. As ISH by itself is a qualitative assay, cell counts were obtained to quantify the number of proliferating cells.

Figure 2. (a-h) Expression of PCNA and DAPI staining in cross sectioned embryos

A. Spinal Cord Example Section
i) **Figure 2a.** Control section from: 0.0ppm Embryo 1, ISH run date 140804

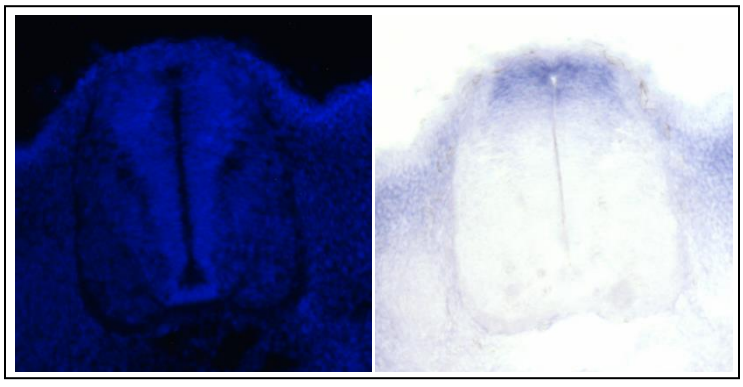

ii) **Figure 2b**. 2.4ppm section from: 2.4ppm Embryo 1, ISH run date 140804

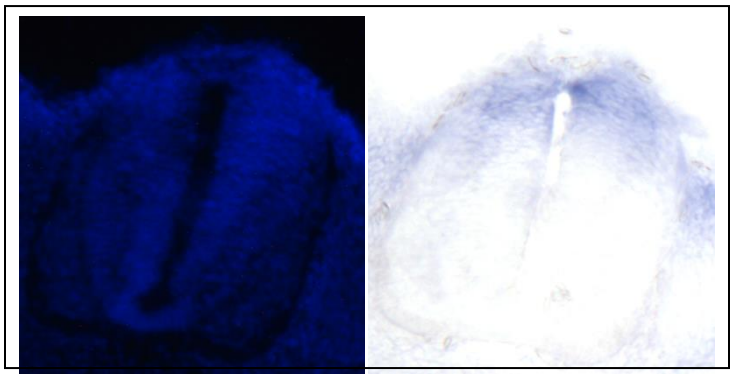

B. Forebrain Example Section

i) **Figure 2c**. Control section from: 0.0ppm Embryo 1, ISH run date 140804

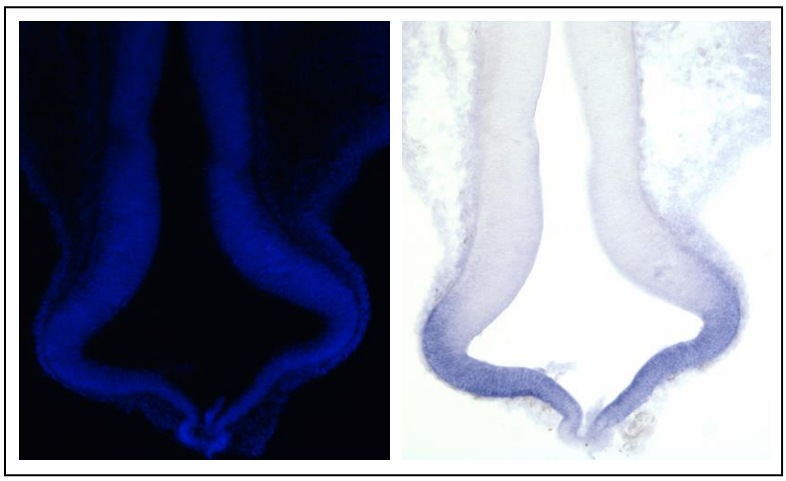

ii) **Figure 2d**. 2.4ppm section from: 2.4ppm Embryo 1, ISH run date 140804

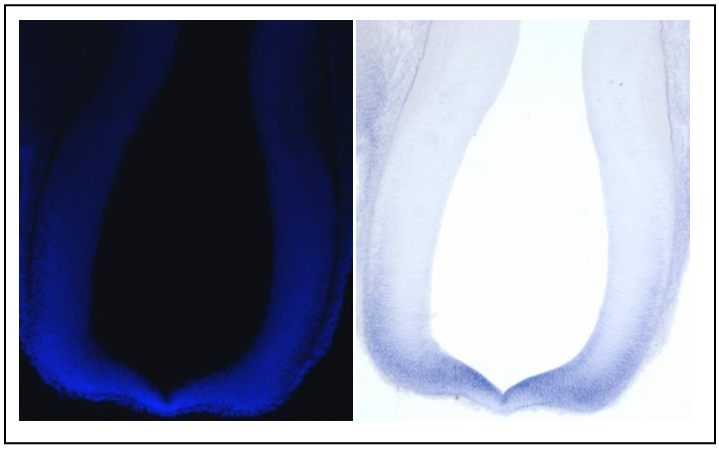

C. Midbrain Example Section

i) **Figure 2e**. Control section from: 0.0ppm Embryo 1, ISH run date 140804

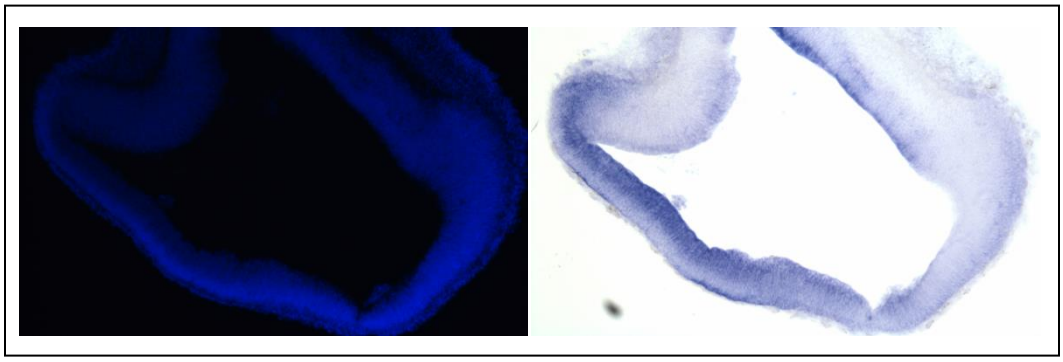

ii) **Figure 2f**. 2.4ppm section from: 2.4ppm Embryo 1, ISH run date 140804

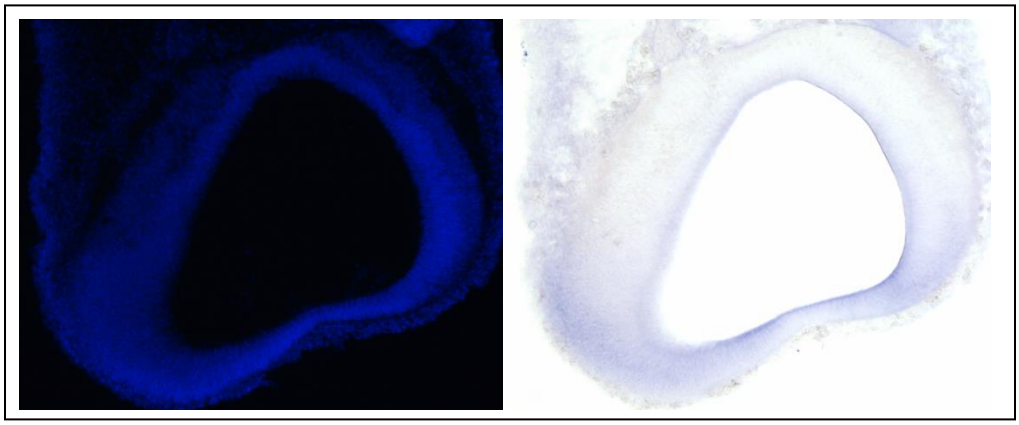

D. Hindbrain Example Section

i) **Figure 2g**. Control section from: 0.0ppm Embryo 1, ISH run date 140804

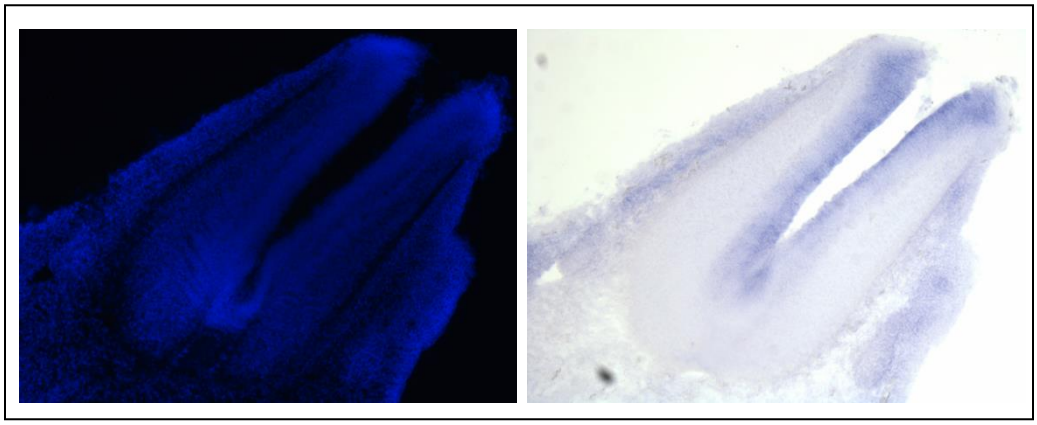

ii) **Figure 2h.** 2.4ppm section from: 2.4ppm Embryo 1, ISH run 140804

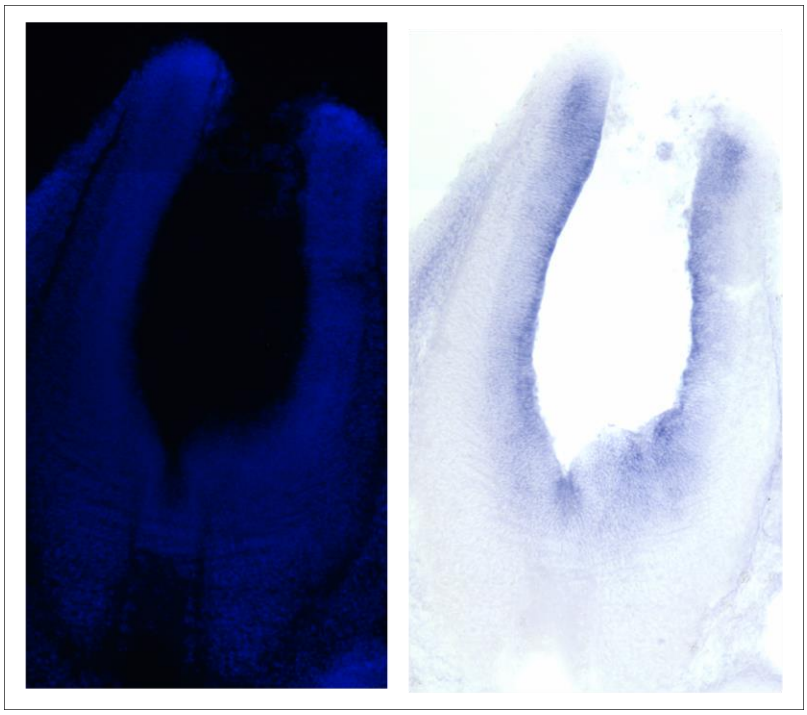

3.2.3. Quantitative Proliferation Data

PCNA cell counts were used to determine the number of proliferating cells in each developing neural region and DAPI cell counts were used to determine the total number of cells in the neural regions. All cell count data was organized by neural region (forebrain, midbrain, hindbrain, spinal cord) in order to determine the total number of cells and proliferating cells, and to compare cell count data for MeHg exposed embryos to control embryos. The average number of overall cells and proliferating cells was calculated for each respective neural region (spinal cord, forebrain, midbrain, and hindbrain) and then the percent proliferation (proliferating cells divided by total cell number) was obtained for each neural region in each control **(Figure 4 (a-d), Tables 2-5)** and treatment **(Figure 5 (a-d), Tables 6-9)** embryo. **Figure 4 (a-d), Tables 2-5** and **Figure 5 (a-d), Tables 6-9** were included to show the levels of individual variation for total cell number and proliferating cell number in each neural region for control and treatment embryos respectively. As seen in the figures and table values, appeared to be relatively large amounts of individual variation for all embryos. The large amount of individual variation observed may be from normal differences in development. Overall, a significant decrease in proliferation was found in the midbrain of treatment embryos which supported our prediction that MeHg would decrease proliferation. The results can be seen in **Figure 3** and **Table 1**.

Figure 3a. Average percent proliferation in each neural region

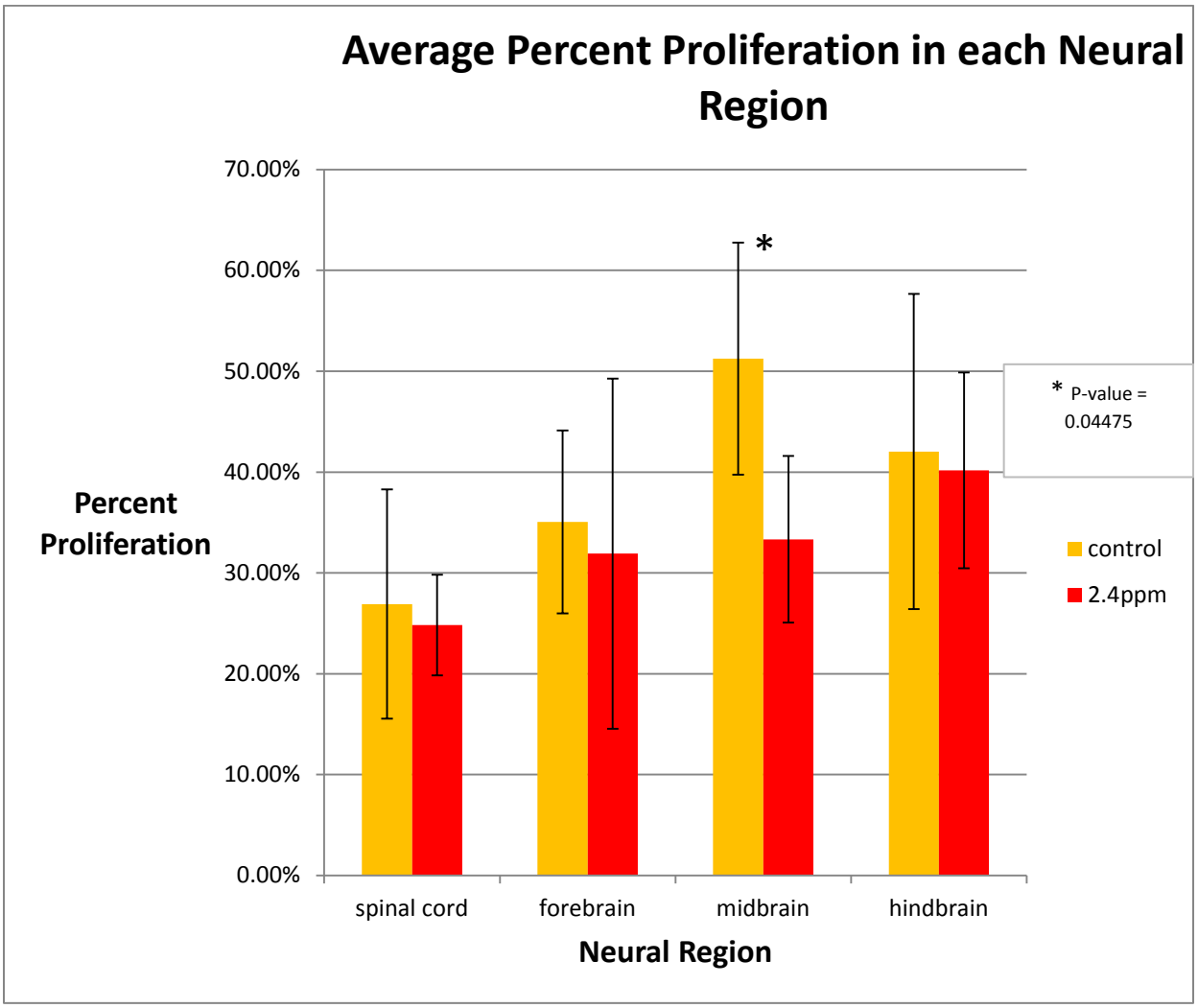

Table 1a. Average percent proliferation in each neural region corresponding to Figure 3

Stage, Embryo #, Treatment, ISH run	% SPC	% Forebrain	% Midbrain	% Hindbrain
st 25, E1, 0.0ppm, 140630	34.77%	39.76%	47%	58.33%
st 25, E2, 0.0ppm, 140630	38.55%	30.73%	63.73%	52.40%
st 25, E1, 0.0ppm, 140804	16.83%	24.75%	56.88%	30.28%
st 25, E2, 0.0ppm,140804	17.48%	45.02%	37.39%	27.13%
st 25, E1, 2.4ppm, 140630	25.19%	24.82%	35.43%	29.94%
st 25, E2, 2.4ppm, 140630	31.20%	56.84%	40.03%	53.21%
st 25, E1, 2.4ppm, 140804	19.12%	29.08%	36.58%	40.08%
st 25, E2, 2.4ppm, 140804	23.82%	16.90%	21.29%	37.46%
T-Test, P-value	0.74947952	0.758313143	0.044752477	0.846233596

The average percent proliferation was determined for both control and treatment embryos for each respective neural region. %SPC, %Forebrain, %Midbrain, and % Hindbrain in **Table 1** all refer to the average percent proliferation found in that respective neural area. There was no significant difference (meaning p value <0.05 determined using a two tailed, unpaired Student's t-test) in the percent of proliferating cells in control and treatment embryos in the spinal cord, forebrain, or hindbrain, with the exception of the midbrain. A significant decrease in proliferating cells was found in 2.4ppm-exposed embryos with a p value of 0.0447, as seen above. As all other neural regions were strongly statistically insignificant, the significant p-value found for decreased proliferation in the midbrain of MeHg exposed embryos is promising. This significant decrease shows that MeHg inhibits/decreases proliferation in the midbrain of 2.4ppm stage 25 embryos during neural development.

Figure 4 (a-d) Average count data for control embryos

Figure 4a. Control Spinal Cord Average Counts

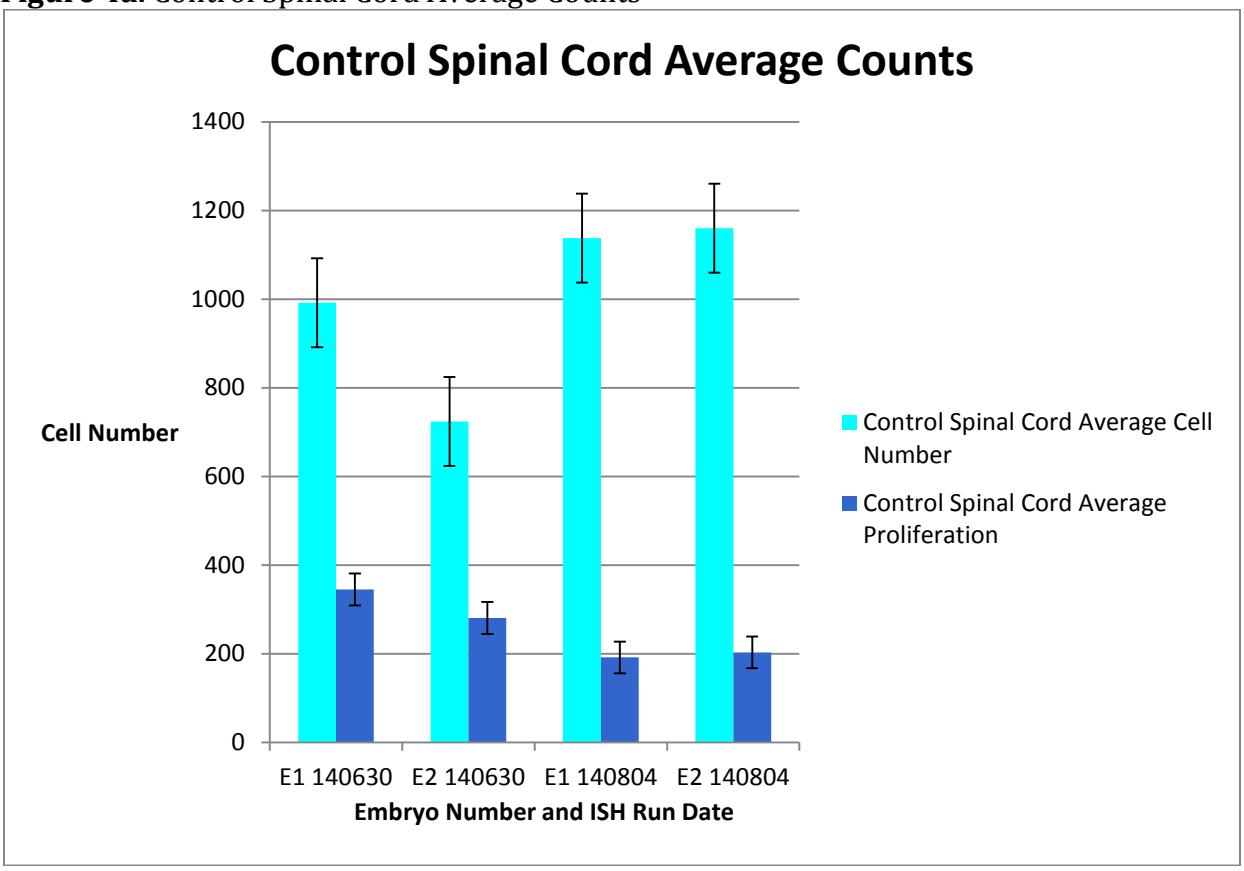

Table 2. Average counts in each neural region corresponding to Figure 4a

Stage, Embryo #, Treatment, ISH run	Avg Count Spinal Cord	Avg PCNA SPC	% SPC
st 25, E1, 0.0ppm, 140630	991.5698925	344.7956989	34.77%
st 25, E2, 0.0ppm, 140630	723.7777778	280.5777778	38.55%
st 25, E1, 0.0ppm, 140804	1137.335938	191.4453125	16.83%
st 25, E2, 0.0ppm,140804	1159.967213	202.8442623	17.48%
AVERAGE	1003.162705	254.9157629	26.91%
STDEV	200.6493134	71.8259033	0.1136956

Average cell counts (for number of neural cells and number of proliferating cells in the spinal cord) were obtained for each control embryo. '%SPC' in **Table 2** refers to the percentage of average number of proliferating cells divided by the average number of total cells in the spinal cord. The average number of total cells in the spinal cord (for all control embryos) was 1003.16 with a standard deviation of 200.65. The average number of

proliferating cells in the spinal cord was 254.92 with a standard deviation of 71.83. The average percent of proliferating cells in the spinal cord came out to be 26.91% with a standard deviation of 0.11. The standard error was 100.33 for average spinal cord cell counts and 35.92 for proliferation cell counts. Embryo number 2 from 140630 ISH run date had a much lower average cell count in the spinal cord compared to the other embryos. This embryo may have been a younger stage 25 compared to the other control embryos.

Figure 4b. Control Forebrain Average Counts

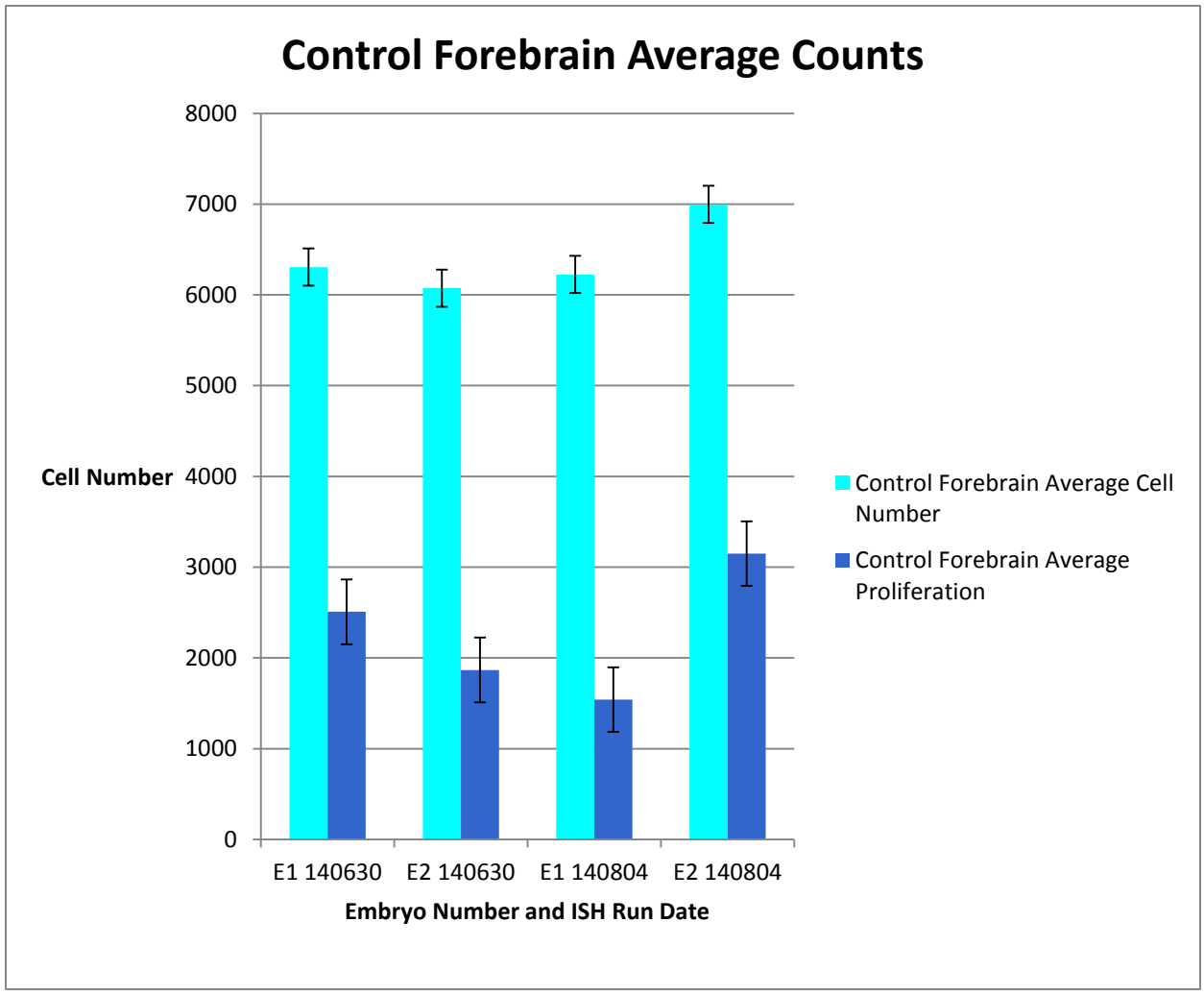

Table 3. Average counts in each neural region corresponding to Figure 4b

Stage, Embryo #, Treatment, ISH run	Avg Count Forebrain	Avg PCNA Forebrain	%Forebrain
st 25, E1, 0.0ppm, 140630	6307	2507.8	39.76%
st 25, E2, 0.0ppm, 140630	6074.541667	1866.583333	30.73%
st 25, E1, 0.0ppm, 140804	6224.580645	1541.032258	24.75%
st 25, E2, 0.0ppm,140804	6997.138889	3149.777778	45.02%
AVERAGE	6400.8153	2266.298342	35.07%
STDEV	409.0298565	712.8912832	0.090615764

Average cell counts (for number of neural cells and number of proliferating cells in the forebrain) were obtained for each control embryo. '%Forebrain' in **Table 3** refers to

the percentage of average number of proliferating cells divided by the average number of total cells in the forebrain. The average number of total cells in the forebrain (for all control embryos) was 6400.8153 with a standard deviation of 409.03. The average number of proliferating cells in the forebrain was 2266.30 with a standard deviation of 712.89. The average percent of proliferating cells in the forebrain came out to be 35.07% with a standard deviation of 0.091. The standard error was 204.52 for average forebrain cell counts and 356.45 for proliferation cell counts.

Figure 4c. Control Midbrain Average Counts

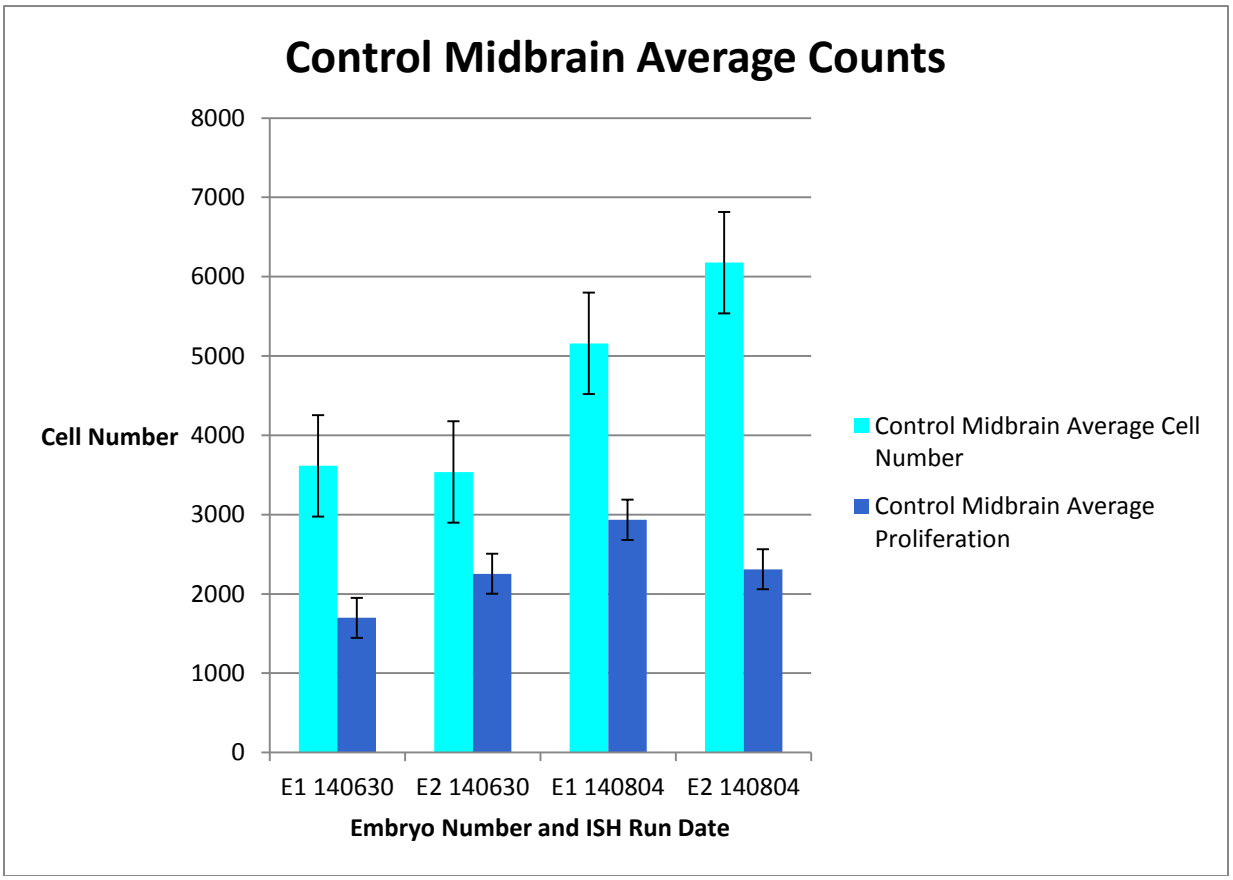

Table 4. Average counts in each neural region corresponding to Figure 4c

Stage, Embryo #, Treatment, ISH run	Avg Count Midbrain	Avg PCNA Midbrain	%Midbrain
st 25, E1, 0.0ppm, 140630	3614.695652	1698.869565	47%
st 25, E2, 0.0ppm, 140630	3537.807692	2254.461538	63.73%
st 25, E1, 0.0ppm, 140804	5159.35	2934.8	56.88%
st 25, E2, 0.0ppm,140804	6177.347826	2310.043478	37.39%
AVERAGE	4622.300293	2299.543645	51%
STDEV	1277.756697	505.4709453	0.115124483

Average cell counts (for number of neural cells and number of proliferating cells in the midbrain) were obtained for each control embryo. '%Midbrain' in **Table 4** refers to the percentage of average number of proliferating cells divided by the average number of total cells in the midbrain. The average number of total cells in the midbrain (for all control embryos) was 4622.30 with a standard deviation of 1277.76. The average number of

proliferating cells in the midbrain was 2299.54 with a standard deviation of 505.47. The average percent of proliferating cells in the midbrain came out to be 51% with a standard deviation of 0.115. The standard error was 638.88 for average midbrain cell counts and 252.74 for proliferation cell counts.

Figure 4d. Control Hindbrain Average Counts

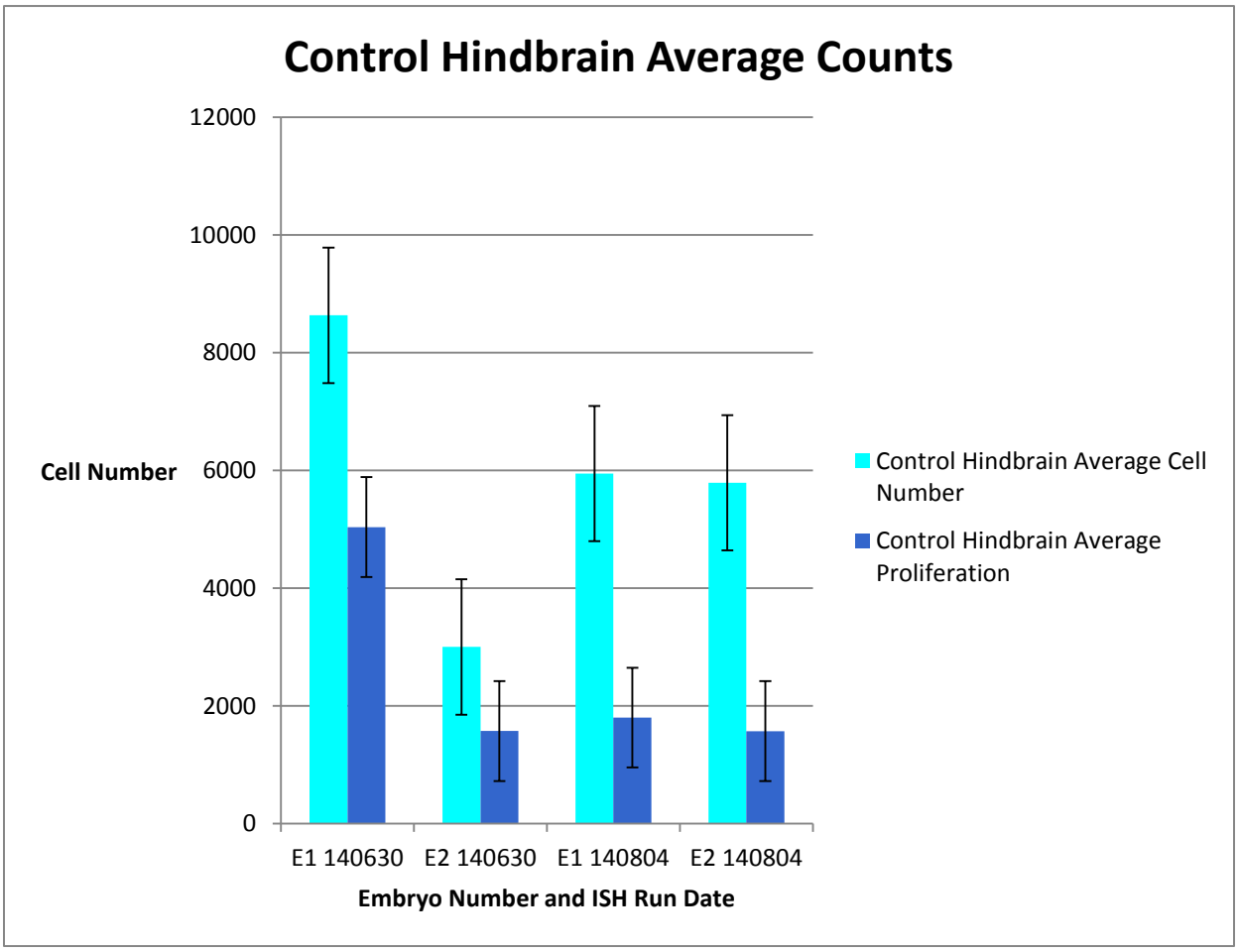

Table 5. Average counts in each neural region corresponding to Figure 4d

Stage, Embryo #, Treatment, ISH run	Avg Count Hindbrain	Avg PCNA Hindbrain	%Hindbrain
st 25, E1, 0.0ppm, 140630	8632.461538	5035.384615	58.33%
st 25, E2, 0.0ppm, 140630	3001.444444	1572.888889	52.40%
st 25, E1, 0.0ppm, 140804	5944.652174	1800.086957	30.28%
st 25, E2, 0.0ppm,140804	5788.166667	1570.933333	27.13%
AVERAGE	5841.681206	2494.823449	42.04%
STDEV	2299.917865	1697.119728	0.156343564

Average cell counts (for number of neural cells and number of proliferating cells in the hindbrain) were obtained for each control embryo. '%Hindbrain' in **Table 5** refers to the percentage of average number of proliferating cells divided by the average number of

total cells in the midbrain. The average number of total cells in the hindbrain (for all control embryos) was 5841.68 with a standard deviation of 2299.92. The average number of proliferating cells in the hindbrain was 2494.82 with a standard deviation of 1697.12. The average percent of proliferating cells in the hindbrain came out to be 42.04% with a standard deviation of 0.156. The standard error was 1149.96 for average hindbrain cell counts and 848.56 for proliferation cell counts. As in the spinal cord region, embryo number 2 from 140630 ISH run date had a much lower average cell count in the spinal cord compared to the other embryos. This embryo may have been a younger stage 25 compared to the other control embryos.

Figure 5. (a-d) Average count data for 2.4ppm embryos

Figure 5a. 2.4ppm Spinal Cord Average Counts

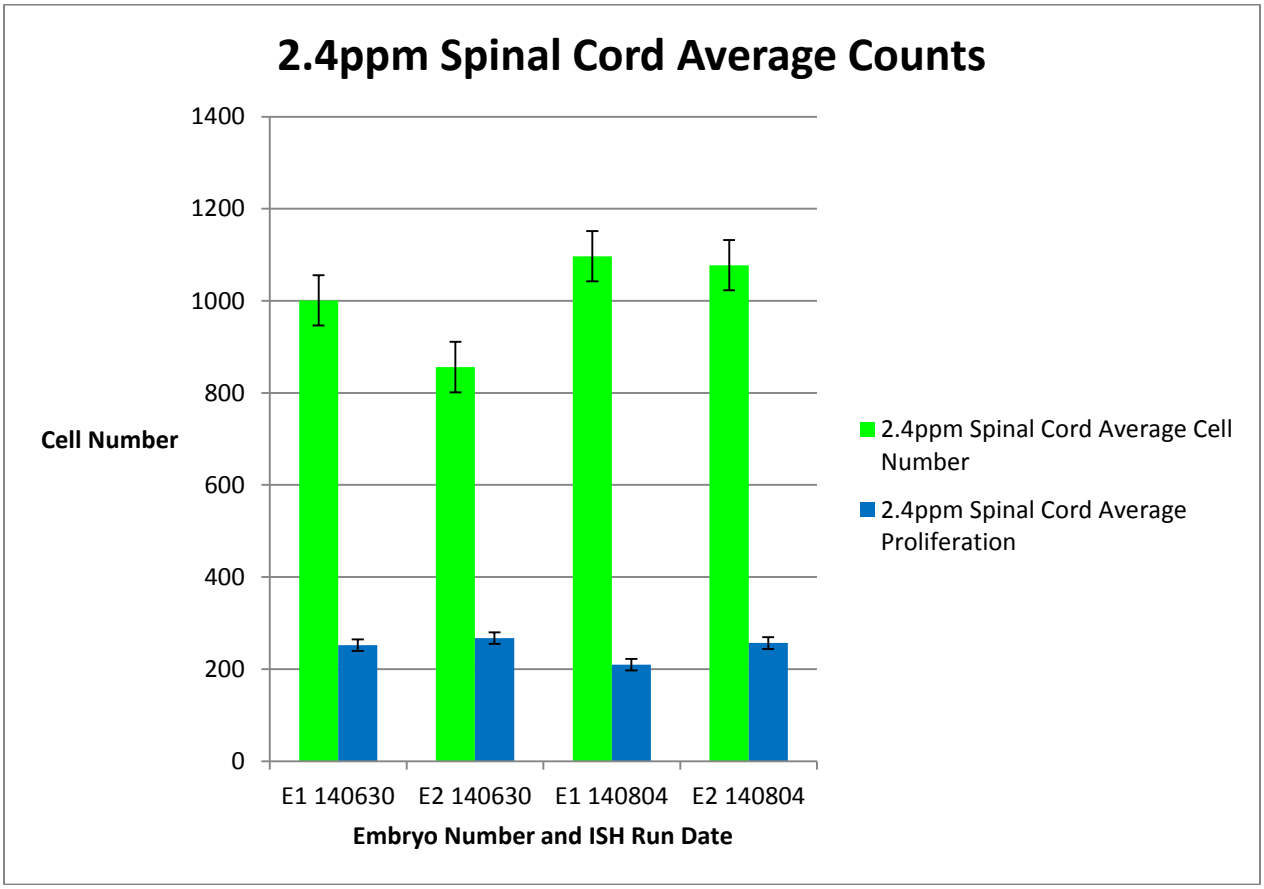

Table 6. Average counts in each neural region corresponding to Figure 5a

Stage, Embryo #, Treatment, ISH run	Avg Count Spinal Cord	Avg PCNA SPC	%SPC
st 25, E1, 2.4ppm, 140630	1000.956044	252.1648352	25.19%
st 25, E2, 2.4ppm, 140630	856.1081081	267.0720721	31.20%
st 25, E1, 2.4ppm, 140804	1096.95	209.75	19.12%
st 25, E2, 2.4ppm, 140804	1077.333333	256.6285714	23.82%
AVERAGE	1007.836871	246.4038697	24.83%
STDEV	109.3006119	25.22177632	0.049776392

Average cell counts (for number of neural cells and number of proliferating cells in the spinal cord) were obtained for each 2.4ppm exposed embryo. '%SPC' in **Table 6** refers

to the percentage of average number of proliferating cells divided by the average number of total cells in the spinal cord. The average number of total cells in the spinal cord (for all treatment embryos) was 1007.84 with a standard deviation of 109.30. The average number of proliferating cells in the spinal cord was 246.40 with a standard deviation of 25.22. The average percent of proliferating cells in the spinal cord came out to be 24.83% with a standard deviation of 0.050. The standard error was 54.65 for average spinal cord cell counts and 12.61 for proliferation cell counts.

Figure 5b. 2.4ppm Forebrain Average Counts

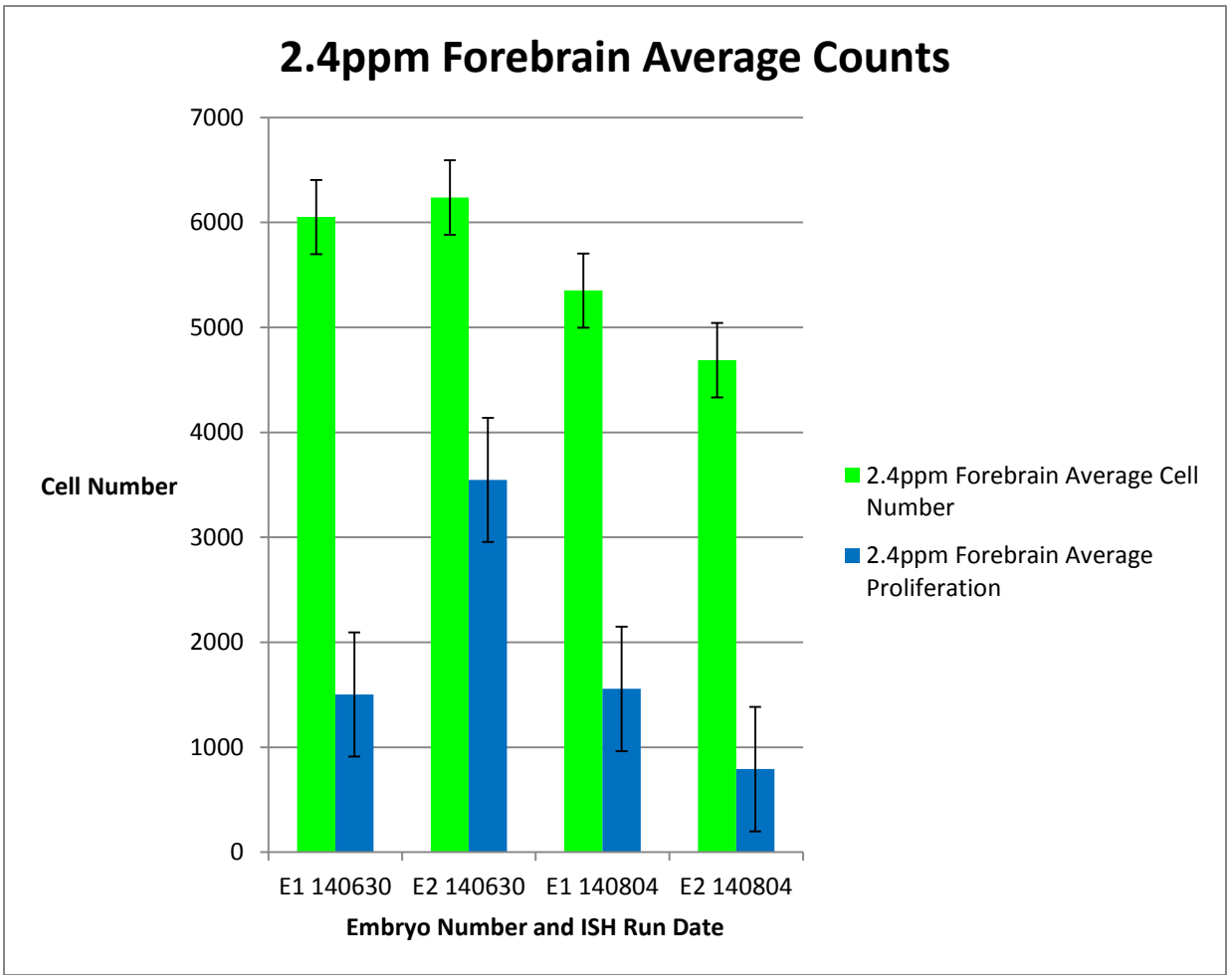

Table 7. Average counts in each neural region corresponding to Figure 5b

Stage, Embryo #, Treatment, ISH run	Avg Count Forebrain	Avg PCNA Forebrain	%Forebrain
st 25, E1, 2.4ppm, 140630	6051.090909	1502.045455	24.82%
st 25, E2, 2.4ppm, 140630	6237.714286	3546.047619	56.84%
st 25, E1, 2.4ppm, 140804	5350.483871	1555.677419	29.08%
st 25, E2, 2.4ppm,140804	4687.382353	791.1764706	16.90%
AVERAGE	5581.667855	1848.736741	31.91%
STDEV	708.0366084	1183.973051	0.173693408

Average cell counts (for number of neural cells and number of proliferating cells in the forebrain) were obtained for each 2.4ppm exposed embryo. '%Forebrain' in **Table 7** refers to the percentage of average number of proliferating cells divided by the average

number of total cells in the forebrain. The average number of total cells in the forebrain (for all treatment embryos) was 5581.67 with a standard deviation of 708.04. The average number of proliferating cells in the forebrain was 1848.74 with a standard deviation of 1183.97. The average percent of proliferating cells in the forebrain came out to be 31.91% with a standard deviation of 0.174. The standard error was 354.02 for average forebrain cell counts and 591.99 for proliferation cell counts.

Figure 5c. 2.4ppm Midbrain Average Counts

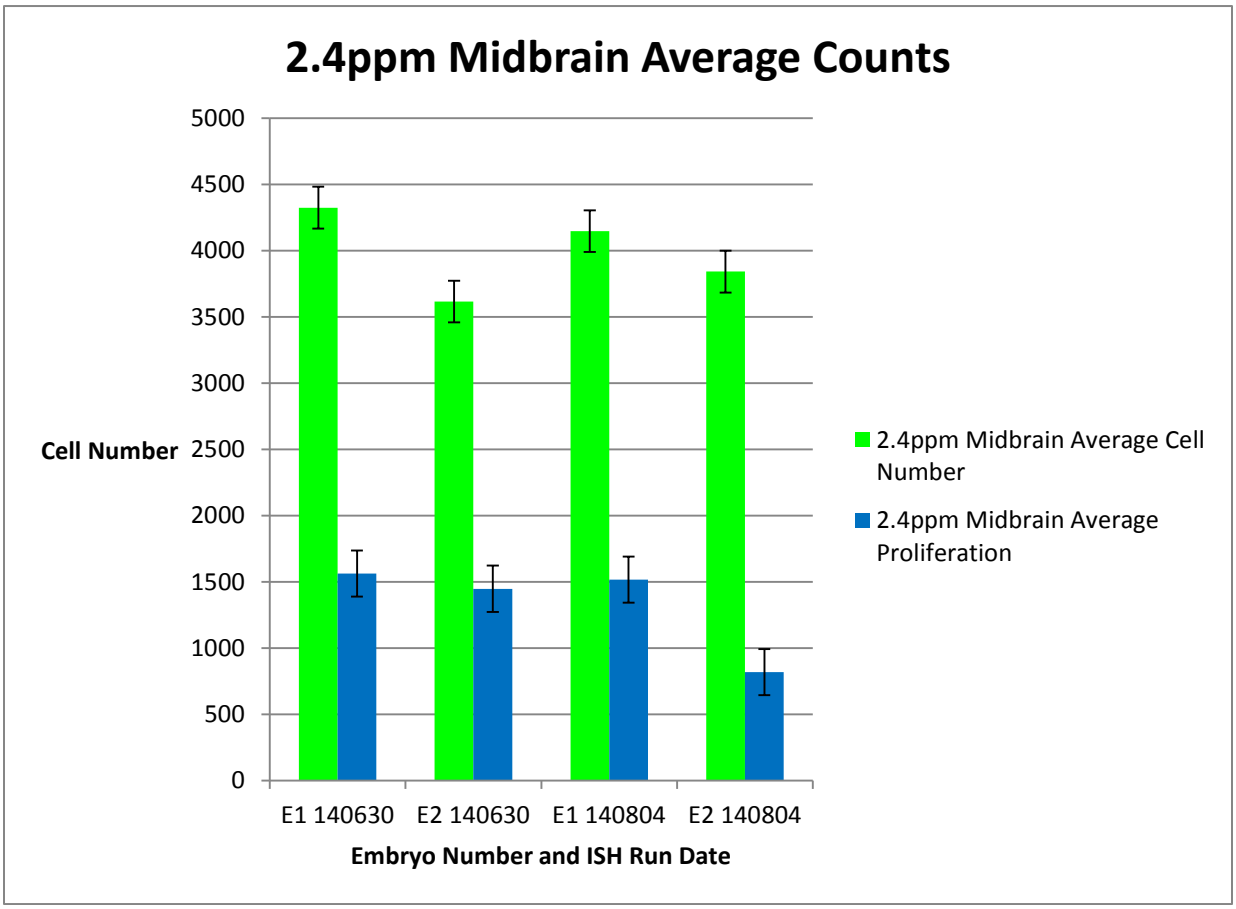

Table 8. Average counts in each neural region corresponding to Figure 5c

Stage, Embryo #, Treatment, ISH run	Avg Count Midbrain	Avg PCNA Midbrain	%Midbrain
st 25, E1, 2.4ppm, 140630	4323.789474	1562.277778	35.43%
st 25, E2, 2.4ppm, 140630	3614.869565	1447.173913	40.03%
st 25, E1, 2.4ppm, 140804	4146.241379	1516.758621	36.58%
st 25, E2, 2.4ppm,140804	3841.15	817.7	21.29%
AVERAGE	3981.512605	1335.977578	33.33%
STDEV	315.3927728	348.7452932	0.082628501

Average cell counts (for number of neural cells and number of proliferating cells in the midbrain) were obtained for each 2.4ppm exposed embryo. '%Midbrain' in **Table 8** refers to the percentage of average number of proliferating cells divided by the average number of total cells in the midbrain. The average number of total cells in the midbrain (for

all treatment embryos) was 3981.51 with a standard deviation of 315.39. The average number of proliferating cells in the midbrain was 1335.98 with a standard deviation of 348.75. The average percent of proliferating cells in the midbrain came out to be 33.33% with a standard deviation of 0.083. The standard error was 157.70 for average midbrain cell counts and 174.38 for proliferation cell counts.

Figure 5d. 2.4ppm Hindbrain Average Counts

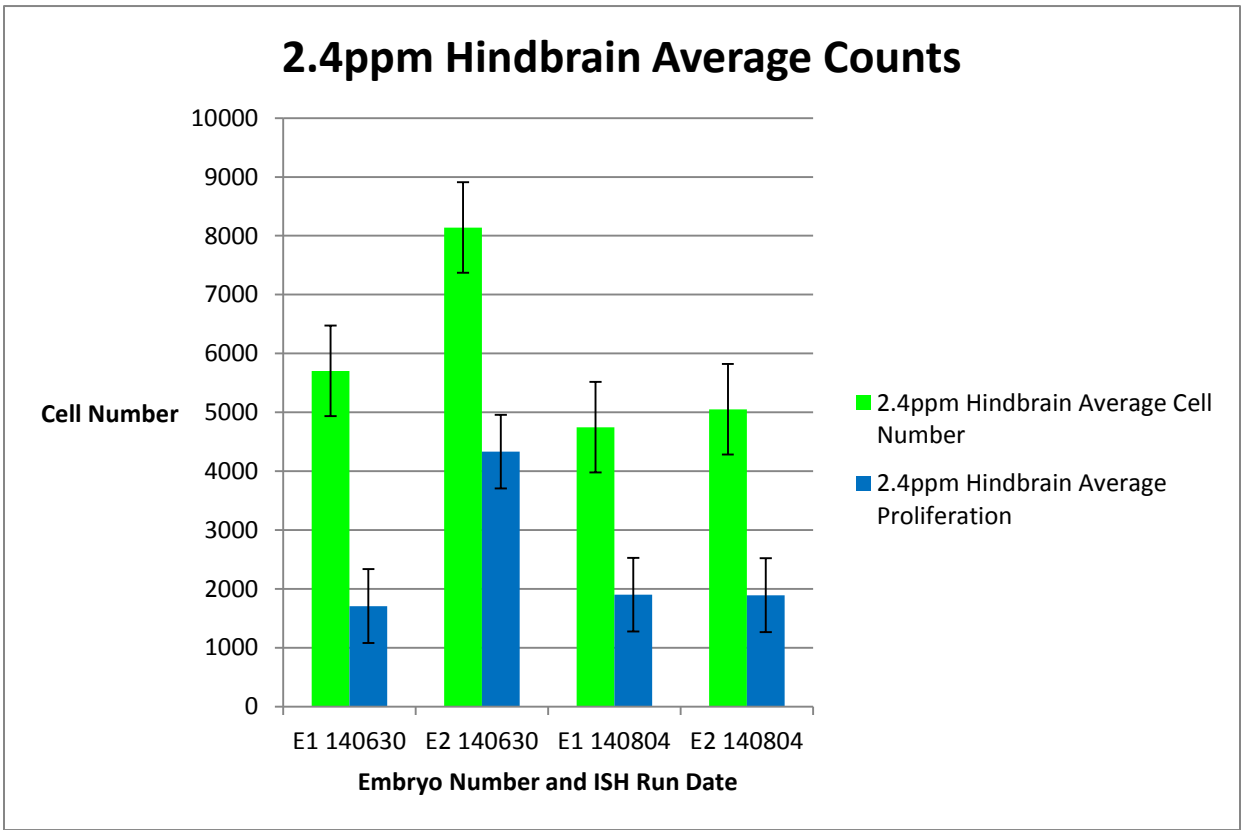

Table 9. Average counts in each neural region corresponding to Figure 5d

Stage, Embryo #, Treatment, ISH run	Avg Count Hindbrain	Avg PCNA Hindbrain	%Hindbrain
st 25, E1, 2.4ppm, 140630	5702.2	1707.466667	29.94%
st 25, E2, 2.4ppm, 140630	8139.923077	4331.461538	53.21%
st 25, E1, 2.4ppm, 140804	4745.482759	1901.758621	40.08%
st 25, E2, 2.4ppm,140804	5052.095238	1892.333333	37.46%
AVERAGE	5909.925268	2458.25504	40.17%
STDEV	1539.246432	1252.003915	0.09696162

Average cell counts (for number of neural cells and number of proliferating cells in the hindbrain) were obtained for each 2.4ppm exposed embryo. '%Midbrain' in **Table 9** refers to the percentage of average number of proliferating cells divided by the average number of total cells in the hindbrain. The average number of total cells in the hindbrain

(for all treatment embryos) was 5909.93 with a standard deviation of 1539.25. The average number of proliferating cells in the hindbrain was 2458.26 with a standard deviation of 1252.00. The average percent of proliferating cells in the hindbrain came out to be 40.17% with a standard deviation of 0.097. The standard error was 769.63 for average hindbrain cell counts and 626.00 for proliferation cell counts.

3.3. TUNEL apoptotic labeling in stage 25 embryos during development

TUNEL (terminal deoxynucleotidyl transferase dUTP nick end labeling) was used in whole mount stage 25 control and 2.4ppm exposed zebra finch embryos to label apoptotic cells. The TUNEL assay detects DNA degradation that occurs in later apoptotic stages and TUNEL positive cells are visualized from the color reaction as entailed in the methods section. A total of three TUNEL runs were performed with an n of four embryos per treatment group. The first run date (150115) had one embryo in each treatment group. The second run date (150125) had one embryo in each treatment group. The final TUNEL run (150225) had two embryos in each treatment group. In whole mounts, it was not possible to see punctate TUNEL apoptotic labeling, therefore embryos were immediately cross sectioned.

3.3.1. TUNEL apoptotic labeling in embryo sections

After performing a TUNEL run to label apoptotic cells, all control and treatment embryos were cross-sectioned on the cryostat and sections were DAPI stained to stain all nuclei. Spinal cord, forebrain, midbrain, and hindbrain regions were imaged for DAPI and TUNEL positive images and cell counts were obtained for each respective neural region. **Figures 6a-h** show how each respective neural region appeared in control and treatment embryo sections after imaging. In **Figures 6 a-h**, the left image is the DAPI image and the right image is the RGB image to see TUNEL positive cells. TUNEL positive cells appear as punctate dark purple/blue regions. Overall cell counts of a neural region were obtained by cell-counting the selected neural region of the DAPI images. In order to count labeled

TUNEL positive cells, the DAPI counter plug in Image J software was used to detect dark peaks. A threshold value defined TUNEL positive cells in order to quantify apoptotic cells. As seen in the figures and table values there were large amounts of individual variation for all embryos. The large amount of individual variation observed may be from normal differences in development. Overall, there was no statistically significant difference in apoptosis between control and treatment embryos and our prediction that MeHg would increase apoptosis in treatment embryos was not supported. However, as apoptosis was only analyzed for stage 25 embryos, there is the potential that MeHg has an impact on apoptotic processes later in embryonic neural development.

Figure 6 (a-h). TUNEL apoptotic labeling and DAPI staining in cross sectioned embryos

Spinal Cord Example Section

i) **Figure 6a**. Control section from: 0.0ppm Embryo 2, TUNEL run 150125

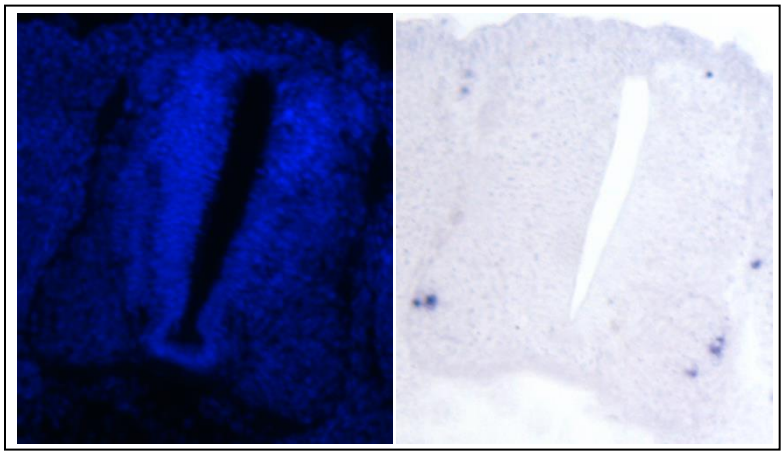

ii) **Figure 6b.** 2.4ppm section from: 2.4ppm Embryo 2, TUNEL run 150125

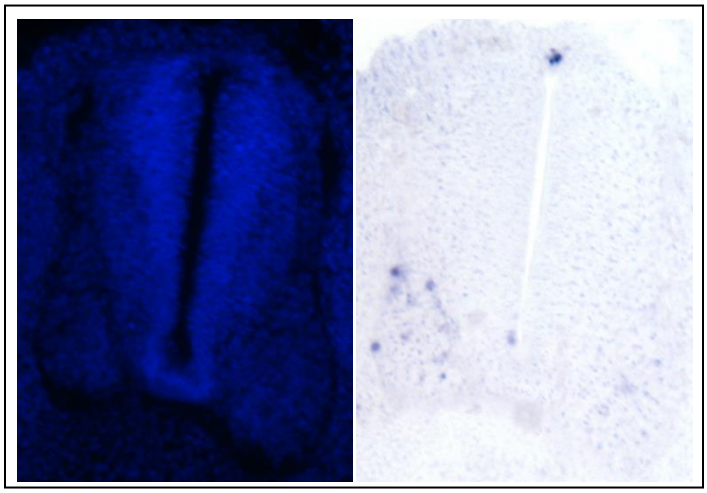

Forebrain Example Section

i) **Figure 6c.** Control section from: 0.0ppm Embryo 2, TUNEL run 150125

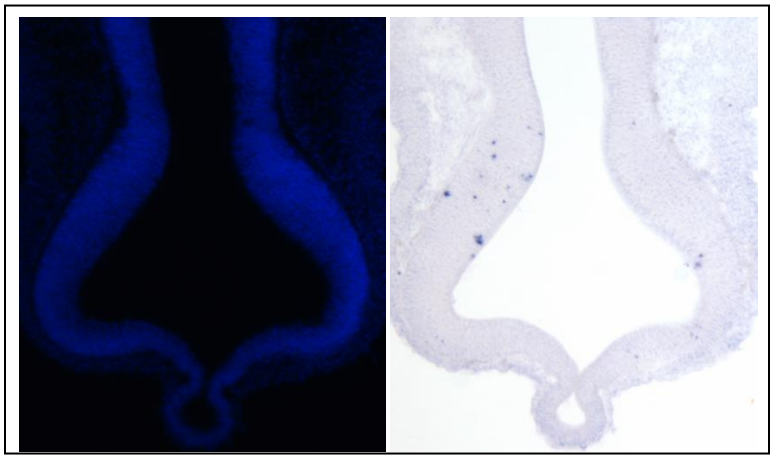

ii) **Figure 6d.** 2.4ppm section from: 2.4ppm Embryo 2, TUNEL run 150125

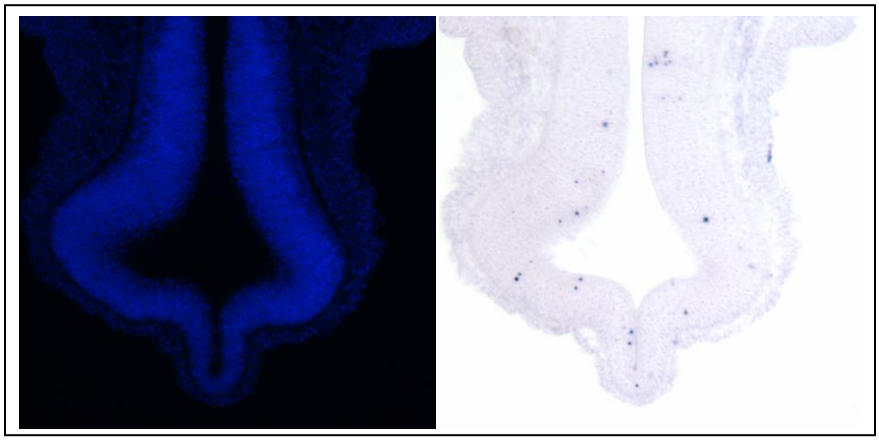

Midbrain Example Section

i) **Figure 6e.** Control section from: 0.0ppm Embryo 2, TUNEL run 150125

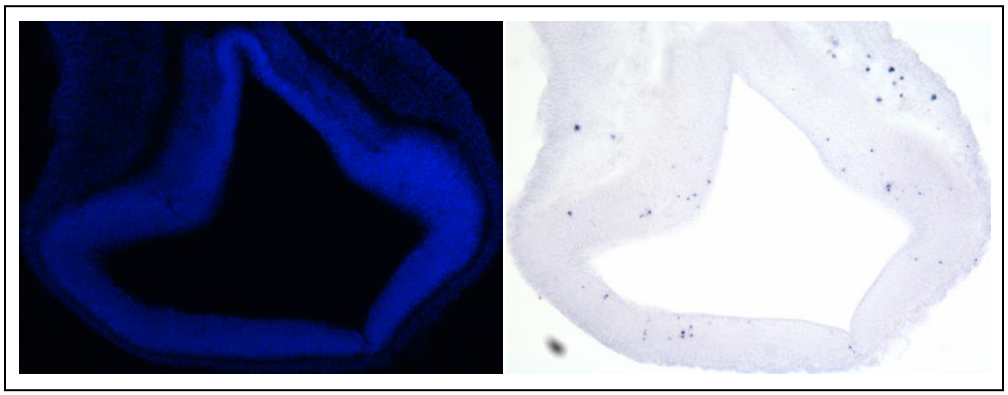

ii)**Figure 6f.** 2.4ppm section from: 2.4ppm Embryo 2, TUNEL run 150125

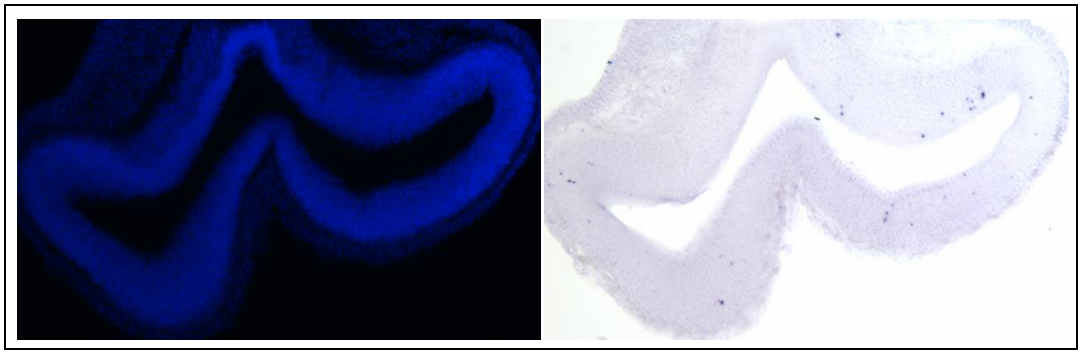

Hindbrain Example Section

i) **Figure 6g.** Control section from: 0.0ppm Embryo 2, TUNEL run 150125

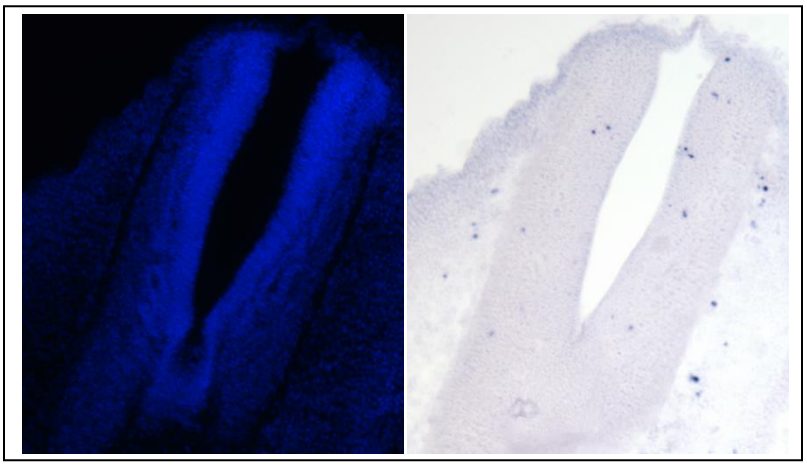

ii) **Figure 6h.** 2.4ppm section from: 2.4ppm Embryo 2, TUNEL run 150125

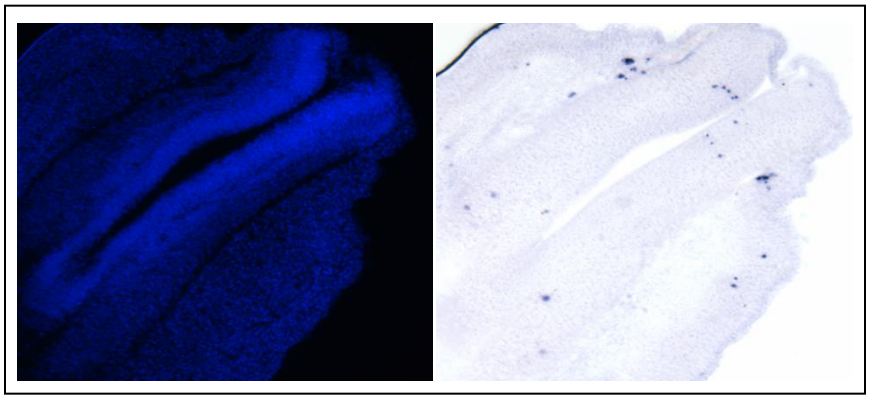

Figure 7a. Average percent apoptosis in each neural region

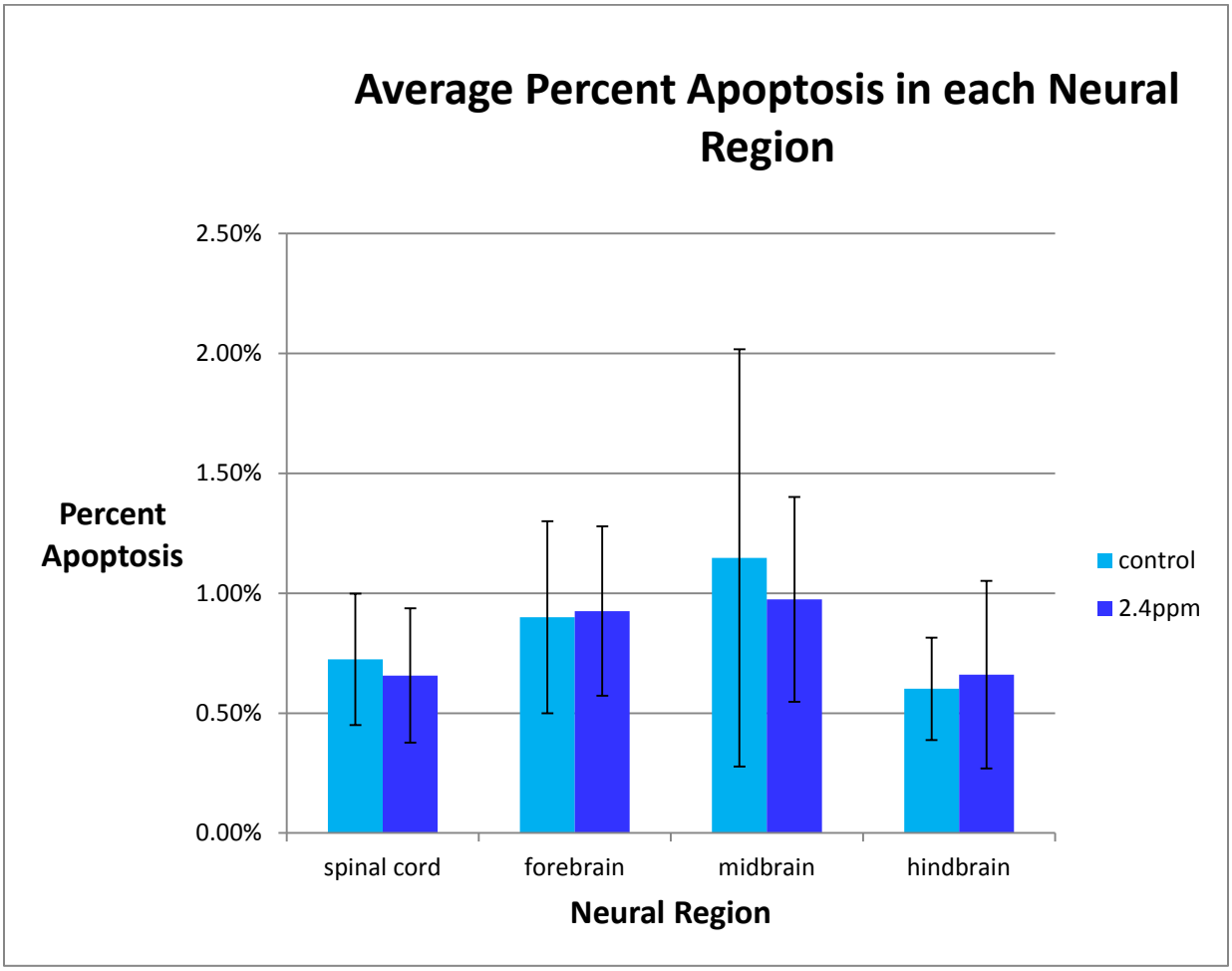

Table 10a. Average percent apoptosis in each neural region corresponding to Figure 7a

Stage, Embryo #, Treatment, TUNEL run	% SPC	% Forebrain	% Midbrain	% Hindbrain
st 25, E1, 0.0ppm, 150115	0.66%	1.45%	2.45%	0.86%
st 25, E2, 0.0ppm, 150125	1.06%	0.91%	0.64%	0.43%
st 25, E1, 0.0ppm, 150225	0.40%	0.52%	0.77%	0.69%
st 25, E2, 0.0ppm,150225	0.78%	0.72%	0.73%	0.42%
st 25, E1, 2.4ppm, 150115	0.45%	0.76%	0.89%	0.59%
st 25, E2, 2.4ppm, 150125	0.93%	0.61%	0.56%	0.37%
st 25, E1, 2.4ppm, 150225	0.87%	1.42%	1.57%	1.23%
st 25, E2, 2.4ppm, 150225	0.39%	0.92%	0.88%	0.45%
T-Test, P-value	0.7429974	0.925577752	0.732844849	0.801754489

The average percent apoptosis (apoptotic cells being TUNEL positive cells) was determined for both control and treatment embryos for each respective neural region.

%SPC, %Forebrain, %Midbrain, and % Hindbrain in **Table 10a** all refer to the average percent apoptosis found in that respective neural area. There was no significant difference (meaning p value <0.05 determined using a two tailed, unpaired Student's t-test) in the percent of apoptotic cells in control and treatment embryos in the spinal cord, forebrain, midbrain, or hindbrain. This lack of significance decrease indicates that MeHg does not affect apoptosis for 2.4ppm stage 25 embryos during neural development.

Figure 8 (a-d). Average count data for control embryos

Figure 8a. Control Spinal Cord Average Counts

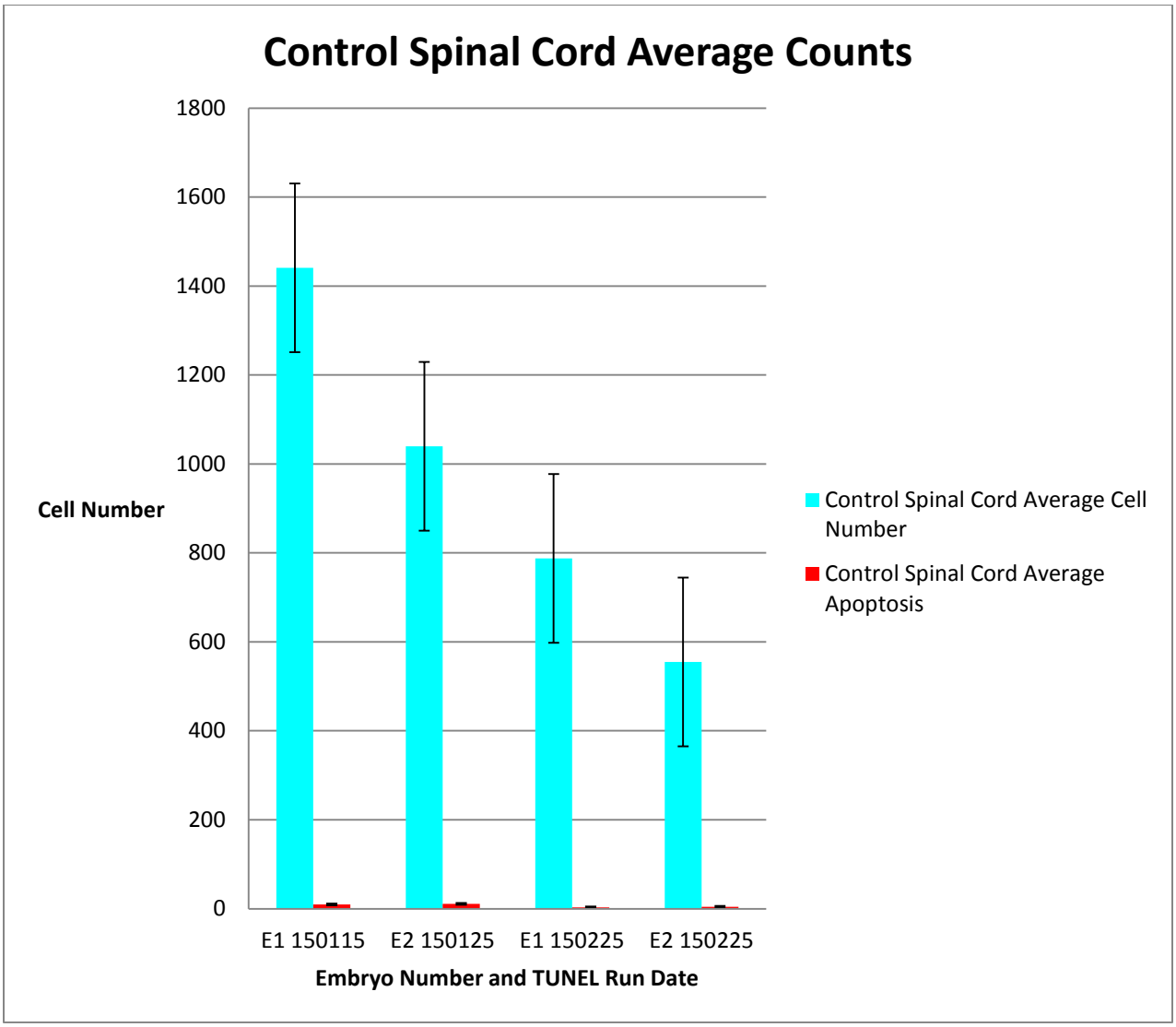

Table 11. Average counts in each neural region corresponding to Figure 8a

Stage, Embryo #, Treatment, TUNEL run	Avg Count Spinal Cord	Avg TUNEL SPC	% SPC
st 25, E1, 0.0ppm, 150115	1440.888889	9.5	0.66%
st 25, E2, 0.0ppm, 150125	1039.676692	11.06015038	1.06%
st 25, E1, 0.0ppm, 150225	787.531746	3.150793651	0.40%
st 25, E2, 0.0ppm,150225	554.8833333	4.308333333	0.78%
AVERAGE	955.745165	7.00481934	0.72%
STDEV	379.2074614	3.864202683	0.002738041

Average cell counts (for number of neural cells and number of TUNEL positive apoptotic cells in the spinal cord) were obtained for each control embryo. '%SPC' in **Table 11** refers to the percentage of average number of apoptotic cells divided by the average number of total cells in the spinal cord. The average number of total cells in the spinal cord (for all control embryos) was 955.75 with a standard deviation of 379.21. The average number of apoptotic cells in the spinal cord was 7.00 with a standard deviation of 3.86. The average percent of apoptotic cells in the spinal cord came out to be 0.72% with a standard deviation of 0.003. The standard error was 189.6 for average spinal cord cell counts and 1.93 for apoptosis counts.

Figure 8b. Control Forebrain Average Counts

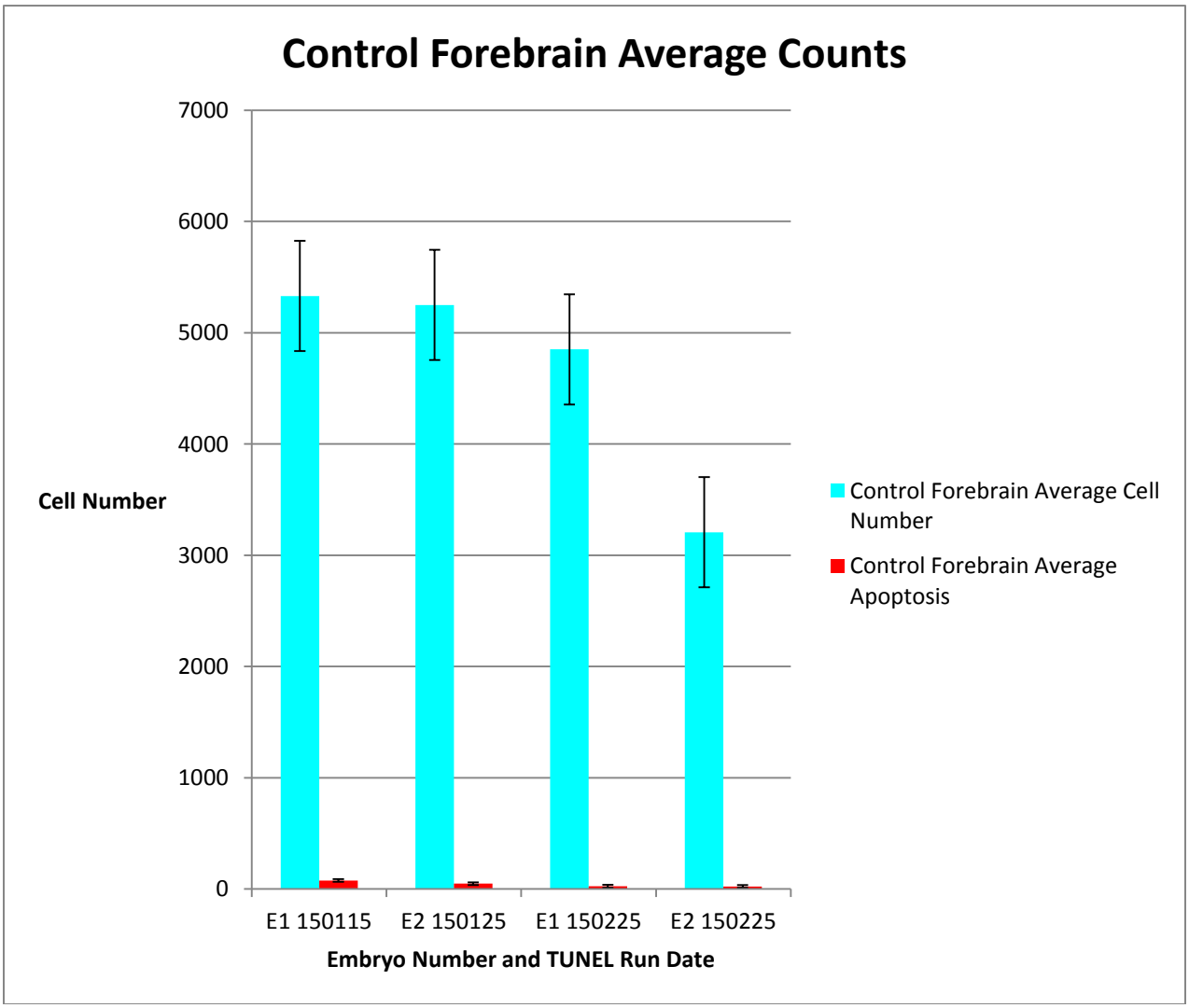

Table 12. Average counts in each neural region corresponding to Figure 8b

Stage, Embryo #, Treatment, TUNEL run	Avg Count Forebrain	Avg TUNEL Forebrain	% Forebrain
st 25, E1, 0.0ppm, 150115	5330.023256	77.09302326	1.45%
st 25, E2, 0.0ppm, 150125	5248.953488	47.79069767	0.91%
st 25, E1, 0.0ppm, 150225	4850.425	25.125	0.52%
st 25, E2, 0.0ppm,150225	3206.681818	23.09090909	0.72%
AVERAGE	4659.020891	43.27490751	0.90%
STDEV	990.6544905	25.17187748	0.004003844

Average cell counts (for number of neural cells and number of TUNEL positive apoptotic cells in the forebrain) were obtained for each control embryo. '%Forebrain' in

Table 12 refers to the percentage of average number of apoptotic cells divided by the average number of total cells in the forebrain. The average number of total cells in the forebrain (for all control embryos) was 4659.02 with a standard deviation of 990.65. The average number of apoptotic cells in the forebrain was 43.27 with a standard deviation of 25.17. The average percent of apoptotic cells in the forebrain came out to be 0.90% with a standard deviation of 0.004. The standard error was 495.33 for average forebrain cell counts and 12.59 for apoptosis cell counts. Embryo one from TUNEL assay run date 150115 may have been an outlier, as that embryo exhibited a great deal more apoptosis. There is the possibility that the embryo would never have fully developed. However, when removed from the group, the percent apoptosis in the forebrain between control and treatment embryos in **Figure 10a** is still statistically insignificant.

Figure 8c. Control Midbrain Average Counts

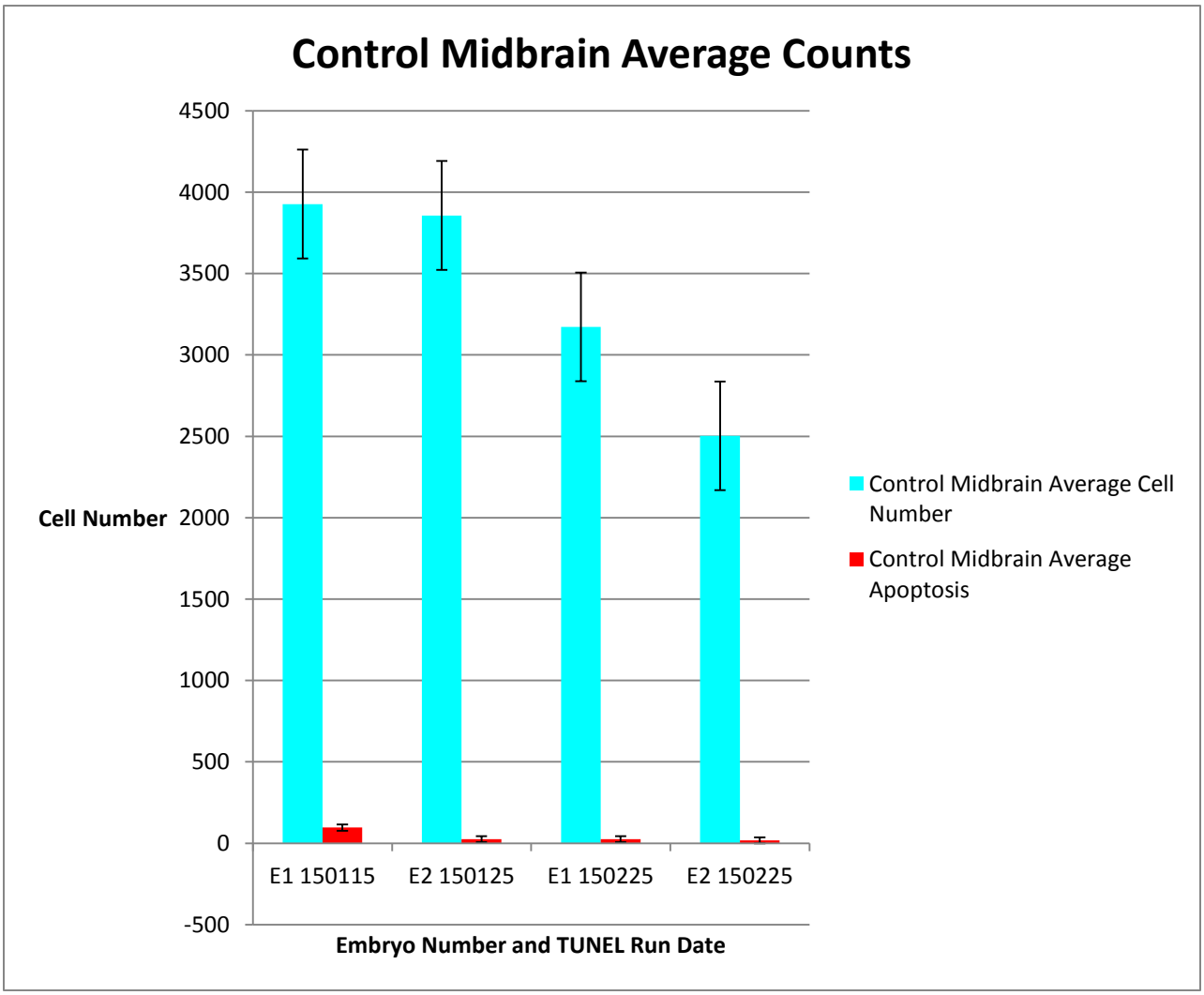

Table 13. Average counts in each neural region corresponding to Figure 8c

Stage, Embryo #, Treatment, TUNEL run	Avg Count Midbrain	Avg TUNEL Midbrain	% Midbrain
st 25, E1, 0.0ppm, 150115	3926.769231	96.17948718	2.45%
st 25, E2, 0.0ppm, 150125	3856.59375	24.71875	0.64%
st 25, E1, 0.0ppm, 150225	3172.5	24.31818182	0.77%
st 25, E2, 0.0ppm,150225	2502.333333	18.33333333	0.73%
AVERAGE	3364.549079	40.88743808	1%
STDEV	667.9566598	36.97686241	0.008697967

Average cell counts (for number of neural cells and number of TUNEL positive apoptotic cells in the midbrain) were obtained for each control embryo. '%Midbrain' in

Table 13 refers to the percentage of average number of apoptotic cells divided by the average number of total cells in the midbrain. The average number of total cells in the midbrain (for all control embryos) was 3364.55 with a standard deviation of 667.96. The average number of apoptotic cells in the midbrain was 40.89 with a standard deviation of 36.98. The average percent of apoptotic cells in the midbrain came out to be 1.00% with a standard deviation of 0.009. The standard error was 333.98 for average midbrain cell counts and 18.49 for apoptosis cell counts. Once again, embryo one from TUNEL assay run date 150115 may have been an outlier, as that embryo exhibited a great deal more apoptosis. If allowed to completely develop, the embryo may have died on its own. However, when removed from the group, the percent apoptosis in the midbrain between control and treatment embryos in **Figure 10a** is still statistically insignificant.

Figure 8d. Control Hindbrain Average Counts

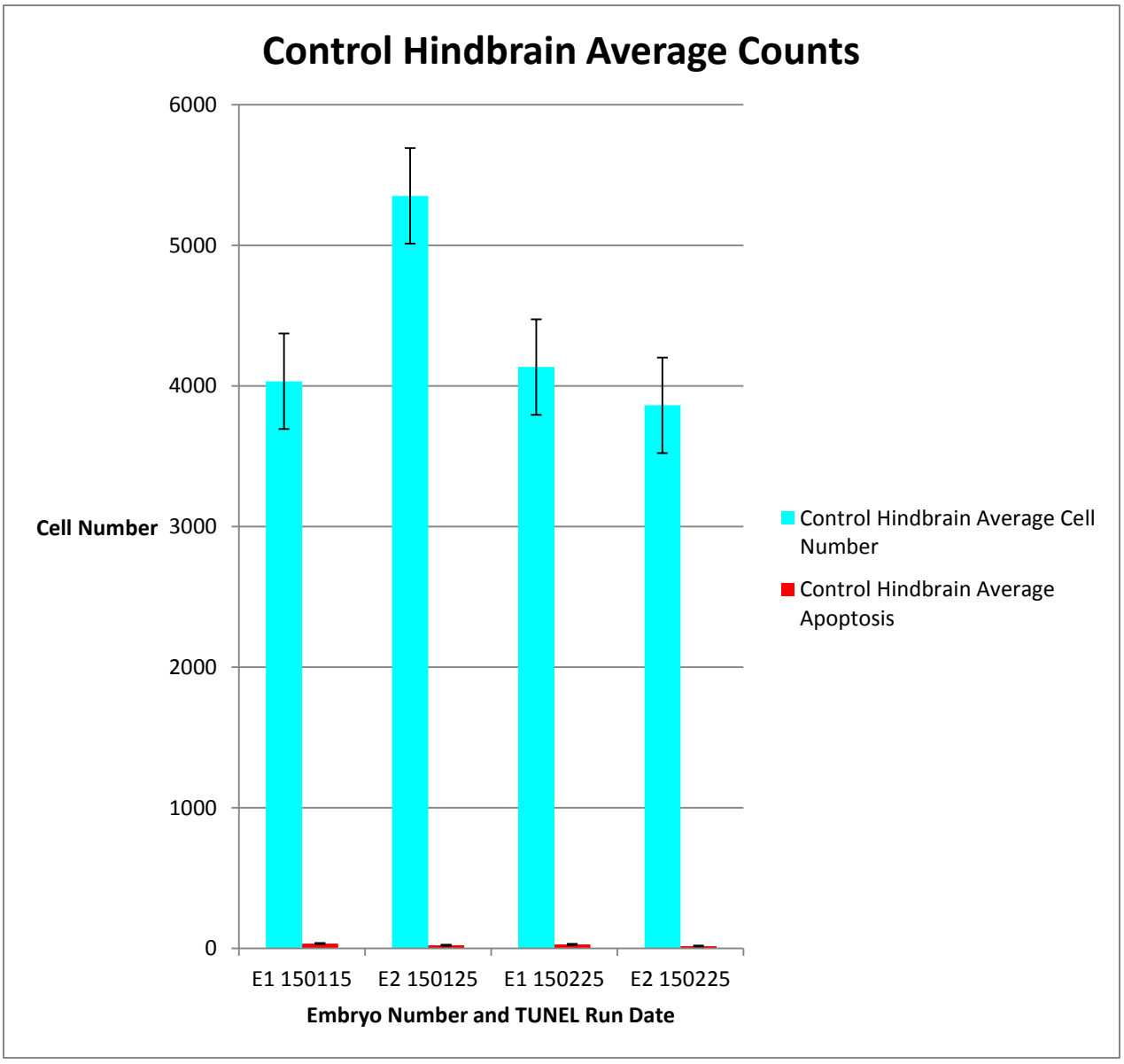

Table 14. Average counts in each neural region corresponding to Figure 11d

Stage, Embryo #, Treatment, TUNEL run	Avg Count Hindbrain	Avg TUNEL Hindbrain	% Hindbrain
st 25, E1, 0.0ppm, 150115	4032.418605	34.69767442	0.86%
st 25, E2, 0.0ppm, 150125	5350.741935	23.06451613	0.43%
st 25, E1, 0.0ppm, 150225	4133.692308	28.61538462	0.69%
st 25, E2, 0.0ppm,150225	3862.034483	16.31034483	0.42%
AVERAGE	4344.721833	25.67198	0.60%
STDEV	679.9829144	7.843593382	0.00213558

Average cell counts (for number of neural cells and number of TUNEL positive apoptotic cells in the hindbrain) were obtained for each control embryo. '%Hindbrain' in **Table 14** refers to the percentage of average number of apoptotic cells divided by the average number of total cells in the hindbrain. The average number of total cells in the hindbrain (for all control embryos) was 4344.72 with a standard deviation of 679.98. The average number of apoptotic cells in the hindbrain was 25.67 with a standard deviation of 7.84. The average percent of apoptotic cells in the hindbrain came out to be .60% with a standard deviation of 0.002. The standard error was 339.99 for average hindbrain cell counts and 3.92 for apoptosis cell counts.

Figure 9 (a-d). Average count data for 2.4ppm embryos

Figure 9a. 2.4ppm Spinal Cord Average Counts

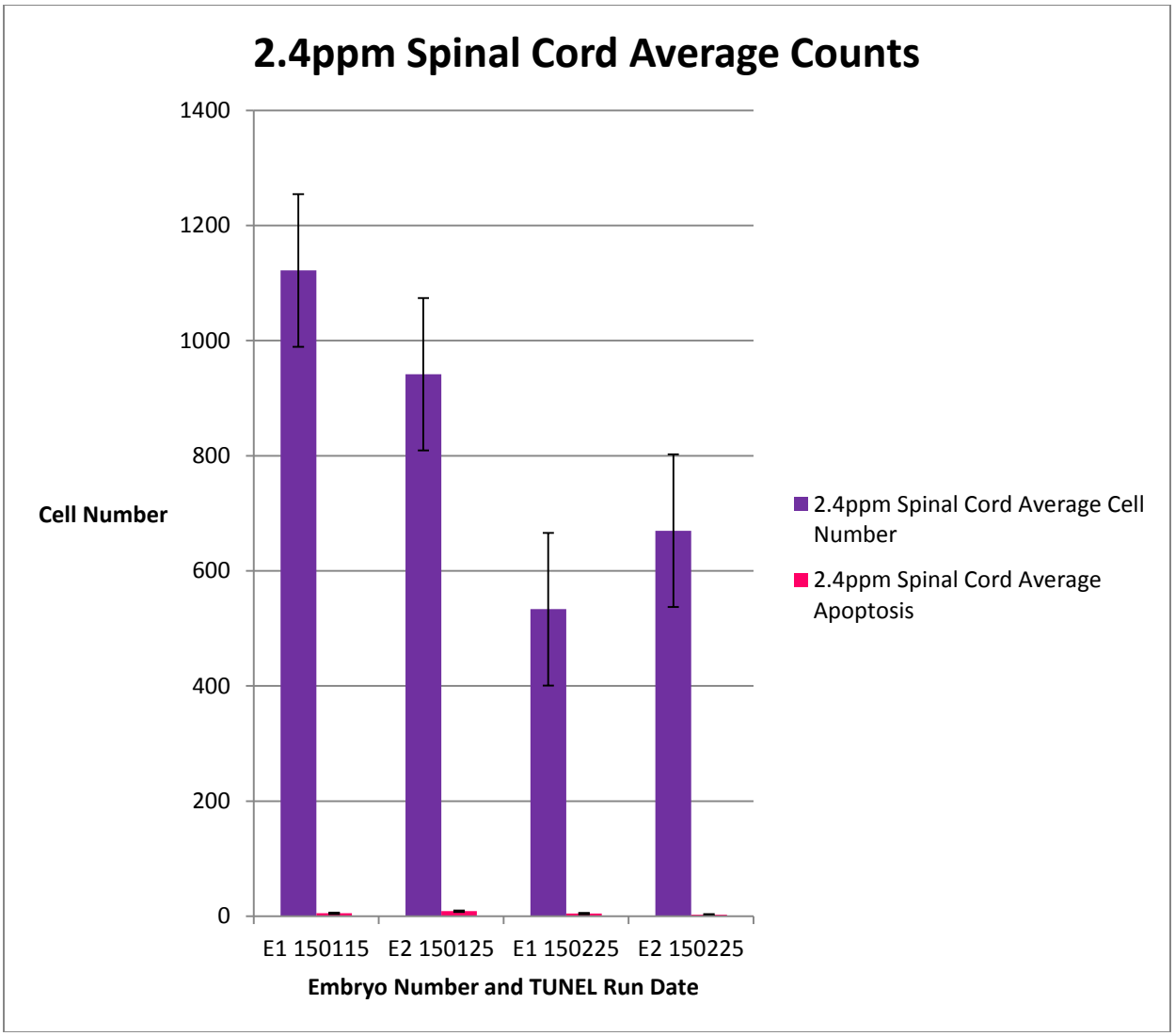

Table 15. Average counts in each neural region corresponding to Figure 9a

Stage, Embryo #, Treatment, TUNEL run	Avg Count Spinal Cord	Avg TUNEL SPC	% SPC
st 25, E1, 2.4ppm, 150115	1121.833333	4.991666667	0.45%
st 25, E2, 2.4ppm, 150125	941.5677966	8.728813559	0.93%
st 25, E1, 2.4ppm, 150225	533.3513514	4.625	0.87%
st 25, E2, 2.4ppm, 150225	669.7421384	2.591194969	0.39%
AVERAGE	816.6236549	5.234168799	0.66%
STDEV	264.941103	2.557847179	0.002800385

Average cell counts (for number of neural cells and number of TUNEL positive apoptotic cells in the spinal cord) were obtained for each 2.4ppm exposed treatment embryo. '%SPC' in **Table 15** refers to the percentage of average number of apoptotic cells divided by the average number of total cells in the spinal cord. The average number of total cells in the spinal cord (for all treatment embryos) was 816.62 with a standard deviation of 264.94. The average number of apoptotic cells in the spinal cord was 5.23 with a standard deviation of 2.56. The average percent of apoptotic cells in the spinal cord was 0.66% with a standard deviation of 0.003. The standard error was 132.47 for average spinal cord cell counts and 1.28 for apoptosis cell counts.

Figure 9b. 2.4ppm Forebrain Average Counts

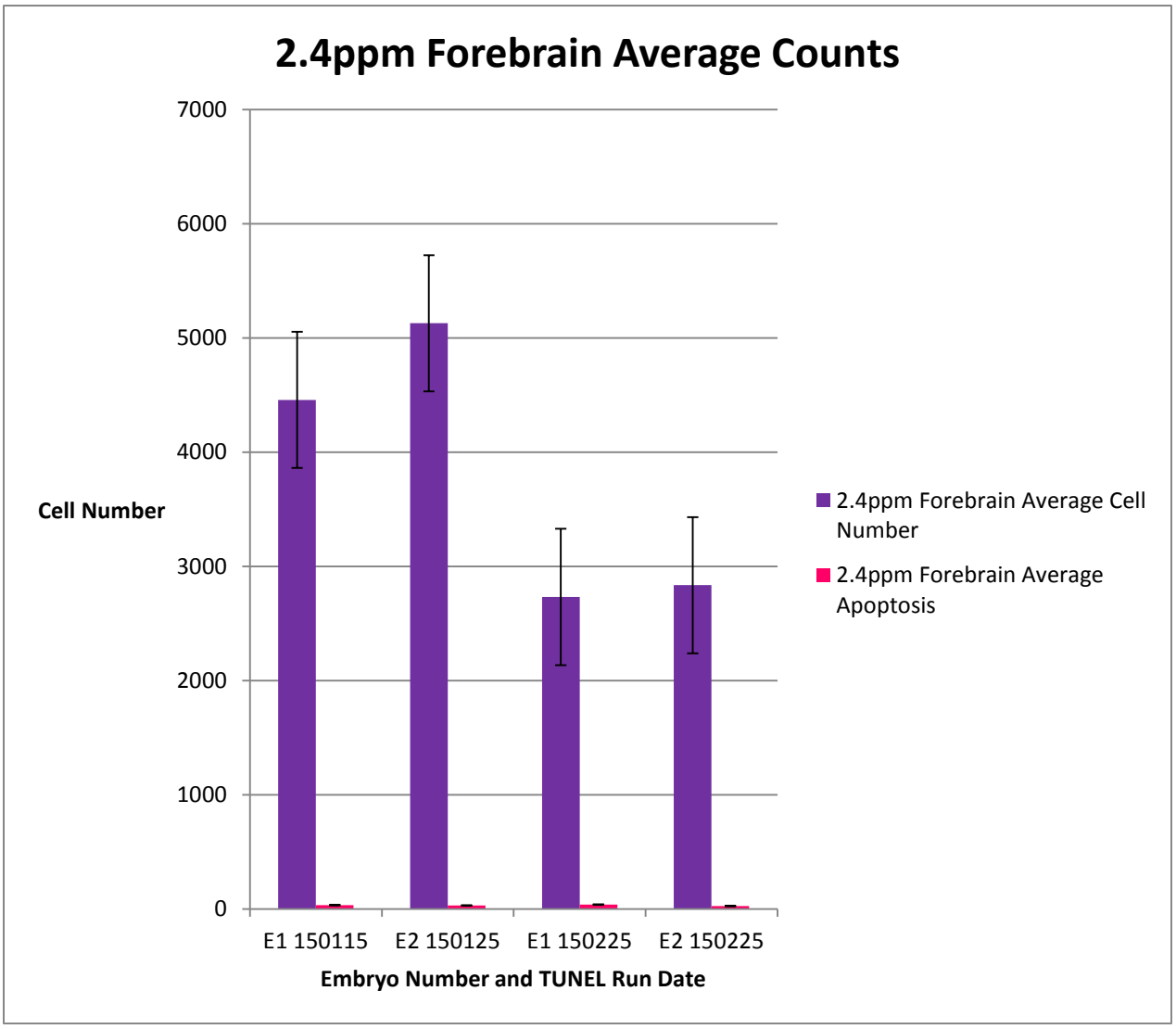

Table 16. Average counts in each neural region corresponding to Figure 9b

Stage, Embryo #, Treatment, TUNEL run	Avg Count Forebrain	Avg TUNEL Forebrain	% Forebrain
st 25, E1, 2.4ppm, 150115	4457.517241	33.86206897	0.76%
st 25, E2, 2.4ppm, 150125	5128.258065	31.09677419	0.61%
st 25, E1, 2.4ppm, 150225	2731.694444	38.69444444	1.42%
st 25, E2, 2.4ppm, 150225	2834.533333	25.96666667	0.92%
AVERAGE	3788.000771	32.40498857	0.93%
STDEV	1192.955032	5.318011917	0.003531246

Average cell counts (for number of neural cells and number of TUNEL positive apoptotic cells in the forebrain) were obtained for each 2.4ppm exposed treatment embryo. '%Forebrain' in **Table 16** refers to the percentage of average number of apoptotic cells divided by the average number of total cells in the forebrain. The average number of total cells in the forebrain (for all treatment embryos) was 3788.00 with a standard deviation of 1192.96. The average number of apoptotic cells in the forebrain was 32.40 with a standard deviation of 5.32. The average percent of apoptotic cells in the spinal cord was 0.93% with a standard deviation of 0.004. The standard error was 596.48 for average forebrain cell counts and 2.66 for apoptosis cell counts.

Figure 9c. 2.4ppm Midbrain Average Counts

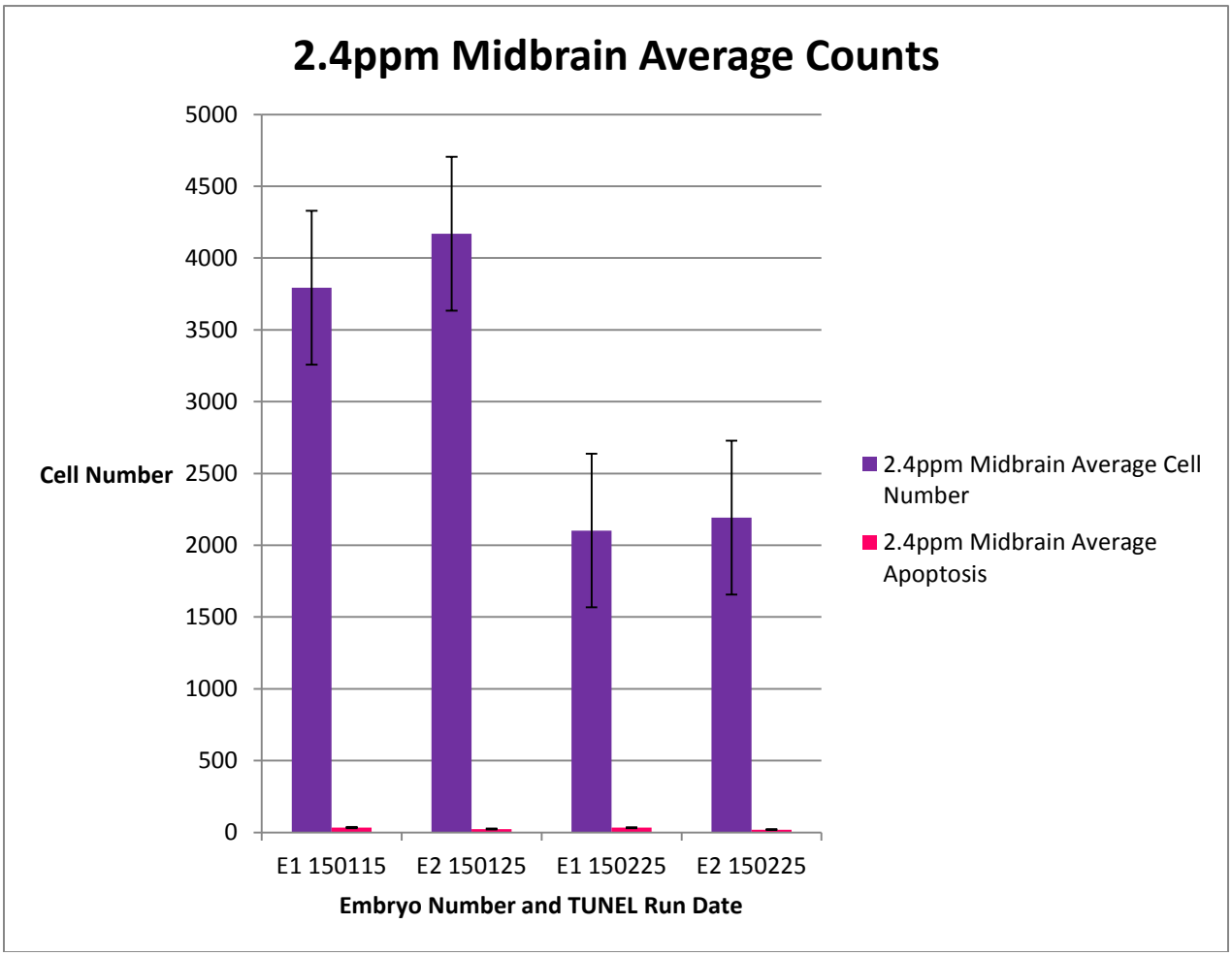

Table 17. Average counts in each neural region corresponding to Figure 9c

Stage, Embryo #, Treatment, TUNEL run	Avg Count Midbrain	Avg PCNA Midbrain	% Midbrain
st 25, E1, 2.4ppm, 150115	3793.777778	33.77777778	0.89%
st 25, E2, 2.4ppm, 150125	4169.464286	23.14285714	0.56%
st 25, E1, 2.4ppm, 150225	2102.518519	33.07407407	1.57%
st 25, E2, 2.4ppm, 150225	2191.8	19.36	0.88%
AVERAGE	3064.390146	27.33867725	0.97%
STDEV	1070.794995	7.202337337	0.004266587

Average cell counts (for number of neural cells and number of TUNEL positive apoptotic cells in the forebrain) were obtained for each 2.4ppm exposed treatment embryo. '%Midbrain' in **Table 17** refers to the percentage of average number of apoptotic cells divided by the average number of total cells in the midbrain. The average number of total cells in the midbrain (for all treatment embryos) was 3064.39 with a standard deviation of

1070.79. The average number of apoptotic cells in the forebrain was 27.34 with a standard deviation of 7.20. The average percent of apoptotic cells in the spinal cord was 0.97% with a standard deviation of 0.004. The standard error was 535.40 for average midbrain cell counts and 3.60 for apoptosis cell counts.

Figure 9d. 2.4ppm Hindbrain Average Counts

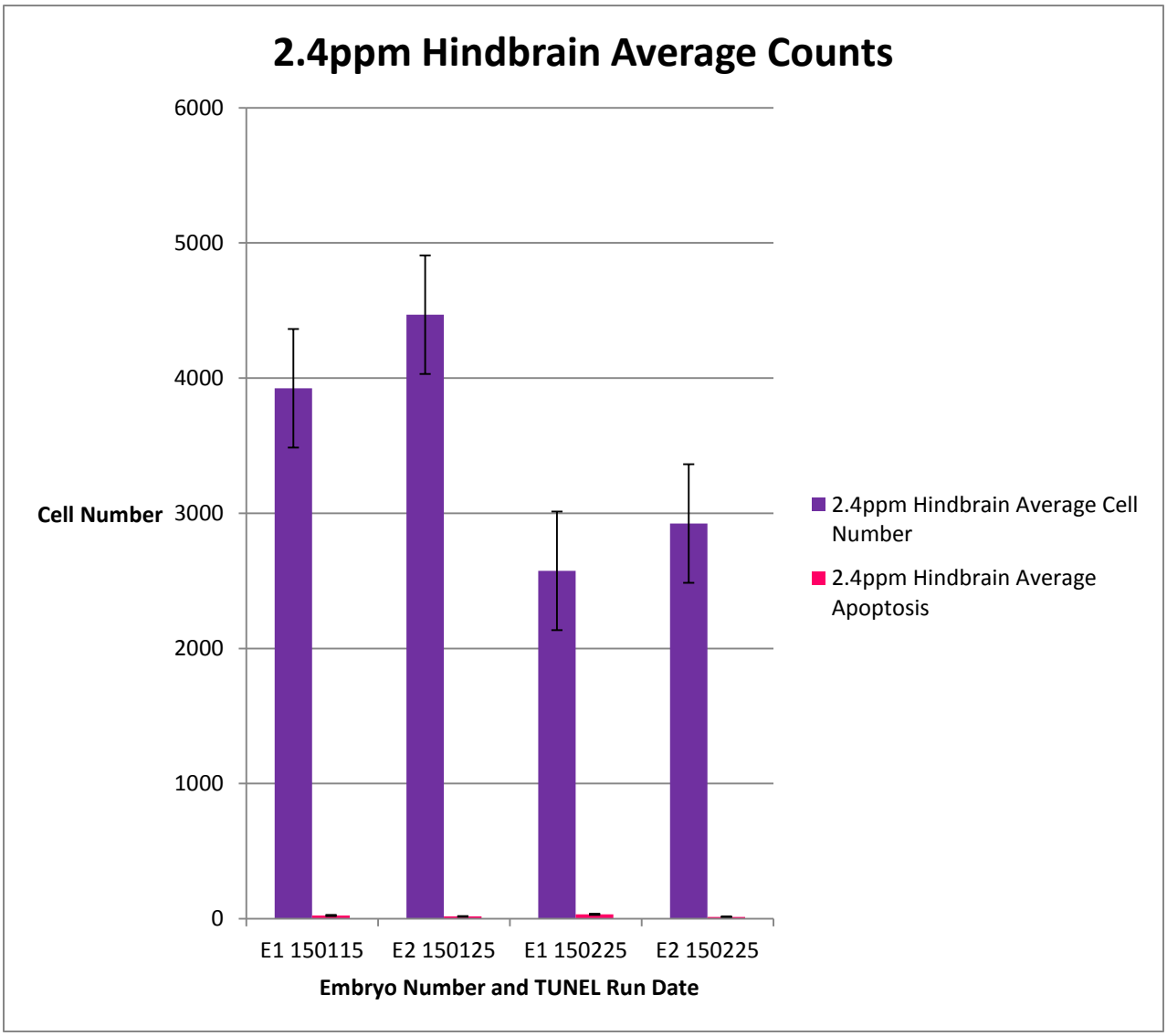

Table 18. Average counts in each neural region corresponding to Figure 9d

Stage, Embryo #, Treatment, TUNEL run	Avg Count Hindbrain	Avg TUNEL Hindbrain	% Hindbrain
st 25, E1, 2.4ppm, 150115	3924.78125	23.21875	0.59%
st 25, E2, 2.4ppm, 150125	4469.814815	16.2962963	0.37%
st 25, E1, 2.4ppm, 150225	2573.896552	31.72413793	1.23%
st 25, E2, 2.4ppm, 150225	2923.269231	13.23076923	0.45%
AVERAGE	3472.940462	21.11748836	0.66%
STDEV	877.1805189	8.213008932	0.003913217

Average cell counts (for number of neural cells and number of TUNEL positive apoptotic cells in the forebrain) were obtained for each 2.4ppm exposed treatment embryo. '%Midbrain' in **Table 17** refers to the percentage of average number of apoptotic cells divided by the average number of total cells in the midbrain. The average number of total cells in the midbrain (for all treatment embryos) was 3064.39 with a standard deviation of 1070.79. The average number of apoptotic cells in the forebrain was 27.34 with a standard deviation of 7.20. The average percent of apoptotic cells in the spinal cord was 0.97% with a standard deviation of 0.004. The standard error was 438.90 for average hindbrain cell counts and 4.11 for apoptosis cell counts.

3.4. Movement of Hg in developing embryos

To measure Hg distribution during zebra finch embryonic development, eggs were dissected at stage 25 (day 4 ¾), stage 32 (day 6 ¾), and stage 38 (day 8 ½). For reference, zebra finches eggs typically hatch within 14-15 days after being laid. For each developmental stage the eggshell, embryo, and yolk-plus-albumin were pooled together. The yolk and albumin were pooled as I was unable to separate them reliably without contaminating one with the other. For all figures below (**Figures 10-16**) the word 'yolk' refers to the pooled yolk and albumin. The eggshell Hg was not included in my consideration of Hg distribution during development, as the Hg amounts in eggshell were typically negligible. However, some eggshell samples did have higher mercury content (see in appendix, **Table 26**), probably due to contamination during sample preparation. Overall, all samples were analyzed for total Hg (mg/kg) concentration using the DMA-80 and a trend was found that mercury accumulated in the developing embryo as development progressed as seen in **Figures 10-12**.

Figure 10. Concentration of Hg in control and 2.4ppm yolk during development

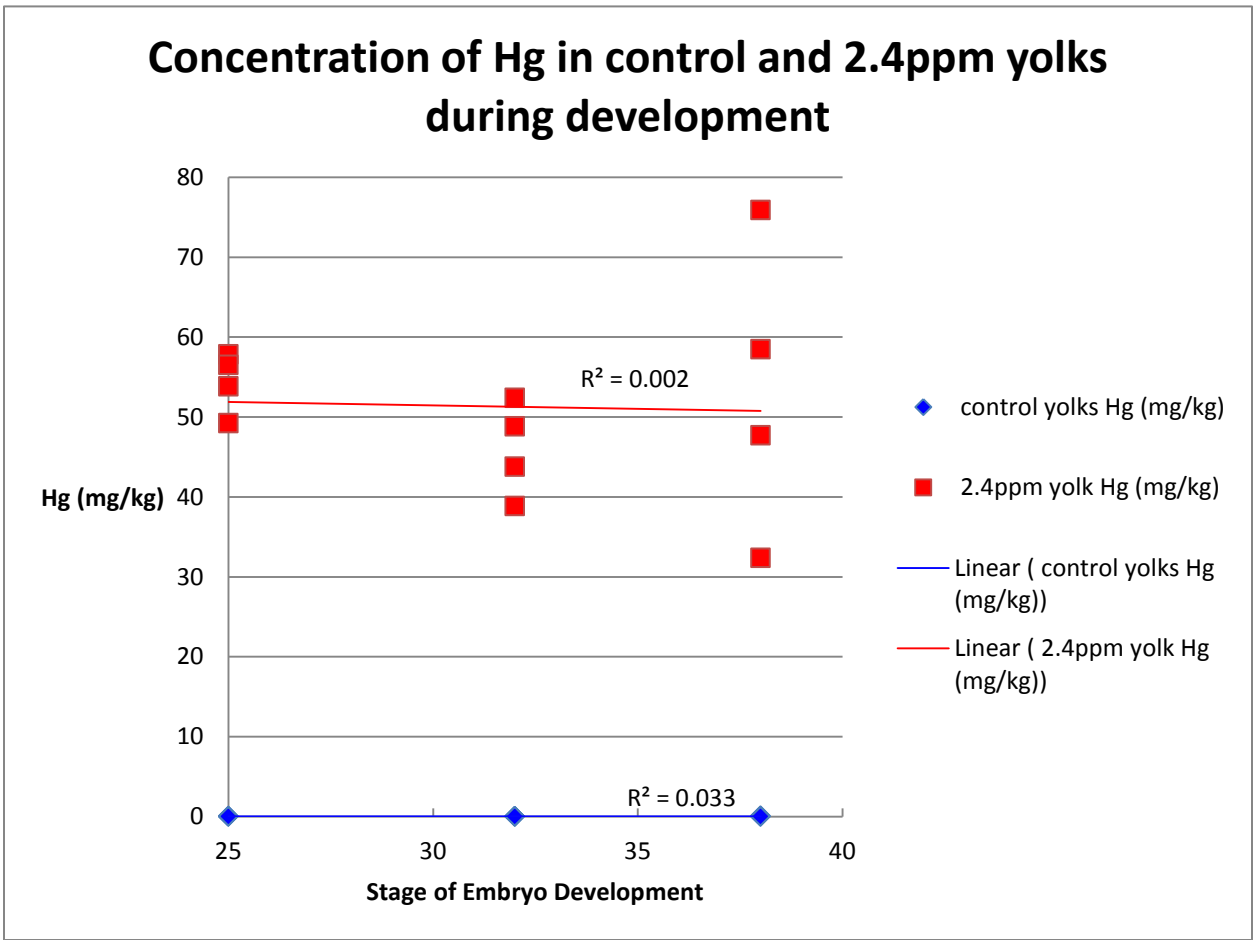

In **Figure 10**, mercury content in the 'yolk' (as in combined yolk/albumin) exhibited a downwards trend as zebra finch embryos progressed along the three measured stages of development. Each separate point on the graph was a yolk that came from a separately analyzed egg. The very slight downwards trend in Hg content in the 'yolk' for 2.4ppm embryos is more apparent when compared alongside with the control embryo yolk values. Later stages of development and an increased sample size are needed to determine if the slight downwards trend continues and is relevant. Overall, despite a slight decrease over time, mercury content was highest in the combined yolk and albumin for all stages of

development analyzed. As the developing embryo absorbs more yolk during development, it raises the question of whether decreased mercury content in the pooled yolk and albumin correspond to increased levels of mercury toxicity. Another potential question is if the rate of yolk absorption influences mercury toxic effects in a developing embryo. Separate graphs of respective treatment and control yolks can be found in the **Appendix** in **Figures 13-14** with corresponding values in **Tables 21-22**.

Figure 11. Concentration of Hg in control and 2.4ppm embryos during development

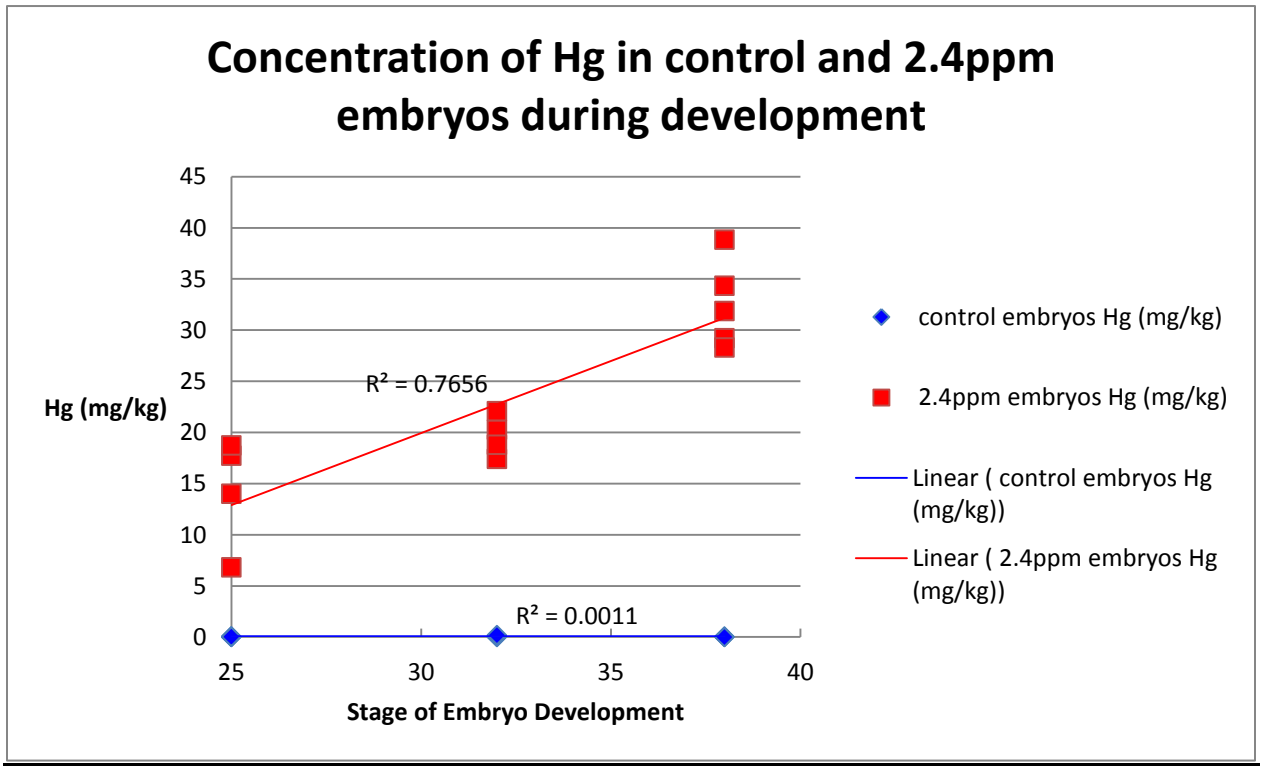

Figure 11 there is an evident trend of increasing mercury content in treatment embryos as development progresses. Each separate point on the graph was an embryo that came from a separately analyzed egg. The trend is supported by the 2.4ppm treatment embryo trend line R^2 value being closer to 1 at 0.7656. As stage 25 embryos had the lowest embryo mercury concentrations and stage 38 embryos had the highest mercury concentrations, the developing embryo may be at a greater risk of MeHg neurotoxic effects for later embryonic stages. Separate graphs of respective treatment and control embryos can be found in the **Appendix** in **Figures 15-16** with corresponding values in **Tables 23-24**.

Figure 12. Concentration of Hg in 2.4ppm embryos compared to yolks during development

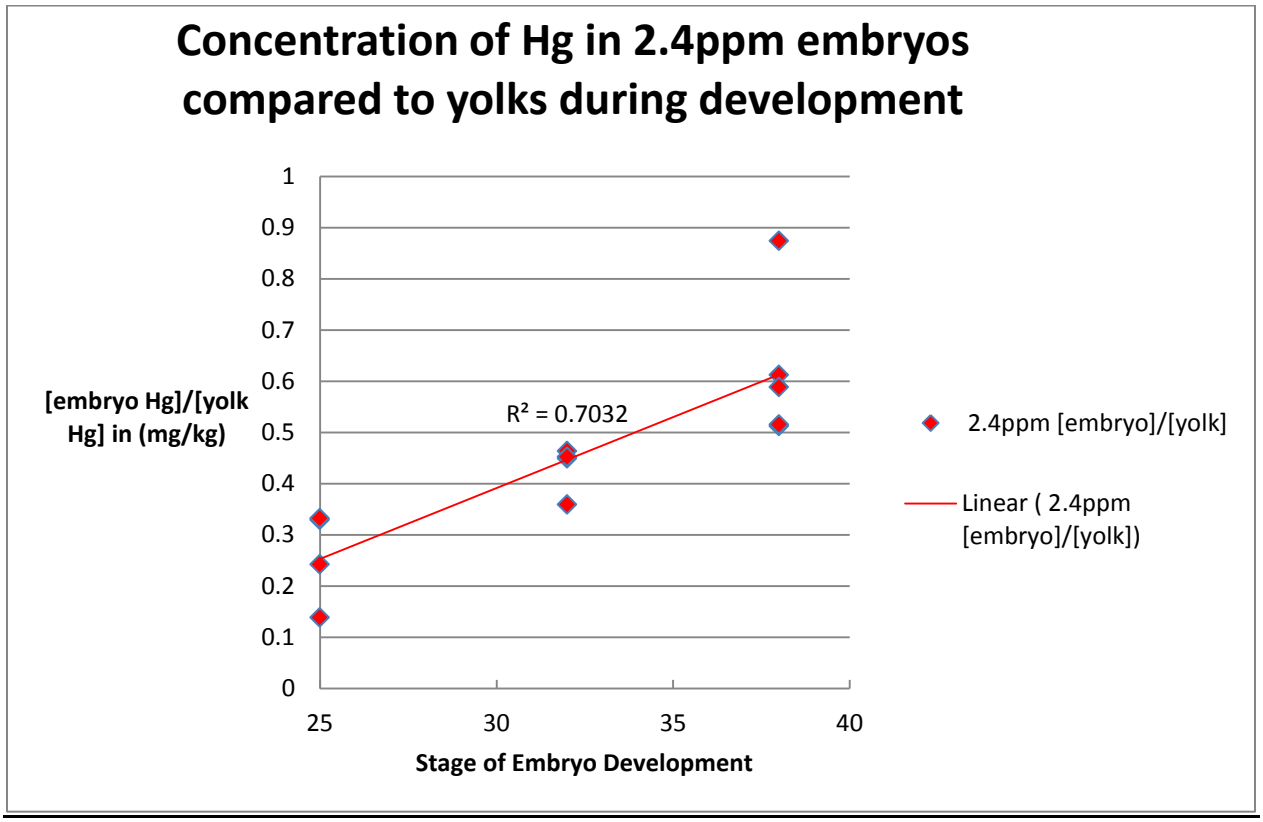

Figure 12 displays the concentration of mercury in the embryo directly compared to the concentration of the yolk that originated from the same egg. Each separate point on the graph was the mercury content of an embryo divided by its respective yolk that came from a separately analyzed egg. The trend seen in **Figure 11** is continued where treatment embryos uptake more mercury as development proceeds. The trend also supports that mercury content in the yolk decreases as the embryo absorbs greater amounts of mercury. Again, the trend may indicate that mercury has a more toxic effect at later stages of development due to increased absorption. Values for **Figure 12** may be found in **Table 25** of the **Appendix**.

3.5. Blood Hg parental concentration

In order to confirm that the parental generations were at the correct treatment level, blood samples were collected of all control and 2.4ppm adult pairs to determine blood mercury concentration. Samples were collected by pricking the brachial vein and collecting 15-40μL of blood. Blood samples were analyzed for total Hg concentration (mg/kg) using the DMA-80. Blood samples were used to determine current mercury dosage of the parental generation, in order to ensure that the females maternally transferred mercury into their eggs for their respective treatment groups. **Table 20** shows the blood mercury data.

Table 19. Blood Hg (mg/kg) of control and 2.4ppm birds

Control, Bird Band Number	Hg [mg/kg]	2.4ppm, Bird Band Number	Hg [mg/kg]
Hg882_male_control	0.0192	2.4ppm Hg1780	36.61538
Hg3895_male_control	0.00843	2.4ppm Hg3084	27.98978
Hg3053_male_control	0.0077	2.4ppm Hg3070	63.61478
Hg920_female_control	0.01837	2.4ppm Hg4345	21.23037
Hg1561_female_control	0.00402	2.4ppm Hg1808	28.65509
Hg1084_female_control	0.02546	2.4ppm Hg2967	21.12869
Hg3077_male_control	0.01561	2.4ppm Hg654	39.53723
Hg3072_female_control	0.00679	2.4ppm Hg1580	32.58473
Hg1594_female_control	0.03199	2.4ppm Hg1256	36.60577
Hg1560_female_control	0.00403	2.4ppm Hg1256 dup	39.15404
Hg3030_male_control	0.00694	2.4ppm Hg2955	23.64869
Hg659_female_control	0.00751	2.4ppm Hg594	45.59954
Average Hg (mg/kg)	0.013004167	2.4ppm Hg745	33.42663
Standard Deviation (stdev)	0.009072759	2.4ppm Hg1409	35.72171
		2.4Hg3051	27.46593
		2.4Hg4280	30.87485
		2.4Hg1718	40.97373
		2.4ppm Hg2770	32.88095
		2.4ppm Hg2845	31.33766
		Average Hg (mg/kg)	34.16029211
		Standard Deviation (stdev)	9.710406889

As seen in **Table 19**, the average Hg (mg/kg) blood content of the control parental generation was 0.013 mg/kg with a standard deviation of 0.009. The average Hg (mg/kg) blood concentration of the treatment parental generation (that were fed a diet of 2.4ppm) was 34.16mg/kg with a standard deviation of 9.71. Whole egg mercury content, which was similar to treatment group parental blood data, can be seen in the **Appendix** in **Table 27**.

3.6. Feather Hg parental concentration

Feathers from all control and 2.4ppm adult pairs were collected to confirm that the parental generations were at the correct treatment level. Feathers were collected by plucking approximately 9 feathers (taken from the breast and nape regions) and analyzed using the DMA-80. Unlike blood, feathers indicate long term mercury exposure and accumulation in the parental generation.

Table 20. Feather Hg (mg/kg) of control and 2.4ppm birds

Control, Bird Band Number	Hg [mg/kg]		2.4ppm, Bird Band Number	Hg [mg/kg]
Hg1560 0.0ppm	0.1665		Hg1718 2.4ppm	405.75803
Hg3895 0.0ppm	0.23275		Hg4345 2.4ppm	366.25619
Hg3072 0.0ppm	0.14606		Hg2845 2.4ppm	491.82184
Hg 3372 0.0ppm	0.35909		Hg2967 2.4ppm	395.43691
Hg3591 0.0ppm	0.12367		Hg2967 2.4ppm duplicate	369.91331
Hg659 0.0ppm (only 3 feathers)	0.2498		Hg654 2.4ppm	578.93988
Hg1561 0.0ppm	0.64787		Hg1808 2.4ppm	549.29569
Hg1594 0.0ppm	0.61143		Hg745 2.4ppm	467.39922
Hg3053 0.0ppm	0.13838		Hg3051 2.4ppm	513.46775
Hg3077 0.0ppm	0.2288		Hg1780 2.4ppm	530.61613
Hg1084 0.0ppm	0.22153		Hg1780 2.4ppm duplicate	573.9745
Hg3030 0.0ppm	0.09875		Hg3084 2.4ppm	479.14766
Average Hg (mg/kg)	0.2687192		Hg1256 2.4ppm	515.13294
Standard Deviation (stdev)	0.1827209		Hg1580 2.4ppm	519.32988
			Hg2955 2.4ppm	383.956
			Hg2970 2.4ppm	491.30194
			Hg1409 2.4ppm	581.97906
			Average Hg (mg/kg)	483.16041
			Standard Deviation (stdev)	73.945225

As seen in **Table 20**, the average Hg (mg/kg) feather content of the control parental generation was 0.269 mg/kg with a standard deviation of 0.182. The average Hg (mg/kg) feather concentration of the treatment parental generation (that were fed a diet of 2.4ppm) was 483.16 mg/kg with a standard deviation of 73.95.

3.7. DMA-80 Quality Assurance and Quality Control (QA/QC)

To check for quality control, duplicates of the same sample were run to determine machine and human error in weighing. The relative percent difference (RPD) was calculated for each duplicated and the average RPD was taken for all of the duplicate RPD values. The resulting average RPD for all duplicates was 7.9%. Assays were run only when standard reference materials were found to be within 7.5% of the manufacturer provided values. Recovery of total mercury from standard reference samples was 97.79% ± 2.65% for DORM-4 (n=32) and 96.77% ± 3.35% (n=32) for DOLT-4.

4. Discussion

4.1 Experimental results and conclusions

Methylmercury is a potent environmental neurotoxin that has many adverse effects on the health of an organism. MeHg is able to exert its toxic effects at low doses and is most harmful during early development. At the cellular level, the literature shows that MeHg adversely impacts important neural developmental processes such as neuronal migration, neuronal differentiation, cell proliferation, and apoptosis[46–48,53]. However, despite progress in understanding how MeHg affects normal development in many model organisms, fewer cellular and molecular studies have been conducted in birds and even fewer in altricial songbird species. Also, the majority of avian specific studies use MeHg injections into eggs which are an unnatural route of exposure and not as biologically relevant as natural maternal MeHg transfer. The decreased biological relevance of MeHg injections may limit conclusions drawn from such studies when understanding the risk that MeHg poses to wild birds. This project examined the effects of MeHg exposure via maternal transfer on proliferation and apoptosis during zebra finch neural development. The project tested the hypothesis that alterations in cell proliferation and apoptosis during embryonic development mediate the adverse effects that MeHg exposure has zebra finch neural development. The original prediction was that proliferating cell nuclear antigen (PCNA) expression levels would decrease and apoptotic levels would increase in neural regions of embryos developmentally exposed to MeHg. The project also investigated Hg toxicokinetics during zebra finch embryo development by assessing the relative concentration of Hg in the developing embryo, pooled yolk and albumin.

4.1.2 PCNA results from in situ hybridization and cell counting analysis

It was hypothesized that cell proliferation would alter during zebra finch embryonic development to mediate the effects of MeHg exposure. The original prediction was that proliferating cell nuclear antigen (PCNA) expression levels would decrease in 2.4ppm treatment embryos. To test this prediction, whole mount *in situ* hybridization (ISH) (with an n=4 per treatment group) was used to determine differences in spatiotemporal patterns of PCNA expression in stage 25 control and mercury exposed embryos. Embryos were cross sectioned and processed to quantify the average percent of proliferating cells in the developing spinal cord, forebrain, midbrain, and hindbrain to determine area-specific differences in cell proliferation. There was no statistically significant difference in average percent proliferation between control and treatment embryos in the spinal cord, forebrain, and hindbrain. The p-values for the spinal cord, forebrain, and hindbrain were respectively p=0.7495, p=0.7583, and p=0.8462. A significant difference (p-value <0.05) was found in the midbrain, where there was a significant decrease (p-value of 0.0447) of proliferation within treatment embryos compared to control embryos. This decrease in proliferation indicates that MeHg affects neural proliferation in the midbrain of stage 25 embryos. In all neural regions for both control and treatment embryos there was a great deal of individual variation in the amount of average percent proliferation, average proliferation, and average number of cells. As both control and treatment embryos displayed large amounts of individual variation, the differences in cell count data are due to normal developmental differences. Overall, a larger sample size may be needed in order to determining if the p-value is significant for decreased proliferation in the midbrain for treatment embryos after increasing the sample size. However, because all other neural regions were strongly

statistically insignificant with very high p-values, the significant p-value found for decreased proliferation in the midbrain of MeHg exposed embryos is promising.

4.1.3 Apoptosis results from TUNEL assay and cell counting analysis

The TUNEL assay was performed on whole mount stage 25 control and 2.4ppm treatment zebra finch embryos in order to test if changes in apoptosis would mediate the effects of MeHg. TUNEL assay embryos (n=4 per treatment group) were analyzed to determine the percent of apoptosis. It was predicted that embryos developmentally exposed to MeHg would have increased levels of apoptosis in neural regions compared to control embryos. There was no statistically significant difference found in the average percent apoptosis in the neural regions of control and treatment embryos. The p-values for the average percent apoptosis in the neural regions were: spinal cord p-value=0.743, forebrain p-value=0.925, midbrain p-value=0.733, and hindbrain p-value=0.802. Similarly to the proliferation data, there were large amounts of individual variation for the average percent apoptosis, average overall cell counts, and average apoptosis counts. In regards to individual variation, the stage 25, eI, control embryo from TUNEL run date 150115 appeared to be an outlier in the control data in the forebrain and midbrain region, as that embryo had much greater amounts of apoptosis than any other control or even treatment embryo in those neural regions. There is the possibility that the embryo itself was not developing normally (despite appearing morphologically normal when dissected) and would not have hatched if allowed to develop completely. However, even if the aforementioned embryo is removed from the data, the p-values for average percent apoptosis remain statistically insignificant. A larger sample size would be ideal in order to

help control for individual variation and potential outliers. As there was no statistically significant difference in apoptosis, our prediction that MeHg would increase apoptosis in treatment embryos was not supported. However, as apoptosis was analyzed only for stage 25 embryos, if would be interesting to investigate if MeHg effects apoptotic processes in later embryonic neural development. Overall, from this data, it appears that MeHg does not impact apoptosis in stage 25 zebra finch embryos.

4.1.4 Mercury distribution results from DMA analysis

In order to better understand the toxicokinetics of maternally transferred MeHg during zebra finch development, stage 25 (day 4 ¾), stage 32 (day 6 ¾), and stage 38 (day 8 ½) embryo stages were analyzed on the DMA-80. Control and 2.4ppm treatment embryos were separated by their eggshell, pooled yolk and albumin, and embryo. All components were subsequently analyzed on the DMA-80 to measure mercury concentration in mg/kg. As inorganic mercury does not easily accumulate or absorb in tissues, the measured mercury content is measured as MeHg content. Generally, the pooled yolk and albumin had the highest mercury concentration for all stages and the eggshells had the lowest mercury values. However, some of the eggshells had high mercury values. The eggshells with high mercury values probably resulted from some leftover yolk/albumin contamination during sample separation. High mercury content in the eggshell did not follow the literature (where eggshells typically have very low mercury content)[71]. The developing embryos generally had lower mercury concentrations than the yolk/albumin but higher amounts than the eggshell. There was a very slight, potentially negligible (as the R^2 value for the trend line was close to zero) trend for the pooled yolk and albumin in treatment embryos

to decrease in mercury content as development proceeded. Mercury content in control developing embryos demonstrated a slight, potentially negligible upwards trend for mercury to accumulate in the embryo as development progressed. What is interesting is that even though these embryos were not directly exposed to mercury (like the treatment embryos) there still appears to be a very slight upwards trend for the embryo to accumulate low amounts of mercury as development progresses. For treatment 2.4ppm exposed embryos, there was a clear trend (with a R^2 value for the trend line was closer to 1 at 0.7656) for mercury to accumulate in the developing embryo tissues as development proceeded from a stage 25 to a stage 38. Overall, when comparing mercury content in the embryo to the pooled yolk and albumin mercury content, there remained an evident trend (with a R^2 value for the trend line at 0.7032) for mercury to increase in the embryo during development.

4.1.5 Overall conclusions

Currently, this is the first cellular, molecular study to have investigated maternal exposure of MeHg in zebra finch embryos. Due to the utilization of maternal exposure, to MeHg, this study has more biological relevance with MeHg exposed birds in the wild than studies that relied on egg injections. This is pertinent, as it has been demonstrated in the literature that injected MeHg is more toxic to avian species than the same amount of MeHg deposited maternally [72].

MeHg distribution during zebra finch development demonstrated a trend to increase in embryonic tissues. As the lowest embryo MeHg concentrations were found in the earliest stage studied (stage 25) and the highest in the oldest stage analyzed (stage 38)

the developing embryo may be at a greater risk of MeHg neurotoxic effects for later embryonic stages. Further studies would be needed to determine if increased MeHg concentrations at later stages is more harmful than lower MeHg concentrations at earlier stages. Increased amounts of mercury may more acutely disrupt embryonic neural development. However, early neural tissue at younger embryonic stages may potentially be more sensitive to even low MeHg concentrations accumulated in embryonic tissue. Another aspect to consider is the rate of mercury absorption into embryonic tissue. It would be interesting to see if later developmental stages not only increased in mercury content but also had an increase rate of mercury content. A quicker rate of mercury absorption in embryonic tissue may parallel acute exposure and cause greater disruption than steady chronic exposure.

It was surprising to find no statistically significant difference in apoptosis for treatment embryos, as the majority of the literature supports increased apoptosis in neural tissue of MeHg exposed organisms[7348]. The majority of studies conducted that found increased levels of apoptotic cells in MeHg exposed organisms used methods including injecting and direct oral exposure of the organisms to MeHg[4874.] To date there have been few studies specifically examining the effect of maternal MeHg transfer on embryonic neural proliferation in either rodent or avian models. The lack of significant change in apoptosis in any neural region of treatment embryos may potentially due to protective elements within the egg such as prolactin[75], selenium sequestration in the egg[60], or the potential ability of embryos to de-methylate MeHg at even early embryonic stages[60]. Another possibility as mentioned earlier, is that injected MeHg is more toxic than maternal

MeHg deposits for avian species[72]. This difference in toxicity may potentially explain why this study did not see a difference in neural apoptotic levels in treatment levels.

Interestingly enough, MeHg exposure via maternal transfer resulted in a statistically significant decrease for cell proliferation in the midbrain of treatment embryos, but without significant change in found for levels of apoptosis. These results indicate that, at least for a stage 25 developing zebra finch, mercury impairs neural cell proliferation in the midbrain and has the potential to cause long term consequences by impairing proliferation necessary for normal neural patterning during development. Current literature supports this result of MeHg decreasing proliferation in the midbrain. Previous studies have found MeHg to inhibit cell proliferation in regions of the developing brain[47,76,53,] and midbrain[77]. *in vitro* studies demonstrate that environmentally relevant levels of MeHg inhibit cell proliferation of neural stem cells (NSCs), affected expression of the p16 and p21 cell cycle regulation genes, but did not cause NSC apoptosis[5345]. This raises the potential that the reduced number of proliferating cells in the midbrain of treatment zebra finch embryos may be from MeHg decreasing NSCs proliferation and disrupting genes involved in cell cycle control. Another possibility is that at stage 25, the embryo has accumulated enough mercury in its tissues to disrupt proliferation but not enough to induce abnormal apoptosis. Further studies would need to be conducted to see if MeHg does increase apoptosis in the developing zebra finch embryo, but at later stages of embryonic development than stage 25.

Decreased levels of proliferation in the midbrain of stage 25 treated zebra finch embryos, but not other neural regions, raises a few intriguing possibilities. The midbrain plays an important role in visual, auditory systems of an organism. Midbrain processing is

important in human auditory and language learning[78,79]. Studies also show that the midbrain in zebra finches is involved in song learning[8081]. Decreased cellular proliferation in the midbrain during embryonic development may potentially mediate later behavioral deficits found in MeHg exposed zebra finches such as less complex songs[22]. As zebra finches are an important model organism for understanding language development in humans[82], alterations in zebra finch midbrain proliferation from MeHg may have implications for understanding how low-level MeHg exposure causes language deficits in humans[52]. Further studies will need to be conducted to understand just what impact decreased proliferation in the midbrain has on later zebra finch development.

4.2 Potential limitations

Due to large amounts of individual variation, this study would benefit for a larger sample size for both proliferation and apoptosis data. The study was limited in sample size due to time constraints involved in processing zebra finch embryos for proliferation and apoptosis analysis. Another limitation is that although all embryos processed for this study were at a stage 25, some embryos may have been an older or younger stage 25. Older/younger stage 25 embryos may potentially account for the vast amount of individual variation seen in both proliferation and apoptosis data. An additional source of variation, as could be seen in the mercury accumulation data, is that the females that laid the eggs from which the embryos were processed from don't deposit the same amounts of mercury as on another. Different mercury deposits in the egg may also arise from laying sequence[71]. Although the zebra finches used in the study had eggs collected from them daily, it is likely that females deposited different amounts of mercury in each egg each day. Lastly, zebra

finch families can significantly vary in tolerance to MeHg which impacts reproductive success[83]. This variation in MeHg tolerance may also be a reason for the high levels of individual variation in embryo data.

4.3 Future Directions

A sample size of four for each treatment group was processed to determine levels of proliferation and apoptosis in zebra finch embryos. Due to high levels of individual variation found in all zebra finch embryo data, processing more samples may improve the data. Therefore, in order to test the strength of the significant p-value found for altered proliferation in treatment embryos and to help even out individual variation, new samples will be collected and processed for both PCNA and TUNEL assays.

In order to see if increasing MeHg concentrations in the embryos increase neurotoxic effects in developing zebra finch embryos, it would be valuable to investigate stages older and younger than stage 25. Running ISH for PCNA and the TUNEL assay on embryonic stages such as stage 15 (day 2 ¾), stage 32 (day 6 ¾) and stage 38 (day ¾) would determine if neural proliferation and apoptosis are affected by increased embryonic accumulation of MeHg during development. Also as for a stage 25 embryos there was no significant difference in apoptosis from MeHg exposure; it would be useful to determine if apoptosis is affected from MeHg at only later stages of development. Such further analysis would also help elucidate which embryonic stage of zebra finch development is most impacted by the neurotoxic effects of MeHg.

To determine how MeHg is decreasing proliferation in the midbrain of 2.4ppm treatment embryos, genes involved in regulating proliferation (such as P16 and P21 that

have been demonstrated to be altered from MeHg exposure in *in vitro* MeHg studies[45]) would be good candidates to study using ISH to determine expression levels. P16 and P21 regulate proliferation by inhibiting of cyclin-dependent kinases and clyclins. If p16 and p21 are found to have increased expression in MeHg exposed embryos (as was found in the *in vitro* studies[45,53]) it would elucidate the mechanisms by which MeHg inhibits neural cell proliferation. Overall, further studies must be conducted in order to determine how MeHg disrupts neuronal proliferation during zebra finch development and if this disruption affects later stages of zebra finch behavior.

Appendix

Extra figures and tables corresponding to data displayed in results section.

Figure 3b. Average overall cell and percent proliferation in each neural region

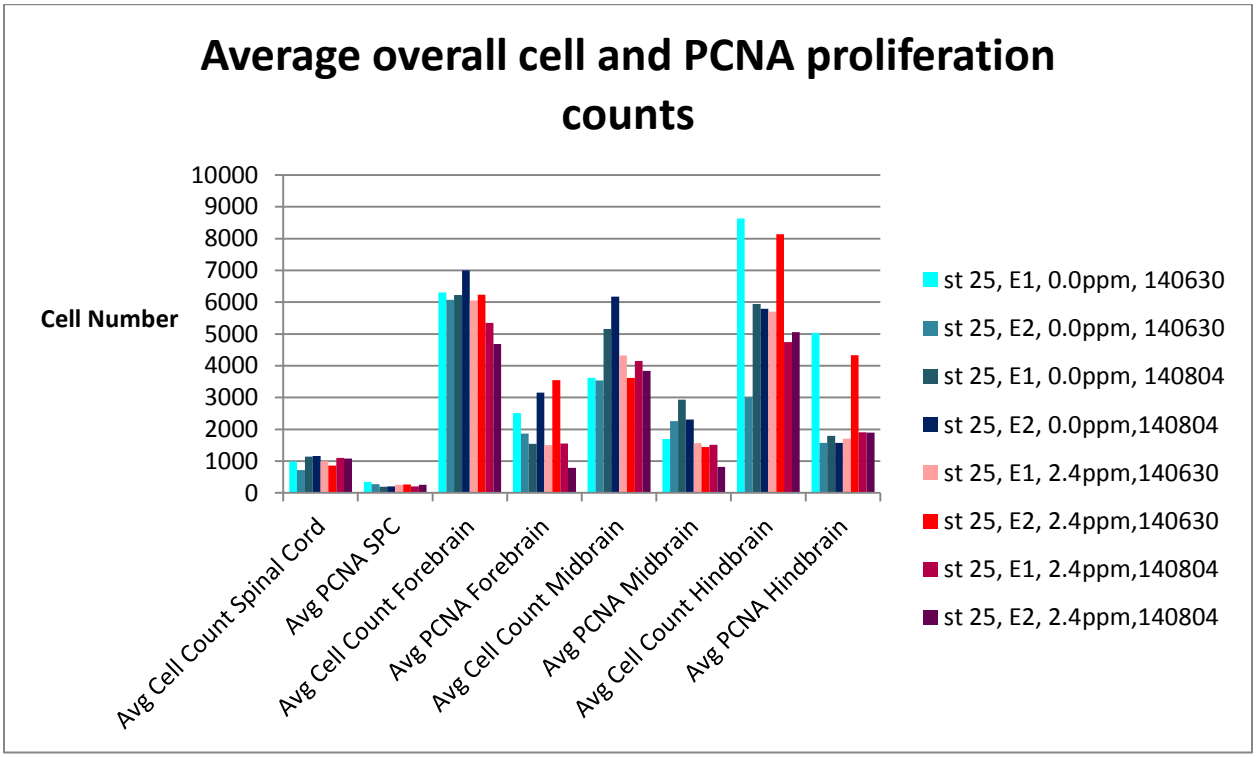

Table 1b. Average counts of total cell number and proliferation in each neural region corresponding to Figure 3b

	Avg Cell Count SPC	Avg PCNA SPC	Avg Cell Count Fore	Avg PCNA Fore	Avg Cell Count Mid	Avg PCNA Mid	Avg Cell Count Hind	Avg PCNA Hind
st 25, E1, 0.0ppm, 140630	991.5698925	344.7956989	6307	2507.8	3614.695652	1698.869565	8632.461538	5035.384615
st 25, E2, 0.0ppm, 140630	723.7777778	280.5777778	6074.541667	1866.583333	3537.807692	2254.461538	3001.444444	1572.888889
st 25, E1, 0.0ppm, 140804	1137.335938	191.4453125	6224.580645	1541.032258	5159.35	2934.8	5944.652174	1800.086957
st 25, E2, 0.0ppm,140804	1159.967213	202.8442623	6997.138889	3149.777778	6177.347826	2310.043478	5788.166667	1570.933333
st 25, E1, 2.4ppm,140630	1000.956044	252.1648352	6051.090909	1502.045455	4323.789474	1562.277778	5702.2	1707.466667
st 25, E2, 2.4ppm,140630	856.1081081	267.0720721	6237.714286	3546.047619	3614.869565	1447.173913	8139.923077	4331.461538
st 25, E1, 2.4ppm,140804	1096.95	209.75	5350.483871	1555.677419	4146.241379	1516.758621	4745.482759	1901.758621
st 25, E2, 2.4ppm,140804	1077.333333	256.6285714	4687.382353	791.1764706	3841.15	817.7	5052.095238	1892.333333
T-Test, P-value	0.96869202	0.830466667	0.091971724	0.567792661	0.36778078	0.020115935	0.96226608	0.973460606

Average cell counts for total cell number and cell proliferation in each neural region for both control and 2.4ppm stage 25 embryos. Just as the midbrain had a significant decrease (p value 0.0447) in

percent proliferation as seen in **Table 1a**, there was a significant decrease in the overall average number of proliferating cells in the midbrain (p value 0.0201) as seen in **Table 1b**. All other neural regions had no significant difference between controls and 2.4ppm embryos.

Figure 7b. Average overall cell and TUNEL apoptosis in each neural region

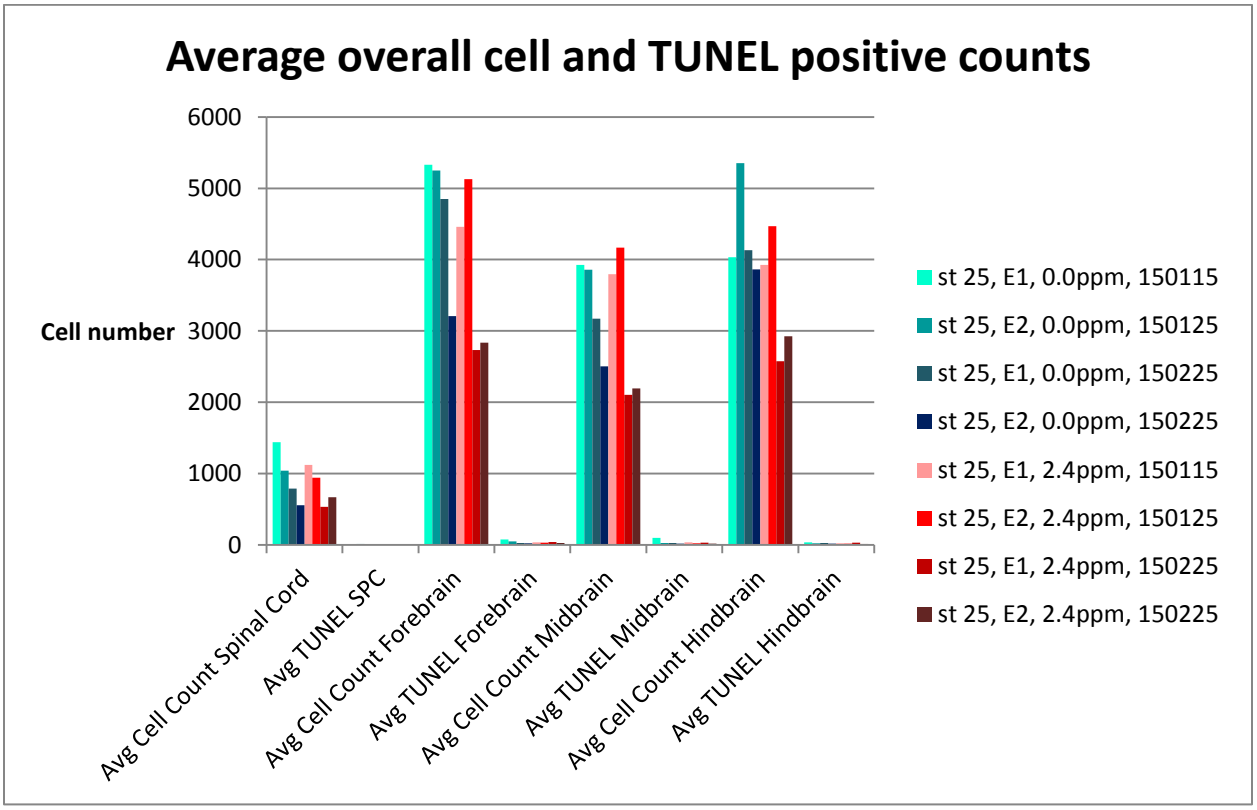

Table 10b. Average counts of total cell number and apoptosis (TUNEL positive cells) in each neural region corresponding to Figure 7b

	Avg Count SPC	Avg TUNEL SPC	Avg Count Fore	Avg TUNEL Fore	Avg Count Mid	Avg TUNEL Mid	Avg Count Hind	Avg TUNEL Hind
st 25, E1, 0.0ppm, 150115	1440.888889	9.5	5330.023256	77.09302326	3926.769231	96.17948718	4032.418605	34.69767442
st 25, E2, 0.0ppm, 150125	1039.676692	11.06015038	5248.953488	47.79069767	3856.59375	24.71875	5350.741935	23.06451613
st 25, E1, 0.0ppm, 150225	787.531746	3.150793651	4850.425	25.125	3172.5	24.31818182	4133.692308	28.61538462
st 25, E2, 0.0ppm, 150225	554.8833333	4.308333333	3206.681818	23.09090909	2502.333333	18.33333333	3862.034483	16.31034483
st 25, E1, 2.4ppm, 150115	1121.833333	4.991666667	4457.517241	33.86206897	3793.777778	33.77777778	3924.78125	23.21875
st 25, E2, 2.4ppm, 150125	941.5677966	8.728813559	5128.258065	31.09677419	4169.464286	23.14285714	4469.814815	16.2962963
st 25, E1, 2.4ppm, 150225	533.3513514	4.625	2731.694444	38.69444444	2102.518519	33.07407407	2573.896552	31.72413793
st 25, E2, 2.4ppm, 150225	669.7421384	2.591194969	2834.533333	25.96666667	2191.8	19.36	2923.269231	13.23076923
T-Test, P-value	0.569529186	0.473726679	0.304188649	0.430508845	0.651133597	0.498997836	0.167249398	0.453095994

Average cell counts for total cell number and apoptotic cells in each neural region for both control and 2.4ppm stage 25 embryos. All neural regions had no significant difference between controls and 2.4ppm embryos.

Figure 13. Concentration of Hg in control yolks during development

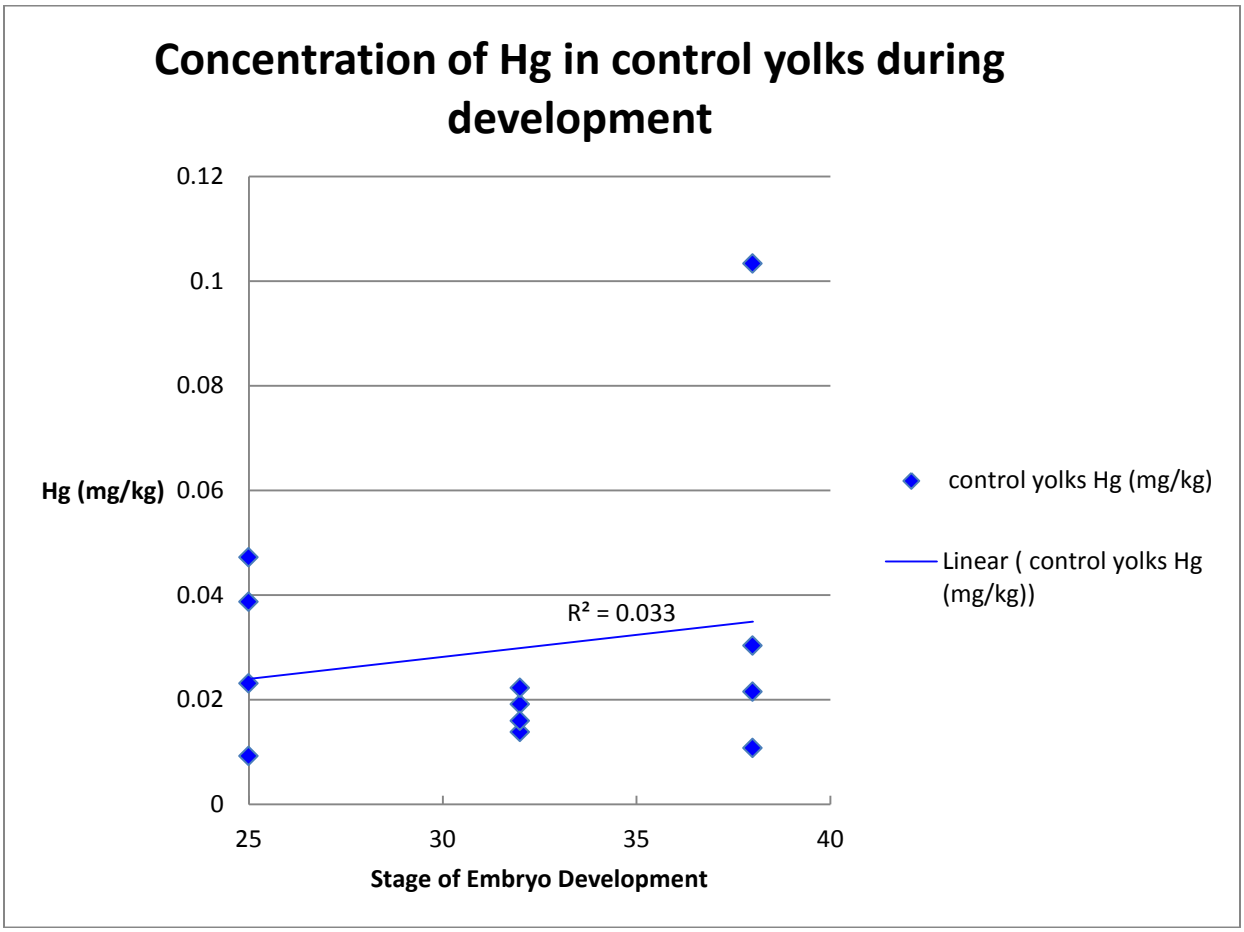

In **Figure 13**, throughout all three measured stages of development 'yolk' (combined yolk/albumin) mercury content was generally very low in control yolks and did not appear to follow any toxicokinetics trend during development. Each separate point on the graph was the mercury concentration a yolk that came from a separately analyzed egg. Values for **Figure 13** may be found in **Table 21** of the **Appendix**.

Table 21. Concentration of Hg in control embryo yolk during development. Values corresponding to **Figure 13**.

Stage, Pair Number, Treatment group, Daid collected and dissected	control yolk Hg (mg/kg)
st 25--P4b,0.0ppm, 150215-150218	0.0387
st 25-- P4c,0.0ppm,150224-150227	0.0472
st 25--P1,0.0ppm,150317-150321	0.0231
st 25--P1,0.0ppm,150321-150325	0.0092
st 32--P4,0.0ppm,150319-150325	0.0191
st 32--P4,0.0ppm,150312-150318	0.0138
st 32--P1b,0,0ppm,150311-150317	0.0222
st 32--P1,0.0ppm,150217-150223	0.0159
st 38--P4, 0.0ppm, 150210-150218	0.1033
st 38--P4,0.0ppm,150302-150310	0.0215
st 38--P1b,0.0ppm,150215-150223	0.0303
st 38--P1c,0.0ppm,150223-150225	0.0107

Figure 14. Concentration of Hg in 2.4ppm yolks during development

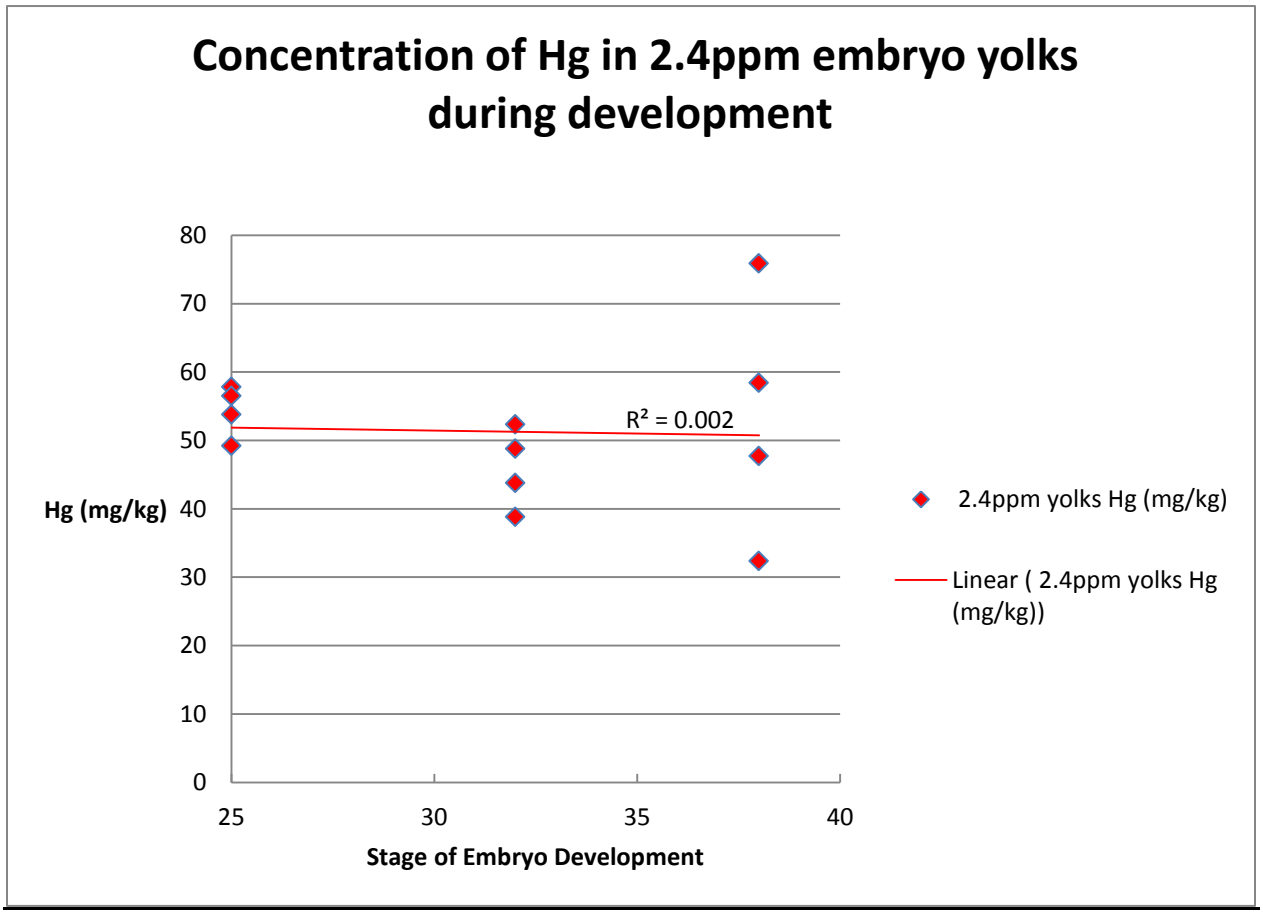

In **Figure 14**, mercury content in the 'yolk' (combined yolk/albumin) of treatment embryos exhibited a slight downwards trend as zebra finch embryos progressed along the three measured stages of development. Each separate point on the graph was the mercury concentration a yolk that came from a separately analyzed egg. Values for **Figure 14** may be found in **Table 22** of the **Appendix**.

Table 22. Concentration of Hg in 2.4ppm embryo yolk during development. Values corresponding to **Figure 14**

Stage, Pair Number, Treatment group, Daid collected and dissected	2.4ppm yolk Hg (mg/kg)
st 25--P15c,2.4ppm,150224-150227	57.8323
st 25--P15,2.4ppm,150318-150322	53.8246
st 25--P16b,2.4ppm,150328-150402	49.2227
st 25--P16a,2.4ppm,150224-150227	56.5148
st 32--P15b,2.4ppm,150311-150317	38.8418
st 32--P15b,2.4ppm,150224-150227	43.7962
st 32--P16,2.4ppm,150318-150324	48.8223
st 32--P16b,2.4ppm,150320-150326	52.3849
st 38--P15,2.4ppm,150304-150312	75.8793
st 38--P15a,2.4ppm,150210-150218	58.4531
st 38--P16b,2.4ppm,150210-150218	47.7144
st 38--P16b,2.4ppm,150301-150309	32.3835

Figure 15. Concentration of Hg in control embryos during development

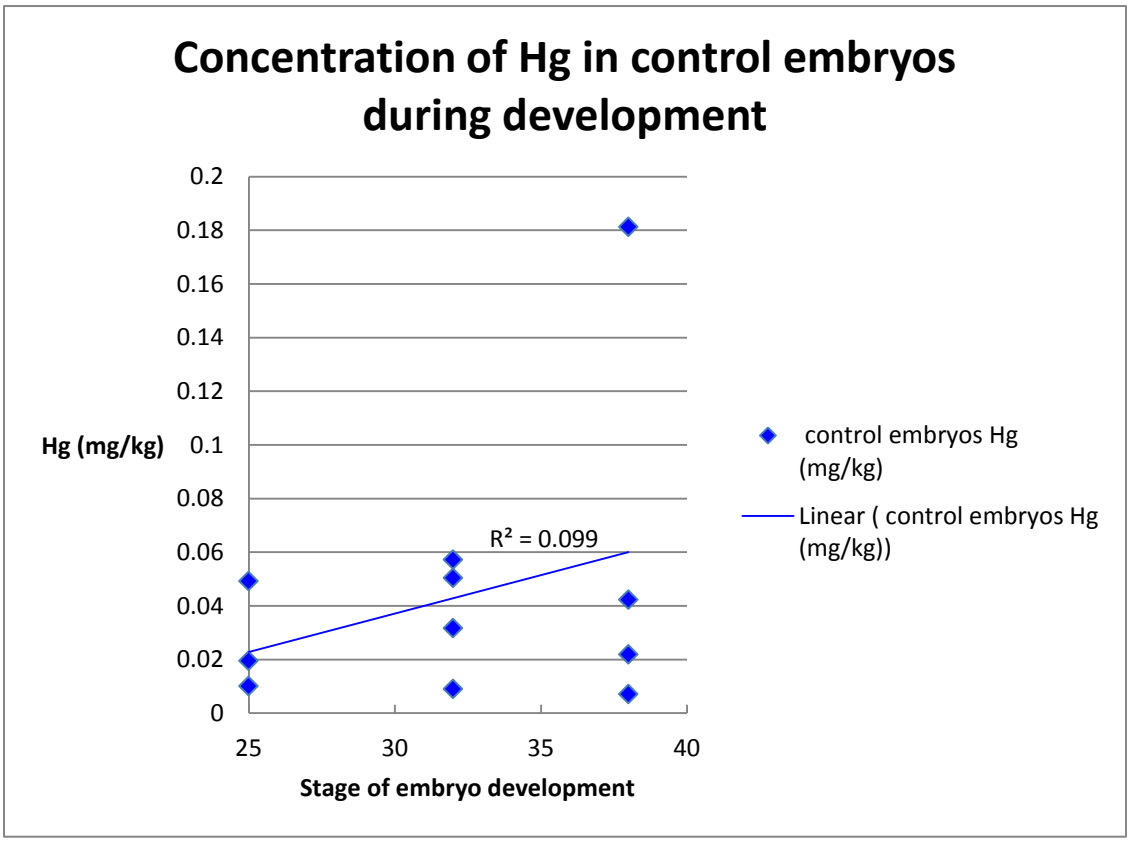

In **Figure 15**, throughout all three measured stages of development 'yolk' (as in combined yolk/albumin) mercury content was generally very low in control embryos. . Each separate point on the graph was the mercury concentration of an embryo that came from a separately analyzed egg. Normal levels of mercury in control embryos during development may potentially follow the same trend as the treatment group. However, as the R^2 value is so low the trend may be meaningless and an increased sample size and inclusion of later stages of development may cause no trend to be observed. Values for **Figure 15** may be found in **Table 23** of the **Appendix**.

Table 23. Concentration of Hg in control embryo s during development. Values corresponding to **Figure 15**

Stage, Pair Number, Treatment group, Daid collected and dissected	control embryo Hg (mg/kg)
st 25--P4b,0.0ppm, 150215-150218	0.0101
st 25-- P4c,0.0ppm,150224-150227	0.0196
st 25--P1,0.0ppm,150317-150321	0.0493
st 32--P4,0.0ppm,150319-150325	0.0317
st 32--P4,0.0ppm,150312-150318	0.009
st 32--P1b,0,0ppm,150311-150317	0.0573
st 32--P1,0.0ppm,150217-150223	0.0505
st 38--P4, 0.0ppm, 150210-150218	0.1813
st 38--P4,0.0ppm,150302-150310	0.0219
st 38--P1b,0.0ppm,150215-150223	0.0423
st 38--P1c,0.0ppm,150223-150225	0.0071

Figure 16. Concentration of Hg in 2.4ppm embryos during development

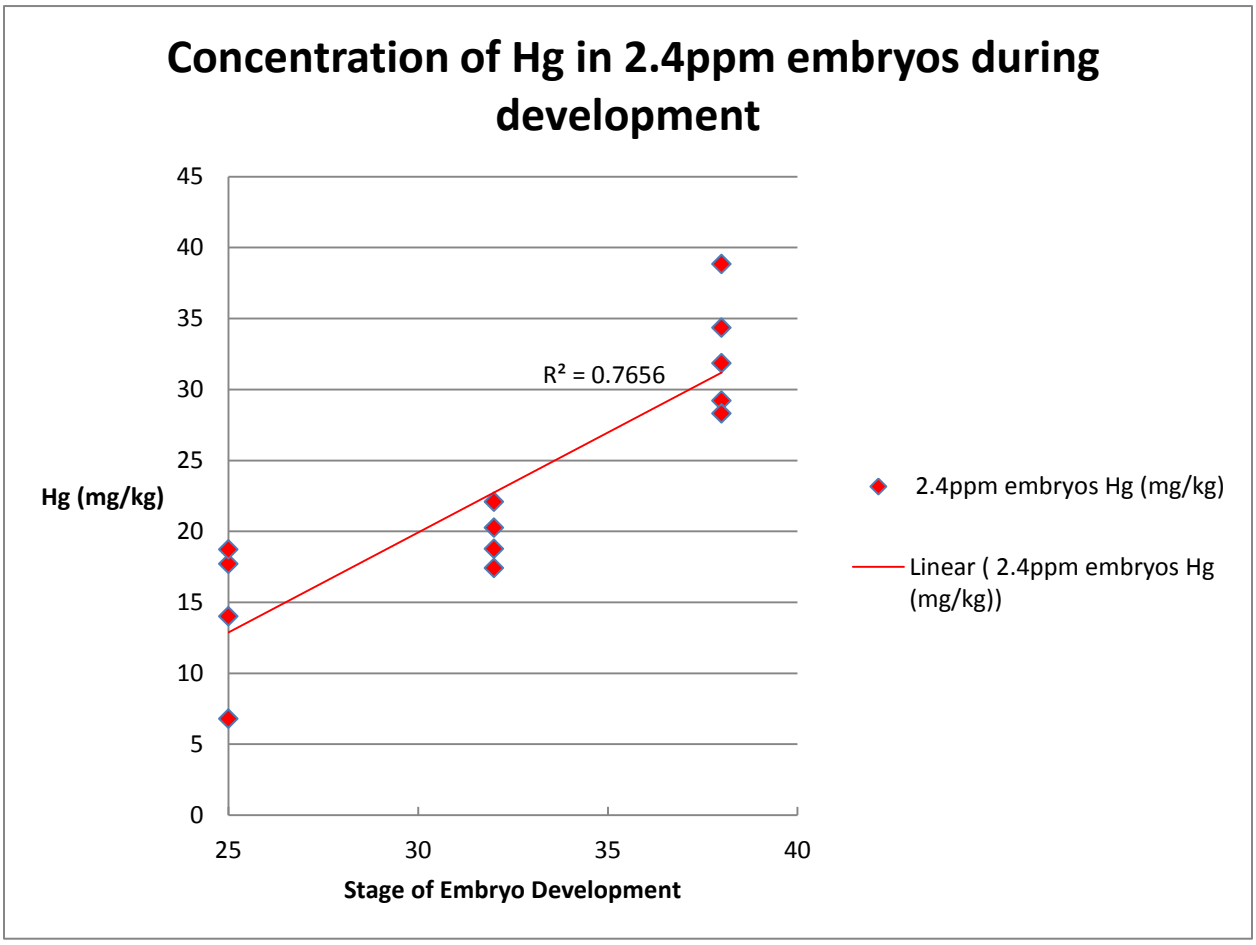

In **Figure 16**, there is an evident trend of increasing mercury content in treatment embryos as development progresses. Each separate point on the graph was the mercury concentration of an embryo that came from a separately analyzed egg. The trend is supported by the R^2 value being closer to 1 at 0.7656. As stage 25 embryos had the lowest embryo mercury concentrations and stage 38 embryos had the highest mercury concentrations, the developing embryo may be at a greater risk of MeHg neurotoxic effects for later embryonic stages. Values for **Figure 16** may be found in **Table 24** of the **Appendix**.

Table 24. Concentration of Hg in 2.4ppm embryos during development. Values corresponding to **Figure 16**

Stage, Pair Number, Treatment group, Daid collected and dissected	2.4ppm embryo Hg (mg/kg)
st 25--P15c,2.4ppm,150224-150227	14.0187
st 25--P15,2.4ppm,150318-150322	17.7242
st 25--P16b,2.4ppm,150328-150402	6.8054
st 25--P16a,2.4ppm,150224-150227	18.7368
st 32--P15b,2.4ppm,150311-150317	17.4267
st 32--P15b,2.4ppm,150224-150227	20.2575
st 32--P16,2.4ppm,150318-150324	22.0898
st 32--P16b,2.4ppm,150320-150326	18.7875
st 38--P15,2.4ppm,150304-150312	29.2206
st 38--P15a,2.4ppm,150210-150218	28.3141
st 38--P16b,2.4ppm,150210-150218	38.8582
st 38--P16b,2.4ppm,150301-150309	34.3528
st 38--P16b,2.4ppm,150224-150304	31.8664

Table 25. Concentration of Hg in 2.4ppm embryo compared to yolk during development. Values corresponding to **Figure 12**.

Stage, Pair Number, Treatment group, Daid collected and dissected	2.4ppm [embryo]/[yolk]
st 25--P15c,2.4ppm,150224-150227	0.242
st 25--P15,2.4ppm,150318-150322	0.329
st 25--P16b,2.4ppm,150328-150402	0.138
st 25--P16a,2.4ppm,150224-150227	0.332
st 32--P15b,2.4ppm,150311-150317	0.449
st 32--P15b,2.4ppm,150224-150227	0.463
st 32--P16,2.4ppm,150318-150324	0.452
st 32--P16b,2.4ppm,150320-150326	0.359
st 38--P16b,2.4ppm,150210-150218	0.612
st 38--P16b,2.4ppm,150301-150309	0.874
st 38--P15,2.4ppm,150304-150312	0.512
st 38--P15a,2.4ppm,150210-150218	0.588
st 38--P16b,2.4ppm,150224-150304	0.515

Table 26. Concentration of Hg in control and 2.4ppm embryos eggshells

Stage, Pair Number, Treatment group, Daid collected and dissected	Control eggshell Hg (mg/kg)
st 25--P4b,0.0ppm, 150215-150218	0.0186
st 25-- P4c,0.0ppm,150224-150227	0.1099
st 25--P1,0.0ppm,150317-150321	0.0415
st 25--P1,0.0ppm,150321-150325	0.0109
st 32--P4,0.0ppm,150319-150325	0.0061
st 32--P4,0.0ppm,150312-150318	0.0058
st 32--P1b,0,0ppm,150311-150317	0.0054
st 32--P1,0.0ppm,150217-150223	0.0218
st 38--P4, 0.0ppm, 150210-150218	0.0933
st 38--P4,0.0ppm,150302-150310	0.0054
st 38--P1b,0.0ppm,150215-150223	0.009
st 38--P1c,0.0ppm,150223-150225	0.003
Stage, Pair Number, Treatment group, Daid collected and dissected	2.4ppml eggshell Hg (mg/kg)
st 25--P15c,2.4ppm,150224-150227	32.9436
st 25--P15,2.4ppm,150318-150322	14.3607
st 25--P16b,2.4ppm,150328-150402	24.87095
st 25--P16a,2.4ppm,150224-150227	19.9262
st 32--P15b,2.4ppm,150311-150317	9.5634
st 32--P15b,2.4ppm,150224-150227	12.3615
st 32--P16,2.4ppm,150318-150324	2.4068
st 32--P16b,2.4ppm,150320-150326	3.288
st 38--P15,2.4ppm,150304-150312	21.6459
st 38--P15a,2.4ppm,150210-150218	13.5724
st 38--P16b,2.4ppm,150210-150218	3.2411
st 38--P16b,2.4ppm,150301-150309	9.7858
st 38--P16b,2.4ppm,150224-150304	5.827

Table 26 results may be due to sample preparation, as the unusually high levels of mercury found in some of the eggshell samples may have been the result of yolk/albumin contamination.

Table 27. Whole egg mercury content

Stage, Pair Number, Treatment group, Daid collected and dissected	stage	Hg (mg/kg)
P4,0.0ppm,150303-150311	38	0.0196
P4,0.0ppm,150308-150316	38	0.0322
P1a,0.0ppm,150311-150331	38	0.0024
P1,0.0ppm,150302-150310	38	0.0073
P4,0.0ppm,150328-150331	32	0.0178
P4a,0.0ppm,150327-150402	32	0.0239
P1,0.0ppm,150313-150319	32	0.0162
P1,0.0ppm,150315-150321	32	0.0208
P4a,0.0ppm,150224-150227	25	0.0376
P4,0.0ppm,150404-150408	25	0.1407
P1,0.0ppm,150403-150407	25	0.2117
P1,0.0ppm,150324-150328	25	0.0098
P15b,2.4ppm,150311-150318	38	37.0447
P15,2.4ppm,150306-150314	38	32.9114
P15,2.4ppm,150311-140318	38	44.2246
P16,2.4ppm,150302-150310	38	34.9501
P16,2.4ppm,150304-150312	38	46.56
P16,2.4ppm,150303-150311	38	47.2987
P15b,2.4ppm,150313-150319	32	25.0728
P15,2.4ppm,150315-150321	32	26.2086
P16,2.4ppm,150322-150328	32	41.1989
P16a,2.4ppm,150320-150326	32	40.7877
P16,2.4ppm,150323-150329	32	32.4378
P15,2.4ppm,150319-150323	25	32.243
P15a,2.4ppm,150327-150331	25	33.1193
P15,2.4ppm,150328-150401	25	49.2688
P16,2.4ppm,150403-150407	25	47.9617
P16,2.4ppm,150320-150403	25	29.2987
P16,2.4ppm,150405-150409	25	45.1342
P16,2.4ppm,150401-150405	25	32.0809

Whole eggs, all components (embryo, yolk/albumin, eggshell) were homogenized and run on the DMA.

References

1. Hsu-Kim, H., Kucharzyk, K. H., Zhang, T. & Deshusses, M. A. Mechanisms regulating mercury bioavailability for methylating microorganisms in the aquatic environment: a critical review. *Environ. Sci. Technol.* **47,** 2441–56 (2013).
2. Mason, R. P. *et al.* Mercury biogeochemical cycling in the ocean and policy implications. *Environ. Res.* **119,** 101–17 (2012).
3. Kim, M.-K. K. & Zoh, K.-D. D. Fate and transport of mercury in environmental media and human exposure. *J Prev Med Public Health* **45,** 335–43 (2012).
4. Krabbenhoft, D. P. & Sunderland, E. M. Environmental science. Global change and mercury. *Science* **341,** 1457–8 (2013).
5. Cristol, D. A. *et al.* The movement of aquatic mercury through terrestrial food webs. *Science* **320,** 335 (2008).
6. Tsui, M. T. *et al.* Variation in terrestrial and aquatic sources of methylmercury in stream predators as revealed by stable mercury isotopes. *Environ. Sci. Technol.* **48,** 10128–35 (2014).
7. Park, J.-D. D. & Zheng, W. Human exposure and health effects of inorganic and elemental mercury. *J Prev Med Public Health* **45,** 344–52 (2012).
8. Farina, M., Aschner, M. & Rocha, J. B. Oxidative stress in MeHg-induced neurotoxicity. *Toxicol. Appl. Pharmacol.* **256,** 405–17 (2011).
9. Bernhoft, R. A. Mercury toxicity and treatment: a review of the literature. *J Environ Public Health* **2012,** 460508 (2012).
10. Pieper, I. *et al.* Mechanisms of Hg species induced toxicity in cultured human astrocytes: genotoxicity and DNA-damage response. *Metallomics* **6,** 662–71 (2014).
11. Farina, M., Rocha, J. B. & Aschner, M. Mechanisms of methylmercury-induced neurotoxicity: evidence from experimental studies. *Life Sci.* **89,** 555–63 (2011).
12. Grandjean, P., Satoh, H., Murata, K. & Eto, K. Adverse effects of methylmercury: environmental health research implications. *Environ. Health Perspect.* **118,** 1137–45 (2010).
13. Buckman, K. L. *et al.* Influence of a chlor-alkali Superfund site on mercury bioaccumulation in periphyton and Low-trophic level fauna. *Environ. Toxicol. Chem.* (2015). doi:10.1002/etc.2964
14. Li, P., Feng, X. & Qiu, G. Methylmercury exposure and health effects from rice and fish consumption: a review. *Int J Environ Res Public Health* **7,** 2666–91 (2010).
15. Ceccatelli, S., Daré, E. & Moors, M. Methylmercury-induced neurotoxicity and apoptosis. *Chem. Biol. Interact.* **188,** 301–8 (2010).
16. Yuan, Y. Methylmercury: a potential environmental risk factor contributing to epileptogenesis. *Neurotoxicology* **33,** 119–26 (2012).
17. Hong, Y.-S. S. *et al.* Four cases of abnormal neuropsychological findings in children with high blood methylmercury concentrations. *Ann Occup Environ Med* **25,** 18 (2013).
18. Newland, M. C., Reed, M. N. & Rasmussen, E. A hypothesis about how early developmental methylmercury exposure disrupts behavior in adulthood. *Behav. Processes* (2015). doi:10.1016/j.beproc.2015.03.007
19. Rand, M. D., Dao, J. C. & Clason, T. A. Methylmercury disruption of embryonic neural development in Drosophila. *Neurotoxicology* **30,** 794–802 (2009).

20. Orenstein, S. T. *et al.* Prenatal organochlorine and methylmercury exposure and memory and learning in school-age children in communities near the New Bedford Harbor Superfund site, Massachusetts. *Environ. Health Perspect.* **122,** 1253–9 (2014).
21. Smith, L. E. *et al.* Developmental selenomethionine and methylmercury exposures affect zebrafish learning. *Neurotoxicol Teratol* **32,** 246–55 (2010).
22. Hallinger, K. K., Zabransky, D. J., Kazmer, K. A. & Cristol, D. A. Birdsong differs between mercury-polluted and reference sites. *The Auk* **127,** 156–161 (2010).
23. Barnea, A. & Pravosudov, V. Birds as a model to study adult neurogenesis: bridging evolutionary, comparative and neuroethological approaches. *Eur. J. Neurosci.* **34,** 884–907 (2011).
24. Capellini, T. D., Zappavigna, V. & Selleri, L. Pbx homeodomain proteins: TALEnted regulators of limb patterning and outgrowth. *Dev. Dyn.* **240,** 1063–86 (2011).
25. McGowan, L. D., Alaama, R. A. & Striedter, G. F. FGF2 delays tectal neurogenesis, increases tectal cell numbers, and alters tectal lamination in embryonic chicks. *PLoS ONE* **8,** e79949 (2013).
26. Tenin, G. *et al.* The chick somitogenesis oscillator is arrested before all paraxial mesoderm is segmented into somites. *BMC Dev. Biol.* **10,** 24 (2010).
27. Winograd, C. & Ceman, S. Exploring the zebra finch Taeniopygia guttata as a novel animal model for the speech-language deficit of fragile X syndrome. *Results Probl Cell Differ* **54,** 181–97 (2012).
28. Chen, Q., Heston, J. B., Burkett, Z. D. & White, S. A. Expression analysis of the speech-related genes FoxP1 and FoxP2 and their relation to singing behavior in two songbird species. *J. Exp. Biol.* **216,** 3682–92 (2013).
29. Henry, K. A., Cristol, D. A., Varian-Ramos, C. W. & Bradley, E. L. Oxidative stress in songbirds exposed to dietary methylmercury. *Ecotoxicology* **24,** 520–6 (2015).
30. Frederick, P. C., Spalding, M. G. & Dusek, R. Wading birds as bioindicators of mercury contamination in Florida, USA: annual and geographic variation. *Environ. Toxicol. Chem.* **21,** 163–7 (2002).
31. Strom, S. M. & Brady, R. S. Mercury in swamp sparrows (Melospiza georgiana) from wetland habitats in Wisconsin. *Ecotoxicology* **20,** 1694–700 (2011).
32. Varian-Ramos, C. W., Swaddle, J. P. & Cristol, D. A. Mercury reduces avian reproductive success and imposes selection: an experimental study with adult- or lifetime-exposure in zebra finch. *PLoS ONE* **9,** e95674 (2014).
33. Bond, A. L., Hobson, K. A. & Branfireun, B. A. Rapidly increasing methyl mercury in endangered ivory gull (Pagophila eburnea) feathers over a 130 year record. *Proc. Biol. Sci.* **282,** (2015).
34. Cristol, D. A., Smith, F. M., Varian-Ramos, C. W. & Watts, B. D. Mercury levels of Nelson's and saltmarsh sparrows at wintering grounds in Virginia, USA. *Ecotoxicology* **20,** 1773–9 (2011).
35. Bond, A., Hobson, K. & Branfireun, B. Rapidly increasing methyl mercury in endangered ivory gull (Pagophila eburnea) feathers over a 130 year record. *Proceedings of the Royal Society B: Biological Sciences* **282**, 20150032-20150032 (2015).
36. Roos, D., Seeger, R., Puntel, R. & Vargas Barbosa, N. Role of calcium and mitochondria in MeHg-mediated cytotoxicity. *J. Biomed. Biotechnol.* **2012,** 248764 (2012).
37. Kanda, H., Shinkai, Y. & Kumagai, Y. S-mercuration of cellular proteins by methylmercury and its toxicological implications. *J Toxicol Sci* **39,** 687–700 (2014).

38. Fujimura, M. & Usuki, F. Methylmercury causes neuronal cell death through the suppression of the TrkA pathway: in vitro and in vivo effects of TrkA pathway activators. *Toxicol. Appl. Pharmacol.* **282,** 259–66 (2015).
39. Kawamata, H. & Manfredi, G. Mitochondrial dysfunction and intracellular calcium dysregulation in ALS. *Mech. Ageing Dev.* **131,** 517–26 (2010).
40. Del Rosario, J. S. *et al.* Death Associated Protein Kinase (DAPK) -Mediated Neurodegenerative Mechanisms in Nematode Excitotoxicity. *BMC Neurosci* **16,** 25 (2015).
41. Polunas, M. *et al.* Role of oxidative stress and the mitochondrial permeability transition in methylmercury cytotoxicity. *Neurotoxicology* **32,** 526–34 (2011).
42. Johnson, W. M., Wilson-Delfosse, A. L. & Mieyal, J. J. Dysregulation of glutathione homeostasis in neurodegenerative diseases. *Nutrients* **4,** 1399–440 (2012).
43. Harrington, A. W. *et al.* Recruitment of actin modifiers to TrkA endosomes governs retrograde NGF signaling and survival. *Cell* **146,** 421–34 (2011).
44. Guo, B.-Q. Q., Yan, C.-H. H., Cai, S.-Z. Z., Yuan, X.-B. B. & Shen, X.-M. M. Low level prenatal exposure to methylmercury disrupts neuronal migration in the developing rat cerebral cortex. *Toxicology* **304,** 57–68 (2013).
45. Ceccatelli, S., Bose, R., Edoff, K., Onishchenko, N. & Spulber, S. Long-lasting neurotoxic effects of exposure to methylmercury during development. *J. Intern. Med.* **273,** 490–7 (2013).
46. Xu, M., Yan, C., Tian, Y., Yuan, X. & Shen, X. Effects of low level of methylmercury on proliferation of cortical progenitor cells. *Brain Res.* **1359,** 272–80 (2010).
47. Huyck, R. W., Nagarkar, M., Olsen, N., Clamons, S. E. & Saha, M. S. Methylmercury exposure during early Xenopus laevis development affects cell proliferation and death but not neural progenitor specification. *Neurotoxicol Teratol* **47,** 102–13 (2015).
48. Sokolowski, K. *et al.* Neural stem cell apoptosis after low-methylmercury exposures in postnatal hippocampus produce persistent cell loss and adolescent memory deficits. *Dev Neurobiol* **73,** 936–49 (2013).
49. Catts, V. S. & Weickert, C. S. Gene expression analysis implicates a death receptor pathway in schizophrenia pathology. *PLoS ONE* **7,** e35511 (2012).
50. Chow, M. L. *et al.* Age-dependent brain gene expression and copy number anomalies in autism suggest distinct pathological processes at young versus mature ages. *PLoS Genet.* **8,** e1002592 (2012).
51. Deroma, L. *et al.* Neuropsychological assessment at school-age and prenatal low-level exposure to mercury through fish consumption in an Italian birth cohort living near a contaminated site. *Int J Hyg Environ Health* **216,** 486–93 (2013).
52. Karagas, M. R. *et al.* Evidence on the human health effects of low-level methylmercury exposure. *Environ. Health Perspect.* **120,** 799–806 (2012).
53. Bose, R., Onishchenko, N., Edoff, K., Janson Lang, A. M. & Ceccatelli, S. Inherited effects of low-dose exposure to methylmercury in neural stem cells. *Toxicol. Sci.* **130,** 383–90 (2012).
54. Watanabe, J. *et al.* Low dose of methylmercury (MeHg) exposure induces caspase mediated-apoptosis in cultured neural progenitor cells. *J Toxicol Sci* **38,** 931–5 (2013).
55. Robinson, J. F. *et al.* Methylmercury induced toxicogenomic response in C57 and SWV mouse embryos undergoing neural tube closure. *Reprod. Toxicol.* **30,** 284–91 (2010).

56. Heinz, GH, Hoffman, DJ & Klimstra, JD. A comparison of the teratogenicity of methylmercury and selenomethionine injected into bird eggs. *Archives of environmental …* (2012). at <http://link.springer.com/article/10.1007/s00244-011-9717-4>
57. Miura, K., Himeno, S., Koide, N. & Imura, N. Effects of methylmercury and inorganic mercury on the growth of nerve fibers in cultured chick dorsal root ganglia. *Tohoku J. Exp. Med.* **192,** 195–210 (2000).
58. Herculano, A. M., Crespo-López, M. E., Lima, S. M., Picanço-Diniz, D. L. & Do Nascimento, J. L. Methylmercury intoxication activates nitric oxide synthase in chick retinal cell culture. *Braz. J. Med. Biol. Res.* **39,** 415–8 (2006).
59. Bertossi, M. *et al.* Effects of methylmercury on the microvasculature of the developing brain. *Neurotoxicology* **25,** 849–57 (2004).
60. Rutkiewicz, J., Bradley, M., Mittal, K. & Basu, N. Methylmercury egg injections: part 2--pathology, neurochemistry, and behavior in the avian embryo and hatchling. *Ecotoxicol. Environ. Saf.* **93,** 77–86 (2013).
61. Murray, J. R., Varian-Ramos, C. W., Welch, Z. S. & Saha, M. S. Embryological staging of the Zebra Finch, Taeniopygia guttata. *J. Morphol.* **274,** 1090–110 (2013).
62. Blom, J. & Lilja, C. A comparative study of embryonic development of some bird species with different patterns of postnatal growth. *Zoology (Jena)* **108,** 81–95 (2005).
63. Rutkiewicz, J. & Basu, N. Methylmercury egg injections: part 1--Tissue distribution of mercury in the avian embryo and hatchling. *Ecotoxicol. Environ. Saf.* **93,** 68–76 (2013).
64. Carvalho, M. C., Nazari, E. M., Farina, M. & Muller, Y. M. Behavioral, morphological, and biochemical changes after in ovo exposure to methylmercury in chicks. *Toxicol. Sci.* **106,** 180–5 (2008).
65. Wang, Y. *et al.* Postnatal exposure to methyl mercury and neuropsychological development in 7-year-old urban inner-city children exposed to lead in the United States. *Child Neuropsychol* **20,** 527–38 (2014).
66. Bisen-Hersh, E. B., Farina, M., Barbosa, F., Rocha, J. B. & Aschner, M. Behavioral effects of developmental methylmercury drinking water exposure in rodents. *J Trace Elem Med Biol* **28,** 117–24 (2014).
67. Bowman, G. D., O'Donnell, M. & Kuriyan, J. Structural analysis of a eukaryotic sliding DNA clamp-clamp loader complex. *Nature* **429,** 724–30 (2004).
68. Strzalka, W. & Ziemienowicz, A. Proliferating cell nuclear antigen (PCNA): a key factor in DNA replication and cell cycle regulation. *Ann. Bot.* **107,** 1127–40 (2011).
69. Mohan, C., Long, K., Mutneja, M. & Ma, J. Detection of end-stage apoptosis by ApopTag® TUNEL technique. *Methods Mol. Biol.* **1219,** 43–56 (2015).
70. Pizard, A. *et al.* Whole-mount in situ hybridization and detection of RNAs in vertebrate embryos and isolated organs. *Curr Protoc Mol Biol* **Chapter 14,** Unit 14.9 (2004).
71. Ou, L., Varian-Ramos, C. W. & Cristol, D. A. Effect of laying sequence on egg mercury in captive zebra finches: An interpretation considering individual variation. *Environ. Toxicol. Chem.* (2015). doi:10.1002/etc.2976
72. Heinz, G. H. *et al.* Species differences in the sensitivity of avian embryos to methylmercury. *Arch. Environ. Contam. Toxicol.* **56,** 129–38 (2009).
73. Chang, S.-H. H. *et al.* Methylmercury induces caspase-dependent apoptosis and autophagy in human neural stem cells. *J Toxicol Sci* **38,** 823–31 (2013).

74. Falluel-Morel, A. *et al.* N-acetyl cysteine treatment reduces mercury-induced neurotoxicity in the developing rat hippocampus. *J. Neurosci. Res.* **90,** 743–50 (2012).
75. Silva-Pereira, L. C. *et al.* Protective effect of prolactin against methylmercury-induced mutagenicity and cytotoxicity on human lymphocytes. *Int J Environ Res Public Health* **11,** 9822–34 (2014).
76. Burke, K. *et al.* Methylmercury elicits rapid inhibition of cell proliferation in the developing brain and decreases cell cycle regulator, cyclin E. *Neurotoxicology* **27,** 970–81 (2006).
77. Lewandowski, T. A., Ponce, R. A., Charleston, J. S., Hong, S. & Faustman, E. M. Effect of methylmercury on midbrain cell proliferation during organogenesis: potential cross-species differences and implications for risk assessment. *Toxicol. Sci.* **75,** 124–33 (2003).
78. Chandrasekaran, B., Kraus, N. & Wong, P. C. Human inferior colliculus activity relates to individual differences in spoken language learning. *J. Neurophysiol.* **107,** 1325–36 (2012).
79. Cacciaglia, R. *et al.* Involvement of the human midbrain and thalamus in auditory deviance detection. *Neuropsychologia* **68,** 51–8 (2015).
80. Nordeen, E. J., Holtzman, D. A. & Nordeen, K. W. Increased Fos expression among midbrain dopaminergic cell groups during birdsong tutoring. *Eur. J. Neurosci.* **30,** 662–70 (2009).
81. Van der Kant, A., Derégnaucourt, S., Gahr, M., Van der Linden, A. & Poirier, C. Representation of early sensory experience in the adult auditory midbrain: implications for vocal learning. *PLoS ONE* **8,** e61764 (2013).
82. Petkov, C. I. & Jarvis, E. D. Birds, primates, and spoken language origins: behavioral phenotypes and neurobiological substrates. *Front Evol Neurosci* **4,** 12 (2012).
83. Varian-Ramos, C. W., Swaddle, J. P. & Cristol, D. A. Familial differences in the effects of mercury on reproduction in zebra finches. *Environ. Pollut.* **182,** 316–23 (2013).